The potential role of Siglec-1 receptor as a therapeutic target against dendritic cell mediated dissemination of enveloped viruses

Xabier Muñiz Trabudua

Universitat Autònoma de Barcelona Department of Cellular Biology, Physiology, and Immunology

The potential role of Siglec-1 receptor as a therapeutic target against dendritic cell mediated dissemination of enveloped viruses

Xabier Muñiz Trabudua

IrsiCaixa AIDS Research Institute

2023

Doctoral thesis to obtain the PhD degree in Advanced Immunology of the Universitat Autònoma de Barcelona

Directors: **Dr. Javier Martínez-Picado**

Dr. Nuria Izquierdo-Useros

Tutor: **Dr. Javier Martínez-Picado**

The Spanish Ministry of Science and Innovation supported the research performed in this thesis through grants SAF2016-80033, grants PID2019-109870RB-I00 and CB21/13/ 00063. Grifols provided additional support. Xabier Muñiz Trabudua was supported by the Spanish Ministry of Science, Innovation and Universities and the European Regional Development Fund under agreement BES-2017-082900. The Spanish AIDS Network 'Red Española de Investigación en SIDA' (RIS) provided additional support for congress assistance.

El Dr. Javier Martínez-Picado, investigador principal y profesor de investigación ICREA en el Instituto de Investigación del SIDA IrsiCaixa.

Certifica:

Que el trabajo experimental y la redacción de la memoria de la Tesis Doctoral titulada "The potential role of Siglec-1 receptor as a therapeutic target against dendritic cell mediated disemination of enveloped viruses" han sido realizados por Xabier Muñiz Trabudua bajo su dirección y tutela, y considera que la citada Tesis es apta para ser presentada para optar al grado de Doctor en Inmunología Avanzada por la Universidad Autónoma de Barcelona.

Y para que quede constancia, firma este documento.

Badalona, 20 de septiembre de 2023.

Dr. Javier Martínez-Picado

La Dra. Nuria Izquierdo-Useros, investigadora principal en el Instituto de Investigación del SIDA IrsiCaixa.

Certifica:

Que el trabajo experimental y la redacción de la memoria de la Tesis Doctoral titulada "The potential role of Siglec-1 receptor as a therapeutic target against dendritic cell mediated disemination of enveloped viruses" han sido realizados por Xabier Muñiz Trabudua bajo su dirección, y considera que la citada Tesis es apta para ser presentada para optar al grado de Doctor en Inmunología Avanzada por la Universidad Autónoma de Barcelona.

Y para que quede constancia, firma este documento.

Badalona, 20 de septiembre de 2023.

Dra. Nuria Izquierdo-Useros

List of abbreviations

- ACE2: Angiotensin-Converting Enzyme 2
- AIDS: Acquired Immunodeficiency Syndrome
- AHF: Argentine Haemorrhagic Fever
- APCs: Antigen Presenting Cells
- ARDS: Acute Respiratory Distress Syndrome

- BSL4: Biosafety Level 4

- CAGGS: Chicken β-Actin promoter with CMV immediate-early enhancer
- CD169: Siglec-1 (Sialoadhesin)
- CD4: Cluster of Differentiation 4
- CCR5: C-C Chemokine Receptor Type 5
- CDRs: Complementarity-Determining Regions
- CMV: Cytomegalovirus
- CNS: Central Nervous System
- COVID-19: Coronavirus Disease 2019
- CRDs: Carbohydrate-Recognition Domains
- CLRs: C-type Lectin Receptors
- CXCL10: Chemokine (C-X-C motif) Ligand 10
- CXCR4: C-X-C Chemokine Receptor Type 4

- DENV: Dengue Virus
- DESC1: Differentially Expressed in Squamous Cell Carcinoma Gene 1
- dsRNA: Double Stranded RNA
- E: Envelope protein
- EBOV: Ebola Virus
- EBV: Epstein-Barr Virus
- ELISA: Enzyme-Linked Immunosorbent Assay
- ER: Endoplasmic Reticulum
- EV: Extracellular Vesicles

- Fabs: Antibody Fragments
- Fc: Fragment Crystallizable
- FITC: Fluorescein Isothiocyanate

- GM1: Ganglioside GM1
- GM3: Ganglioside GM3
- GP: Glycoprotein
- GP1-GP2: Glycoprotein 1-Glycoprotein 2

- HAT: Human Airway Trypsin-Like Protease
- HBV: Hepatitis B Virus
- HEK293T: Human Embryonic Kidney 293T Cells
- HIV-1: Human Immunodeficiency Virus 1

- IFN: Interferon
- IFNα: Interferon-alpha

- IFNβ: Interferon Beta
- IL: Interleukin
- IL-10: Interleukin-10
- IL-4: Interleukin-4
- IL-6: Interleukin-6
- ILRs: I-type Lectin Receptors
- ISGs: Interferon-Stimulated Genes

- JEV: Japanese Encephalitis Virus
- JUNV: Junín Virus

- LASV: Lassa Virus
- L: Large RNA segment
- LPS: Lipopolysaccharide
- LRT: Lower Respiratory Tract

- M: Membrane protein
- MARV: Marburg Virus
- MAVS: Mitochondrial Antiviral Signalling Protein
- M-CSF: Macrophage Colony-Stimulating Factor
- MOI: Multiplicity of Infection
- MΦs: Macropahges

- N: Nucleocapsid protein
- N: Nucleoprotein
- NAM: Nerve-Associated Macrophages
- NHP: Non-Human Primates
- NP: Nucleocapsid Protein
- NPC-1: Niemann-Pick C1 Protein

- ORFs: Open Reading Frames

- PAMP: Pathogen-Associated Molecular Pattern
- PAMPs: Pathogen-Associated Molecular Patterns
- PASylation: Conjugation of a therapeutic protein with Proline-Alanine-Serine repeats for increased half-life
- PEGylation: Conjugation of a therapeutic protein with Polyethylene Glycol for increased stability and half-life
- PFA: Paraformaldehyde
- PCR: Polymerase Chain Reaction
- PerCP: Peridinin Chlorophyll Protein Complex
- PRR: Pattern Recognition Receptor
- PRRs: Pattern Recognition Receptors

- RBD: Receptor-Binding Domain
- RNA: Ribonucleic Acid
- RLRs: Retinoic-acid Inducible Gene I-like Receptors
- RNP: Ribonucleoprotein
- RSV: Respiratory Syncytial Virus

- S: Spike protein

- SARS-CoV: Severe Acute Respiratory Syndrome Coronavirus
- SARS-CoV-2: Severe Acute Respiratory Syndrome Coronavirus 2
- Siglec-1: Sialic Acid-Binding Immunoglobulin-Like Lectin 1, Sialoadhesin or CD169
- SP8 STED: Stimulated Emission Depletion on Leica SP8 Microscope
- ssRNA: Single Stranded RNA

- T-cells: T Lymphocytes
- TLRs: Toll-like Receptors
- TNFα: Tumor Necrosis Factor Alpha
- TMPRSS 2: transmembrane serine protease 2

- URT: Upper Respiratory Tract

- VCC: Virus-Containing Compartment
- VLP: Virus-Like Particle
- VLPs: Viral like particles
- VSV: Vesicular Stomatitis Virus

Table of Contents

SUMMARY

Dendritic cells (DCs) play a key role in initiating specific adaptive immune responses against viruses. They possess the unique capability to capture, process, and present viral antigens to T lymphocytes, a critical step in the immune defence. However, these cells can also contribute to the early stages of viral dissemination during some infections. This is due to the capacity of Siglec-1/CD169 receptor expressed on DCs, which specifically recognizes sialylated gangliosides present on the viral membrane of enveloped viruses such as HIV-1 or Ebola virus. Curiously, Siglec-1 expression is significantly up-regulated when dendritic cells are stimulated with immune-activating factors like interferon-alpha and lipopolysaccharide, both of which are commonly found during different infectious processes.

Our group has previously shown that the recognition of HIV-1 by Siglec-1 leads to the accumulation of viral particles within a sac-like virus-containing compartment (VCC), which allows the virus to remain inside DCs and be transmitted to target $CD4^+$ T cells, which become productively infected by this mechanism known as *trans*-infection. Previous studies have shown that the interaction between Siglec-1 and HIV-1 relies on the recognition of syalilated gangliosides such as GM1, which has been found in HIV-1 membranes, but also in the membranes of other viruses such as Ebola virus (EBOV). Our group has shown that EBOV viral-like particles (VLPs) were captured in a Siglec-1 dependent manner, leading to the formation of a VCC that favour viral fusion. These results suggest that Siglec-1 might act as an auxiliary receptor, facilitating viral entry and dissemination of distinct enveloped viruses.

Following this hypothesis, here we show that SARS-CoV-2, an enveloped virus responsible for the COVID-19 global pandemic, contains GM1 gangliosides in their membrane and is captured via Siglec-1 by DCs and macrophages. While DCs did not get productively infected, SARS-CoV-2 followed a similar *trans*-infection mechanism as to that described for HIV-1. We next studied the possible contribution of Siglec-1 to the capture of arenaviruses, which is another family of enveloped viruses responsible for causing haemorrhagic fevers in humans. We found that the capture of two different VLPs from the Junín and Lassa arenaviruses was Siglec-1 dependent and led to the formation of a VCC in DCs. Given that DCs are the primary target cells for arenavirus infection, Siglec-1 might act as an auxiliary receptor facilitating arenaviruses fusion, as seen for EBOV.

These results prompted us to explore the possible role of Siglec-1 as a therapeutic target against DC mediated dissemination of enveloped viruses. Following our previous work were we have identified 5 distinct murine anti-Siglec-1 monoclonal antibodies (mAbs) abrogating

Siglec-1 mediated viral uptake, we generated anti-Siglec-1 Fabs and humanized anti-Siglec-m Abs in an attempt to develop a host-directed antiviral treatment. Overall, the activity of anti-Siglec-1 Fabs and human mAbs inhibits the infection in *cis* (Ebola virus/Arenavirus) or *trans* (HIV-1/SARS-CoV-2) mediated by Siglec-1 receptor on DCs and suggests their potential use as broad-spectrum antivirals.

RESUM

Les cèl·lules dendrítiques tenen un paper clau en l'inici de respostes immunitàries adaptatives específiques contra els virus. Posseeixen la capacitat única de capturar, processar i presentar antígens virals als limfòcits T, un pas crític en la defensa immunitària. Tanmateix, aquestes cèl·lules també poden contribuir a les primeres etapes de la disseminació viral durant algunes infeccions. Això es deu a la capacitat del receptor Siglec-1/CD169 expressat a la superfície de les cèl·lules dendrítiques, que reconeix específicament gangliòsids sialilats presents a la membrana de virus embolcallats, com el VIH-1 o el virus de l'Ebola (EBOV). Curiosament, l'expressió de Siglec-1 es regula significativament quan les cèl·lules dendrítiques s'estimulen amb factors d'activació immune com l'interferó-alfa o el lipopolisacàrid, els quals es troben habitualment presents durant diferents processos infecciosos.

El nostre grup havia demostrat prèviament que el reconeixement del VIH-1 per part de Siglec-1 condueix a l'acumulació de partícules virals dins d'un compartiment que conté virus semblant a un sac, que permet que el virus romangui intacte dins les cèl·lules dendrítiques i es transmeti als limfòcits T CD4+, la seva diana cel·lular final, els quals s'infecten productivament per aquest mecanisme conegut com a *trans*-infecció. Estudis anteriors han demostrat que la interacció entre Siglec-1 i VIH-1 es basa en el reconeixement de gangliòsids sialats com el GM1, que s'ha trobat a les membranes del VIH-1, però també a les membranes d'altres virus com l'EBOV. El nostre grup ha demostrat que les partícules pseudovirals de l'EBOV també es capturen de manera dependent de Siglec-1, donant lloc a la formació de compartiments virals, la qual cosa afavoreix la fusió viral. Aquests resultats suggereixen que Siglec-1 podria actuar com a receptor auxiliar, facilitant l'entrada viral i la difusió d'altres virus embolcallats.

En línia amb aquesta hipòtesi, aquí mostrem que el SARS-CoV-2, un virus embolcallat responsable de la pandèmia global de COVID-19, conté gangliòsids GM1 a la seva membrana i és capturat mitjançant Siglec-1 per cèl·lules dendrítiques i macròfags. Tot i que les cèl·lules dendrítiques no s'infecten productivament, el SARS-CoV-2 va seguir un mecanisme de *trans*-infecció similar al descrit per al VIH-1. A continuació, vam estudiar la possible contribució de Siglec-1 a la captura d'arenavirus, que és una altra família de virus embolcallats responsables de provocar febres hemorràgiques en humans. Vam trobar que la captura de partícules pseudovirals dels arenavirus Junín i Lassa depenia de Siglec-1 i va provocar la formació de compartiment virals en les cèl·lules dendrítiques. Atès que les cèl·lules dendrítiques són cèl·lules diana per a la infecció dels arenavirus, Siglec-1 podria actuar com a receptor auxiliar facilitant la seva fusió, com s'havia vist per l'EBOV.

Aquests resultats ens vam impulsar a explorar el possible paper de Siglec-1 com a diana terapèutica contra la difusió de virus embolcallats mitjançant cèl·lules dendrítiques. Després del nostre treball anterior en el qual havíem identificat 5 anticossos monoclonals murins anti-Siglec-1 que bloquegen la captura viral mitjançant Siglec-1, vam generar Fabs i anticossos humanitzats anti-Siglec-1, en un intent de desenvolupar un tractament antiviral dirigit contra molècules de l'hoste. Tant els Fabs com els anticossos humanitzats inhibeixen la infecció en *cis* (EBOV/Arenavirus) o *trans* (VIH-1/SARS-CoV-2) mitjançant el receptor Siglec-1 en cèl·lules dendrítiques, tot suggerint el seu potencial us com a antivirals d'ampli espectre.

Chapter 1 – INTRODUCTION

Our organism lives in a constant battle with the threat of viral infections, and our remarkable immune system stands as the determined defender of this endless battle. Yet, through years of evolution, our immune defences have refined their skills to detect and combat these silent invaders swiftly and efficiently.

As viruses penetrate our body barriers, our immune system jumps into action, orchestrating a carefully organized defensive response restricting viral replication, impeding viral dissemination, and setting the stage for the subsequent and more specialized adaptive immune response. At the heart of this remarkable defence mechanism lie the antigen presenting cells (APCs), the frontline of our immune response. These specialized cells are the precursors of our immune response, preparing the way for the complex interplay between viruses and immunity.

In this thesis we explore the role of Siglec-1 (CD169 or Sialoadhesin), a type I lectin receptor expressed by APCs involved in viral recognition, that might contribute to the pathogenesis of life-threatening viruses such as Severe Acute Respiratory Syndrome Coronavirus 2 (SARS-CoV-2) or arenaviruses. We investigate the interaction via Siglec-1 receptor between these viruses and APCs. The potential role of Siglec-1 as an auxiliary receptor for SARS-CoV-2 and arenaviruses holds significant implications. If confirmed, it would highlight the versatility of Siglec-1 as a receptor for multiple enveloped viruses, increasing its relevance as a promising target for antiviral therapies.

1.1. Immune response against viral infections

Our organism is constantly exposed to the threat of viral infections, and our immune system is the first line of defence. Viruses, ubiquitous and ever evolving, can invade our organism and prompt a physio-pathological cascade of potentially devastating consequences. Yet, our immune defences have evolved to efficiently detect and combat these invaders with precision and efficacy.

Upon encountering a virus, the immune system has the capacity to mount two sequentially differentiated immune responses: the innate and the adaptive immune responses.

1.2. The innate immune response

It is characterized by its rapid mobilization of effector cells to fight invading pathogens within minutes to hours. Innate immunity plays a crucial role in limiting viral replication, preventing viral dissemination, and defining the subsequent adaptive immune response. A key component in this defence mechanism are the APCs, which serve as the inducers of the immune response, initiating the intricate series of events that follows upon viral encounter. For example, at the beginning of a viral infection, APCs will initiate the innate immune response after sensing the virus through pattern recognition receptors (PRRs) to pathogen-associated molecular patterns (PAMPs)[1]. These PRRs can be present in cell membranes (i.e., TLR7, TLR8 and TLR9) or cytosolic (RIG-I like receptors)[2]. The interaction of these receptors with viral antigens will be followed by the secretion of type I and type III interferons (IFNs), along with a range of proinflammatory cytokines and chemokines. These molecules will mobilize and activate immune cells such as macrophages (MΦs), NK cells and dendritic cells (DCs) to control virus spread, in addition to activating and modulating the adaptive immune response[1].

1.3. The adaptive immune response

Efficient activation of innate immunity plays a crucial role in restricting viral entry, translation, replication, and assembly within the host cell. This mechanism helps identifying and eliminating infected cells, while enabling a rapid development of adaptive immune responses.

After the innate immune response has activated, viral antigens go through the process of phagocytosis and degradation inside APCs[2]. These antigens are processed into smaller peptides, which are presented on the cell surface via major histocompatibility complex class-II (MHC-II) present in APCs' membranes. MHC-II expression in cells may be induced by interferon-gamma (IFNγ) and modulated by other factors, such as interleukin-4 (IL-4),

interleukin-10 (IL-10), interferon- alpha/beta (IFN-α/β), tumour necrosis factor-alpha (TNFα), and glucocorticoids secreted during the innate immune response[2]. $CD4^+$ T cells, recognize these antigens presented through MHC-II, initiating their activation, progressing into differentiation and proliferation[2]. The activation of $CD4^+$ T-cells by APCs causes them to differentiate into different subtypes with specific functions mediated by cytokine secretion and cell-to-cell contact[2]. Activated T-cells can help B cell maturation by secreting IL-4 and through CD40/CD40L interaction, they can also help B memory cells and long-lived high-affinity antibody-producing plasma cells maturation in germinal centres by interacting with them. Other T-cells differentiate into memory T-helper cells that will remain in the lymph nodes ready to build a quick specific response upon a second contact with the same pathogen, while another subset will activate $CD8^+$ cytotoxic T-cells by simultaneously interacting with APCs. The $CD8^+$ cytotoxic T-cells will cause killing of infected host cells infected. It has been reported that for SARS-CoV-2, a well-built immune response in which all these elements coordinate, correlated with mild COVID-19 development, while an uncoordinated response, more frequently observed in immune-suppressed and elderly populations, was more frequent in patients that developed severe disease[3]. Most COVID-19 vaccine efforts focus on stimulating these defence mechanisms by triggering the generation of neutralizing antibodies, with an additional activation of $CD4^+$ or $CD8^+$ T-cells[3].The coordination of APCs in viral immune response, is crucial for a quick innate response and the induction of the adaptive response. Each cell type plays a key role in the complex interaction, from the moment they interact with the invading virus to the induction of memory cells that will be ready for a second encounter.

1.4. APCs during viral infections

APCs are a diverse group of specialized immune cells that play a crucial role in the initiation and organization of immune responses. APCs include B cells, monocytes, MΦs, and DCs. They are characterized for expressing a repertoire of PRRs that enable them to recognize and respond to viral components known as PAMPs[4]. Different types of molecular structures can act as PAMPs, such as lipopolysaccharide (LPS), endotoxins, peptidoglycan, flagellin, lipoteichoic acid, double stranded RNA (dsRNA), single stranded RNA (ssRNA), DNA, CpG DNA and nucleic acid motifs[5]. To detect such range of different molecules, APCs express a variety of specialized PRRs. Among them we can find: Toll-like Receptors (TLRs), C-type and I-type Lectin Receptors (CLRs and ILRs), RIG-I Like Receptors (RLRs), or NOD-Like Receptor (NLRs). Upon infection, PRRs in APCs recognize viral PAMPs and initiate the innate immune

response by producing proinflammatory cytokines, type I IFNs and antimicrobial proteins[6,7], which will be followed by the adaptive immune response.

Among PRRs, TLRs present a wide range of different PAMP type recognition, and they can be found in the cell surface, or intracellularly on endosomal and endo-lysosomal membranes[8] (**Figure 1.1**). TLRs are usually expressed in MΦs and DCs, but they are also present in B cells. Despite their main role as mediators in the production of antigen-specific immunoglobulin (IgG) directed against invasive pathogens, B cells can act as APCs presenting antigens to T-cells via MHC-II. For example, TLR2 expressed on B cells surface, is known to sense cytomegalovirus (CMV) via viral envelope glycoprotein B and H, and Hepatitis C virus (HCV) via core protein[8,9]. Furthermore, TLR2 mediates innate immune response against Junín virus (JUNV) in mice and plays a critical role in viral clearance of JUNV vaccine Candid 1[10]. Another example is TLR4, which has been reported to sense Ebola virus (EBOV) via glycoprotein[11]. TLR4 has also been reported to modulate activation in human MΦs after interacting with HIV-1 envelope protein gp120[12]. It is worth noting that TLR2 and TLR4 expressed in APCs, not only recognize viral antigens, but bacterial origin lipopolysaccharide (LPS), peptidoglycans and lipoproteins as well[13].

Apart from protein recognition, TLRs can recognize viral genetic material. For example, TLR3 recognizes viral dsRNA, small interfering RNAs (siRNAs), and self-RNAs derived from damaged cells[13]. Examples of viral recognition via TLR3 include respiratory syncytial virus (RSV), rhinovirus, reovirus, Epstein-Barr virus (EBV), and herpes simplex virus-2 (HSV2)[14–18]. TLR7 and TLR8, which are highly expressed in plasmacytoid DCs (pDCs), are involved in recognition of ssRNA viruses in a species-specific way[19]. pDCs, which are known for secreting large amounts of type I IFN, particularly IFNα, in response to viral infection, recognize multiple viruses, such as: Influenza virus, VSV, HIV-1, Sendai virus (SeV), Coxsackievirus B (CBVs), and HCV, via TLR7 and TLR8[19–23]. Similar to TLR7 and TLR8, TLR9 is primarily expressed in pDCs, and it has been described to recognize bacterial and viral DNA that is rich in unmethylated 2'-deoxyribo (cytidine-phosphate- guanosine) CpG-DNA motifs[13]. Viral DNA recognition via TLR9 has been described to induce IFN production in herpes viruses including HSV-1, HSV-2, varicella zoster virus (VZV), cytomegalovirus (CMV), and EBV[24–29].

APCs also express Retinoic-acid inducible gene I (RIG-I)-like receptors or RLRs, which are intracellular pattern recognition receptors to sense viral RNA in the cytoplasm via RNA binding motifs[13] (**Figure 1.1**). They possess a signalling domain that activates a cascade leading to the production of type I IFNs, proinflammatory cytokines, and chemokines[30,31]. These receptors have been found to be essential for the induction of type I IFN in DCs after infection with VSV[32].

Curiously, some viruses can halt IFN production by inhibiting the signalling mediated by RIG-I. For example, SARS-CoV-2 M protein interaction with RIG-I impedes the phosphorylation and nuclear translocation of IFN regulatory factor 3 (IRF3), inhibiting IFN production in infected cells[33].

Other PRRs that can lead to type I IFN production after encountering viral PAMPs are C-type lectin receptor or CLRs. CLRs include a large family of transmembrane and soluble receptors that contain one or more conserved carbohydrate-recognition domain (CRDs) (**Figure 1.1**). These CLRs bind carbohydrate moieties in a $Ca2^{+}$-dependent or $Ca2^{+}$-independent manner using CRDs. CLRs have high affinity for their ligands and are known to be expressed on DCs and MΦs. Internalization via CLRs can lead to different outcomes such as degradation via lysosome or autophagy[34,35], production of type I IFNs, activation of NF-κB, activation of the inflammasome, or antigen presentation on MHC molecules, promoting adaptive immune responses[36,37]. Dendritic cell-specific intercellular adhesion molecule-3-grabbing non-integrin (DC-SIGN) is a CLR which can recognize mannose and fucose structure on the surface of viruses such as HIV-1 and Dengue virus (DENV)[38,39]. Lymph node-specific intercellular adhesion molecule-3-grabbing integrin (L-SIGN, also known as DC-SIGNR) is another CLR similar to DC-SIGN. Both L-SIGN and DC-SIGN have been identified to interact with various viruses, such as EBOV, HBV, SARS-CoV, or Marburg virus (MARV)[36,40]. DAP-12-associating lectin (MDL-1, also known as CLEC5A), is a CLR found in MΦs known to recognize DENV, Influenza virus and Japanese encephalitis virus (JEV)[41–43].

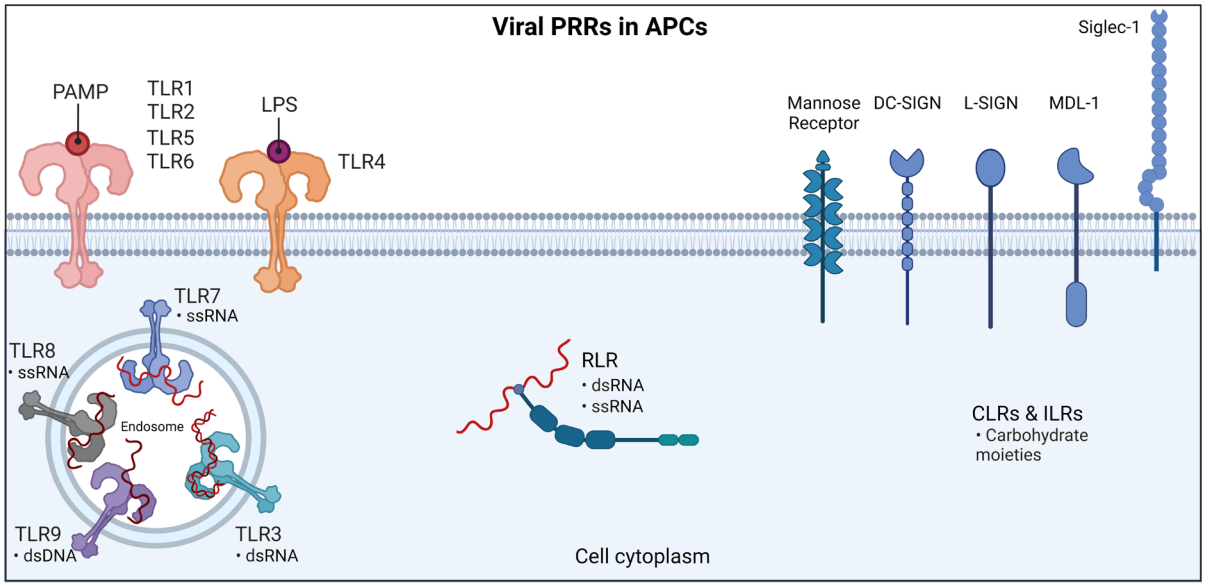

Figure 1.1. Relevant viral PRRs found in APCs. Dcs, MΦs, monocytes and B cells express a variety of PRR to recognize pathogens upon entry in the organism. TLRs present a up to 10 different molecules from which 9 of them recognize multiple viruses, including their proteins or genetic material. RLRs are cytosolic PRRs recognizing viral RNA. CLRs present in cell membrane recognize carbohydrate moieties in viral membranes. Image created using BioRender (https://biorender.com/). PRR: Pattern Recognition Receptors; APCs: Antigen-Presenting Cells; DCs:

Dendritics cells; MΦs: Macrophages; TLRs: Toll-Like Receptors; RLRs: RIG-I-Like Receptors; CLRs: C-type Lectin Receptors; ILRs: I-type Lectin Receptors.

The pro-inflammatory state promoted after the activation of APCs via the PRRs will be followed by some cells like DCs travelling to the lymph nodes in order to present the processed antigens to the T-cells via MHC-II (**Figure 1.2**). Interaction of DCs and T-cells via MHC-II activates naive T-cells, which will promote into T-helper cells that can activate memory B cells or memory cytotoxic T-cells, plus secreting IL-4 to activate B-cells. Activated B-cells will then evolve into plasma cells that will secrete specific antibodies against the virus or differentiate into memory B-cells for long-term immunity.

DCs use sensing receptors to start the immune response, however, this interaction not always helps controlling or fighting the infection. Several pathogens have evolved mechanisms to impair DC function, either interfering with their sensing capacity, maturation program or antigen-presenting function. Interactions between viral PAMPs and PRRs upon viral infection leads to APC stimulation and production of IFNs which function in an autocrine and paracrine fashion inducing an anti-viral state that is characterized by the expression of distinct interferon-stimulated genes (ISGs)[13]. Among the sensing receptors on APCs there is Siglec-1, also known as CD169 or Sialoadhesin, a ILR which might play a versatile role in viral uptake. Siglec-1 is an IFN-inducible receptor[44], and consequently, immune activating signals present throughout the course of viral infections increase the expression of Siglec-1 in myeloid cells[44–46]. Several viruses have been reported to take advantage of DCs function as a way to improve their pathogenicity by interacting with Siglec-1. This is the case of HIV-1 and filoviruses such as Ebola and Marburg. Studying the role of Siglec-1 expressed on DCs in viral infections might help better understanding its relevance in the antiviral immune response.

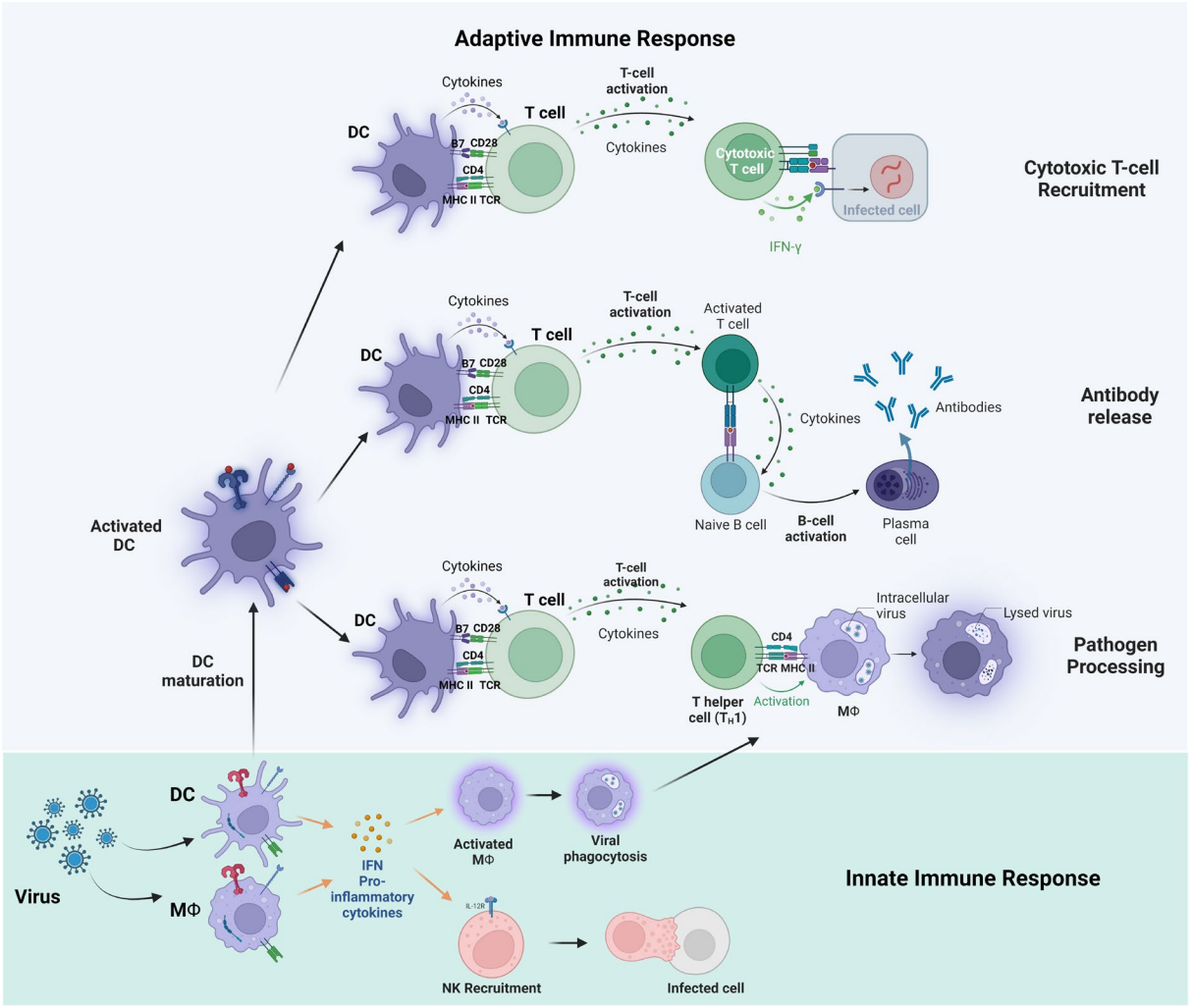

Figure 1.2. Immune response mediated by APCs during viral infections. After recognition of invading viruses via PRRs, MΦs and DCs will initiate the innate immune response by secreting pro-inflammatory cytokines and recruiting more immune cells to control the infection. Pathogen recognition through PRRs will also activate DCs, and after travelling to the lymph nodes they will interact with T cells and initiate the adaptive immune response, specific for the invading pathogen. Image created using BioRender (https://biorender.com/). DCs: Dendritics cells; MΦs: Macrophages; PRR: Pattern Recognition Receptors.

1.5. CD169/Siglec-1 and viral infections

Siglec-1, the first member of the Siglec family, was identified by Paul Crocker and colleagues in the early 90s[47,48]. It is the Siglec member with the longest extracellular part, which is composed of 16 immunoglobulin-like domains and a terminal V-set domain (**Figure 1.3**). The numerous Ig-like domains that separate the ligand-binding site from the membrane favour the interaction in *trans* with external ligands, limiting the binding to cell-surface molecules in *cis*, as it happens with shorter members of the Siglec family[49]. Its cytoplasmic domain lacks a tyrosine containing motif and therefore does not trigger an intracellular signalling cascade[49] (**Figure 1.3**).

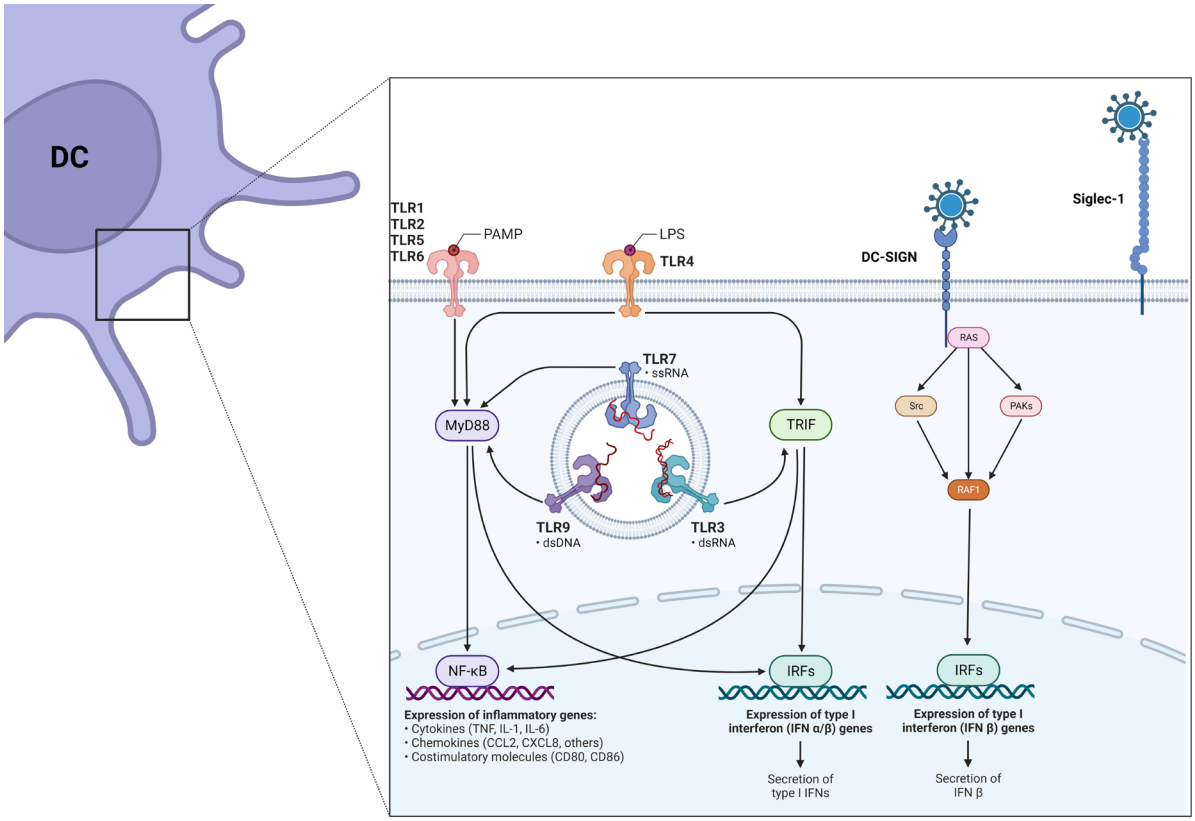

Figure 1.3 Siglec-1 is a ILR. Siglec-1 contains an extracellular V-set domain that holds the sialic acid binding pocket in its N-terminal region. This is followed by 16 C2 immunoglobulin domains that extend the distance from the V-set domain all the way to the extracellular surface, forming the link to the transmembrane domain. It lacks a tyrosine containing motif compared to other CLRs such as DC-SIGN and therefore it is currently thought that it does not activate any intracellular signalling after viral encounter. Image created using BioRender (https://biorender.com/). ILR: I-type Lectin Receptor; CLRs: C-type Lectin Receptor

Siglec-1 recognizes sialylated motives from lipids present in biological membranes[45]. Recent studies have shown that the clustering of these sialylated motives can favour receptor avidity and enhance its ligand interaction[50]. Siglec-1 can bind to multiple target cells in a sialic acid dependent manner, including granulocytes, NK cells, B-cells and erythrocytes[51]. It also exhibits a CD43-dependent binding affinity for T-cells[52], participating in cell-to-cell signalling to modulate cellular immune responses against viral infections[49]. The sialylated motives recognized by Siglec-1 are present not only in human cells, but also in extra-cellular vesicles (EV) secreted by cells containing these motives, bacteria, or enveloped viruses[50]. Immune cells such as DCs, MΦs and monocytes that can recognize pathogens such as bacteria or viruses are known to express Siglec-1 on their surface[45], and it has been shown that they can mediate viral uptake via Siglec-1 interaction with enveloped viruses[53].

Upon viral infection, activated immune cells release pro-inflammatory signals, including IFNs, which upregulate Siglec-1 expression in myeloid cells, as observed in SARS-CoV-2 infected individuals[44,46]. It has been reported that Siglec-1 expression was upregulated on APCs in

SARS-CoV-2 infected individuals[54]. In addition, Siglec-1 expressing monocytes were found to be more prominent in mild cases and the amount of Siglec-1 expression correlated with plasma IFN levels[54,55]. In RSV infections, Siglec-1 expressing alveolar MΦs triggers an early innate protection and recruitment of effector $CD8^+$ T cells to the lung after RSV infection[56]. Another example showed that the absence of Siglec-1 expressing macrophages impedes antigen uptake, leading to a decrease in the $CD8^+$ T-cell responses against VSV[57].

Despite the role of Siglec-1 mediating the immune response against viral infections[56,57], viral capture mediated by Siglec-1 in APCs does not always lead to an effective immune response. Enveloped viruses that constitute a major threat to human health, such as HIV-1 or Ebola virus, incorporate sialylated gangliosides on their membranes and by interacting with Siglec-1 (**Figure 1.4**), could evade the immune response and disseminate the infection within tissues [53,58].

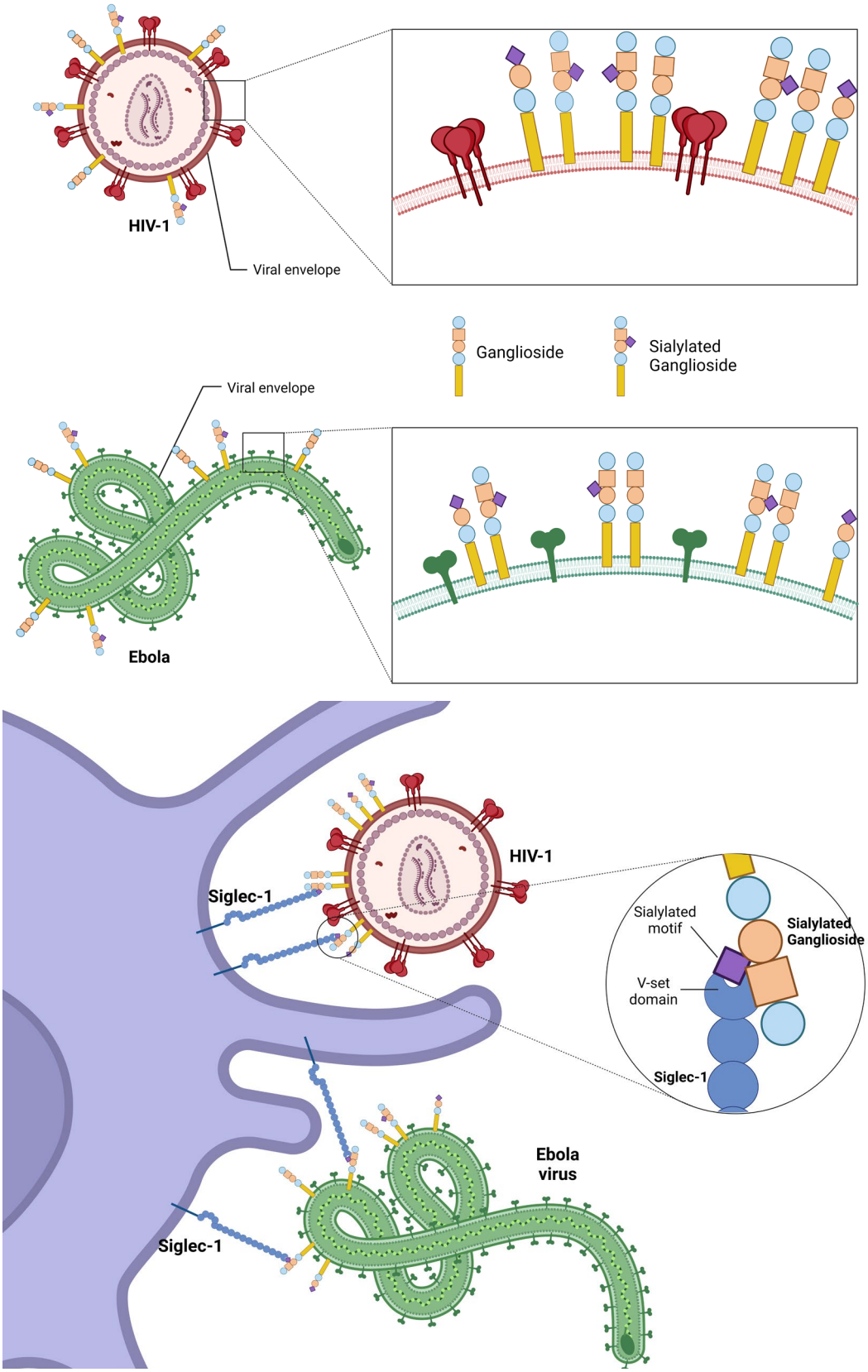

Figure 1.4. HIV-1 and EBOV uptake via Siglec-1. Enveloped viruses such HIV-1 and Ebola virus present sialylated gangliosides in their membrane that can be recognized by Siglec-1. HIV-1: Human Immunodeficiency Virus 1; EBOV: Ebola Virus

The first evidence of how Siglec-1 promotes viral infection of nearby target cells arose from the field of cell-to-cell transmission of HIV-1. This retrovirus is responsible for the AIDS pandemic and preferentially infects $CD4^+$ T lymphocytes expressing the CCR5 or CXCR4 co-receptors[59]. Although Siglec-1-expressing myeloid cells are also susceptible to HIV-1 infection[60,61], several restriction factors limit productive viral replication[62,63]. However, these cells can trap HIV-1 particles, which display specific gangliosides such as GM1 or GM3 in their envelope membranes[50,58], via Siglec-1[64,65]. These virions are then trafficked by Siglec-1 to a virus-containing compartment (VCC)[50] (**Figure 1.5**). In primary cervical tissues from HIV-1-infected individuals, cell-associated viral accumulations have been identified in Siglec-1-positive compartments, confirming the formation of VCCs *in vivo*[66]. Virions accumulated in VCC are effectively transferred to interacting $CD4^+$ T-cells through the formation of an infectious synapse[59]. This mechanism, known as *trans*-infection, was initially observed *in vitro* [67], but it took two additional decades to identify Siglec-1 as the key molecule mediating this process[58,68]. Moreover, this has been confirmed *in vivo*, using a murine model infected with another retrovirus, the MLV, whose robust infection in lymph nodes and spleen required Siglec-1 and *trans*-infection for viral spread[69].

Other enveloped viruses, such as the highly pathogenic EBOV, bind to Siglec-1, but in this particular case the interaction leads to the viral fusion in Siglec-1 expressing cells[53], which can support productive infection[70] (**Figure 1.5**). EBOV sporadic outbreaks are associated with high mortality rates, and viral transmission occurs through contact with body fluids from infected individuals[71]. This results in the infection of a broad cell repertoire including hepatocytes, fibroblasts and myeloid cells like DCs, macrophages and monocytes[70]. Given their patrolling function at the viral entry sites, DCs are among the first cells to encounter EBOV, becoming productively infected early during EBOV disease[70,72]. Following their migration to lymphoid tissues, DCs contribute to EBOV systemic dissemination[70] playing a similar role to that described for HIV-1 infection.

In addition to promoting EBOV dissemination, infected myeloid cells display a dysregulated phenotype that impairs their capacity to mount innate and adaptive immune responses[72,73]. EBOV entry into myeloid cells begins with viral attachment to the cell surface, which involves different viral and host factors[74]. C-type lectins such as DC-SIGN and LSECtin mediate EBOV binding through recognition of the EBOV glycoprotein[75,76], while the TIM/TAM receptors act as attachment factor through the recognition of phosphatidylserine on the viral membrane[77]. Although the overall role of TIM/TAM receptors on EBOV entry has been confirmed, in primary myeloid cells[77], the relative contribution of each family and their particular members on distinct

myeloid cells is not clearly delineated yet. After internalization, EBOV is directed to a late endosome, where cathepsins cleave the viral glycoprotein and via Nieman Pick Receptor 1 (NPC-1), releases viral RNA into the cytoplasm leading to a productive infection. Intriguingly, EBOV incorporate sialylated ganglioside GM1 when they bud from producing cells[78], and Siglec-1 acts as an attachment factor mediating viral entry into these cells through a glycoprotein-independent mechanism[53]. Of note, Siglec-1-inducing factors such as LPS and type I IFNs are present during the course of EBOV infection, especially in fatality cases of the disease[79,80]. This, together with the fact that Siglec-1 allows viral entry into key target cells for EBOV, suggests a role for this receptor in the progression EBOV infection. EBOV captured via Siglec-1 is also directed towards a VCC that is associated with viral *trans*-infection[53] as previously demonstrated for HIV-1[81,82] (**Figure 1.5**). Whether or not this VCC also favours EBOV *trans*-infection remains to be elucidated.

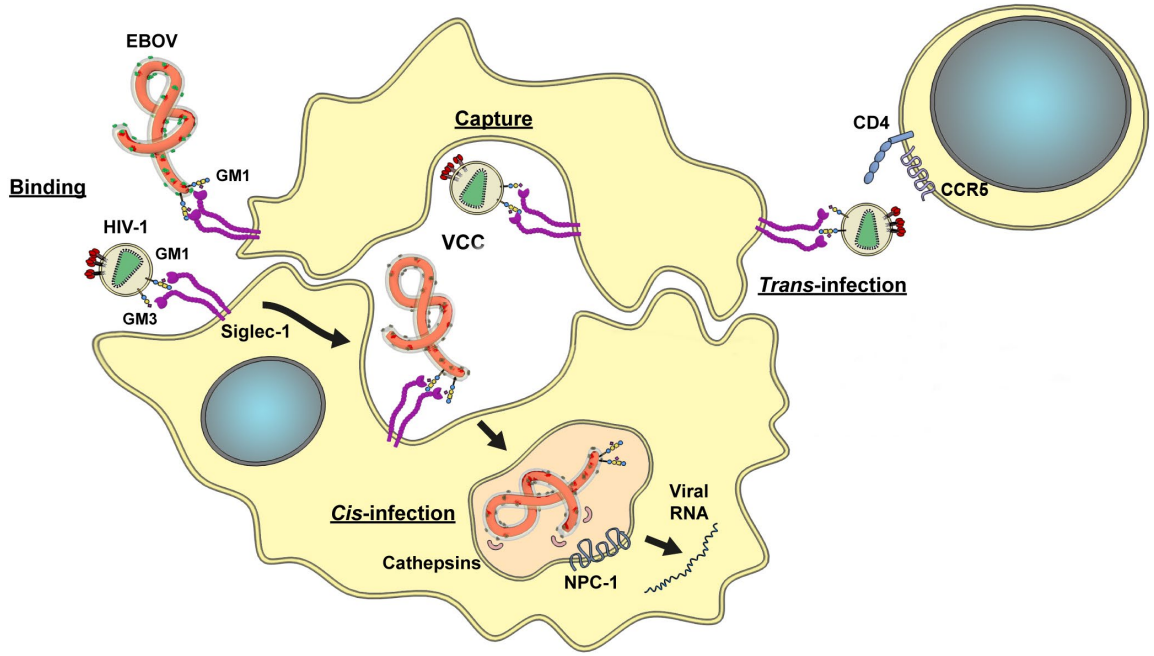

Figure 1.5. Siglec-1 *trans*- and *cis*-infection pathway. EBOV binds to nanoclusters of Siglec-1 molecules via GM1, whereas HIV-1 binds via both GM1 and GM3. Viral binding is followed by accumulation in a virus containing compartment (VCC) within dendritic cells. HIV-1 is subsequently transferred to target cells expressing CD4 and CCR5 (or CXCR4) receptors via trans-infection, whereas EBOV is directed to the late endosome, where cathepsins cleave the viral glycoprotein and via Nieman Pick Receptor 1 (NPC-1), releases viral RNA into the cytoplasm leading to the production of new EBOV via *cis*-infection in dendritic cells. Adapted from Ref [45]

Because Siglec-1 expressed in DCs interacts with sialic acids, which can be present in several enveloped viruses, we believe it harnesses the potential to interact with other enveloped viruses such as SARS-CoV-2 and pathogenic arenavirus family members Junín and Lassa virus.

1.6. Severe Acute Respiratory Syndrome Coronavirus 2 (SARS-CoV-2)

SARS-CoV-2 is an enveloped virus which is responsible for causing the Coronavirus-Disease-19 (COVID-19) global pandemic[83]. A vaccine was developed in a short period of time and plenty of antiviral treatments were rapidly tested, causing severe cases to drop significantly[84]. Despite the efficacy and progress of vaccines and treatments against SARS-CoV-2, future viral variants might overcome these strategies. SARS-CoV-2 variants reported so far have been classified according to mutations in the Spike protein (S) that produced changes in transmission and virulence[84]. Although the S protein is the canonical attachment receptor for SARS-CoV-2[83], other receptors and co-receptors might be involved in viral attachment and entry[83]. Studying the role of these molecules, such as Siglec-1, that might be involved in SARS-CoV-2 attachment and entry could help to improve current vaccines and treatments.

1.6.1. Classification and viral structure

SARS-Cov-2 virus belongs to the *Coronaviridae* family and along with other highly pathogenic coronaviruses, to the *Betacoronavirus* genus, group 2. SARS-CoV-2 virus is enveloped, positive-sense single-stranded RNA virus[85] and its genome has ~80% sequence similarity with SARS-CoV virus and ~50% with MERS-CoV virus[86,87]. It is comprised by 14 open reading frames (ORFs), which encode 16 non-structural proteins, 9 accessory proteins and 4 structural proteins, including: the spike (S), envelope (E), membrane (M) and nucleocapsid (N) [86,88,89] (**Figure 1.6**). The structural proteins, once assembled, form a virion that while budding from the host cell, will incorporate a lipid bilayer completing an enveloped virus[90]. The incorporated lipid bilayer will contain some molecules present in the host cell membrane along with the S protein, which is the one mediating the viral entry into host cells[88].

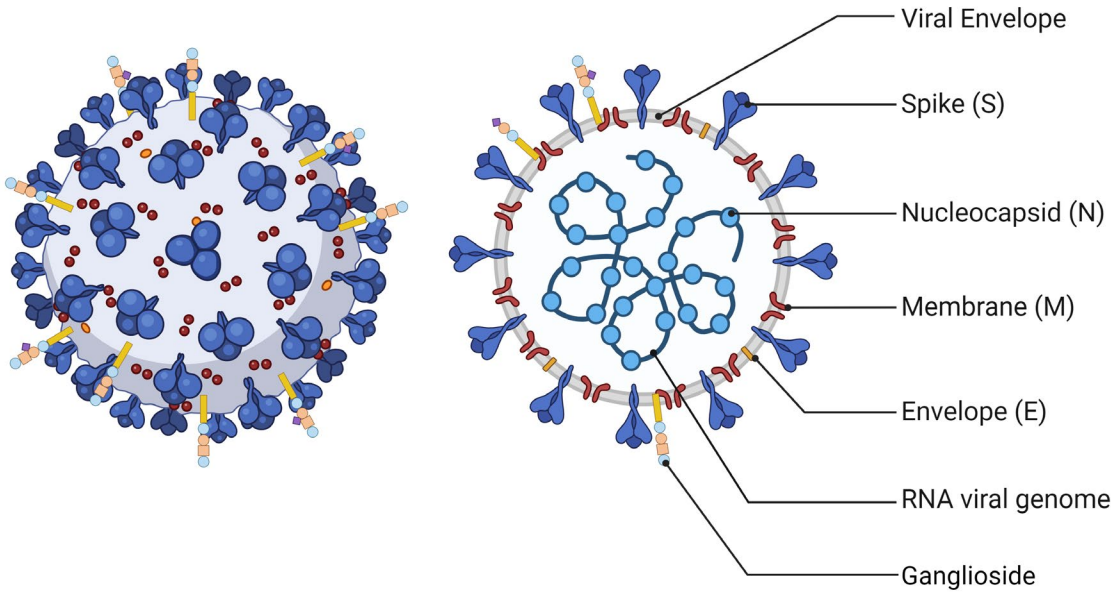

Figure 1.6. SARS-CoV-2 structure. The severe acute respiratory syndrome coronavirus 2 (SARS- CoV-2) virion consists of the following structural proteins: spike protein (S), nucleocapsid protein (N), membrane protein (M) and envelope protein (E). When budding, it incorporates the viral envelope containing gangliosides present in the cell membrane from the host cell. Image created using BioRender (https://biorender.com/).

1.6.2. Epidemiology

The first cases of SARS-CoV-2 reported in humans occurred in late 2019 under the name Coronavirus-Disease-19 (COVID-19)[91]. It started as a contained outbreak in Wuhan city, China[89], but a rapid worldwide spread in early 2020 showed its efficient human to human transmission, and in March 2020 the World Health Organization (WHO) declared COVID-19 as a new pandemic[91,92]. Contact tracing studies revealed high infectiousness at the time of symptom onset, with frequent transmission from pre-symptomatic and mildly symptomatic individuals and transmission also occurring from fully asymptomatic individuals [92–94]. Since no vaccine or treatment was available, non-pharmaceutical interventions, such as lockdowns, social distancing measures, and, eventually, the use of facemasks, were implemented to contain the viral spread[92,95]. Despite these measures, it rapidly expanded worldwide, with only a few countries managing to contain the initial spread. The capacity to slow down the virus spread depended on the capacity to isolate infectious individuals, which depended on early detection of infected individual through a rigorous surveillance and on the proportion of asymptomatic or mildly symptomatic infections and their transmission potential[92,96–98].

A quick development and approval of vaccines against SARS-CoV-2 was accelerated by epidemiological factors such as high incidence of COVID-19 and limited acquired immunity to the virus[92]. The emergence of new variants of concern challenged SARS-CoV-2 vaccine

efficacy, but studies have shown that vaccines still offer significant protection against severe outcomes such as hospitalization and death[92]. These new variants emerged as a result of a few mutations of the spike that allowed immune evasion, better transmission capacity and higher virulence[99,100].

1.6.3. Transmission and viral cycle

SARS-CoV-2 transmission occurs mainly through respiratory droplets and aerosols (**Figure 1.7A**). Although less relevant, direct contact with contaminated surfaces, and faecal–oral transmission was also reported [101–104]. This transmission method is supported by SARS-CoV-2 productively replicating mainly in the upper respiratory tract (URT) and lower respiratory tract (LTR)[91,105] (**Figure 1.7A**). In addition, opposite to SARS-CoV, SARS-CoV-2 was found to be transmitted by non-symptomatic/pre-symptomatic individuals[106–108].

After viral particles enter the host through the respiratory tract, SARS-CoV-2 first target are likely to be multiciliated cells in the nasopharynx or trachea, or sustentacular cells in the nasal olfactory mucosa[109–111] (**Figure 1.7B**). SARS-CoV-2 primarily infects the respiratory system and enters host cells through the interaction of the S protein with angiotensin-converting enzyme 2 (ACE2) receptor[112] (**Figure 1.7B**). The S protein is the main protein mediating the entry of SARS-CoV-2 into the host cell[113]. It has a receptor-binding domain (RBD) which interacts with ACE2, and an S1/S2 polybasic cleavage site that is proteolytically cleaved by cellular cathepsin L and distinct transmembrane serine proteases. Among these proteases, transmembrane serine protease 2 (TMPRSS2) has been established as the most relevant, although other proteases such as TMPRSS4, differentially expressed in squamous cell carcinoma gene 1 (DESC1) or human airway trypsin-like protease (HAT), might also be relevant in SARS-CoV-2 entry[114,115].

Once the genome is released into the cytosol, the virus hijacks the host cell's machinery to synthesize viral proteins and replicate its RNA genome[116]. Efficient replication will produce viral proteins that will assemble the virion which exits the host cells incorporating a lipid bilayer in the budding process. If virus is not cleared from the upper respiratory tract (URT), it can spread to the lower respiratory tract (LRT), although sometimes the initial infection site can directly be the LRT (**Figure 1.7B**). This can ultimately lead to the infection of the alveoli, causing inflammation and limiting gas exchange [90]. COVID-19 also causes epithelial damage, which attracts immune cells to the affected area. Single- cell sequencing of post-mortem COVID-19 lung tissue indicates increased infiltration of monocytes and macrophages in comparison with control lungs, and it was noted that monocyte-derived macrophages and alveolar

macrophages were aberrantly activated[117]. SARS-CoV-2 RNA, including the negative strand replicative intermediate, was also found within inflammatory monocytes and macrophages, suggesting that they may become infected, despite this infection is likely abortive[118,119].

Although there is evidence of SARS-CoV-2 interacting with immune cells, it is worth noting that most of these cells express low or no levels of SARS-CoV-2 receptor ACE2[116]. Studies have suggested that myeloid cell interaction with alternative receptors might have implications promoting immune hyperactivation[116]. SARS-CoV-2 pathogenesis is characterized by triggering an inflammatory response in the host, contributing to the symptoms and tissue damage associated with COVID-19. Understanding the viral cycle of SARS-CoV-2 and the immune response generated is crucial for developing better treatments and prevent severe disease outcomes.

1.6.4. Treatment and prevention

The COVID-19 pandemic caused by the SARS-CoV-2 prompted significant research efforts to develop effective treatments. Antiviral therapies targeting specific viral enzymes required for the virus to replicate have been tested or developed, including: remdesivir, a nucleotide analogue prodrug with broad-spectrum antiviral activity[120,121], molnupiravir that interacts with the RNA-dependent RNA polymerase[122], and nirmatrelvir that inhibits the viral protease[123]. Likewise, plasma from convalescent patients and a variety of specifically developed SARS-CoV-2 neutralizing mAbs, such as bamlanivimab+etesevimab, casirivimab+imdevimab, sotrovimab, or bebtelovimab have been clinically used during the pandemic[124–126]. However, most of the antibody-based therapies have lost their efficacy due to the viral evolution towards the dominant Omicron subvariants. In those cases of more severe infection which resulted in a cytokine storm, antivirals treatment needed to be complemented with anti-inflammatory therapies, mainly corticosteroids such as dexamethasone and hydrocortisone, tocilizumab (anti-IL-6-receptor), or baricitinib (JAK inhibitor)[127–129]. Often, heparin was also used as anticoagulant specially in hospitalized patients[130]. Of note, despite significant research efforts, there is currently no approved treatment that targets the host cell molecules involved in the pathogenesis of SARS-CoV-2 to halt or prevent infection.

Regardless of the efficacy demonstrated by the approved vaccines to protect against severe SARS-CoV-2 infection, they are not effective with immunocompromised individuals[131] and due to the possibility of new escape variants, ongoing clinical trials continue to evaluate the efficacy of existing and novel treatments that could be useful preventing SARS-CoV-2 infection or target key steps of viral pathogenesis. Studying the mechanisms that drive SARS-CoV-2

dissemination and the cellular components involved, might help in the development of new strategies to fight the infection.

2.5. Role of DCs in SARS-CoV-2 infection

DCs are one of the fist immune cells to encounter an invading pathogen and they are distributed all over the organism, patrolling for the detection of new pathogens. Some viruses, such as HIV-1 and Ebola virus, take advantage of DCs capability to travel through the organism to disseminate faster[53,68].

DCs can be found in the respiratory system and are known to respond to inflammation of the airways and lungs[132]. Upon SARS-CoV-2 entry, MΦs and DCs will initiate an antiviral immune response stablishing a pro-inflammatory state[116]. DCs will activate after recognition of the virus via PRRs. This activation triggers a maturation process consisting of cytokine release and upregulated expression of MHC complexes[133]. In addition, other studies have shown that maturation of DCs can enhance the capture and transmission of HIV-1[134]. After recognition, DCs internalize and process the antigens, promoting the innate and adaptive response[133] (**Figure 1.7C**). DC-SIGN, a C-type lectin which is a highly expressed PRR in DCs, has been proposed as one of the receptors able to recognize SARS-CoV-2[83,135]. It has also been reported that SARS-CoV-2 cannot infect DCs, since virus entry into DCs resulted in an abortive infection[119]. Despite being abortive, the study showed that DCs produced multiple antiviral and proinflammatory cytokines such as IFNα, IFNβ, TNF and IL-6 or IL-10[119] (**Figure 1.7C**). Interestingly, HIV-1 is also internalized by DCs, but does not infect them[136].

Earlier studies have highlighted the important role of MΦs and DCs, in mediating an antiviral inflammatory response, which is exacerbated in severe COVID-19 cases[137–140]. A study found that the RBD can trigger the maturation and activation of DCs[133]. This activation increased levels of MHC class I and class II molecules on the surface of DCs, as well as upregulation of CD40, CD80, and CD86 expression[133,141]. These results suggest that maturation and activation of DCs are due to recognition of the S proteins and RBD[133]. In the context of SARS-CoV-2 infection, it has also been reported that DCs in lungs were depleted, while pDCs, which are known for secreting pro-inflammatory cytokines, were increased[135]. The same study reported that despite DCs were able to promote the innate immune response, they failed to present SARS-CoV-2 via MHCII [135].

Taken together, this data suggests that despite not being able to be infected by SARS-CoV-2, the pro-inflammatory state generated by the infection, leads to DCs maturation, increasing viral

capture and providing feedback for the inflammatory state by pDCs, suggesting a role for DCs different from promoting the adaptive immune response.

Overall, our results show that DCs might play a key role in SARS CoV-2 infection, and while factors governing coronavirus entry into DCs are not fully understood, identifying and targeting them poses an interesting option to block early stages of coronavirus pathogenesis. Beyond the unexpected epidemic emergency generated by SARS-CoV-2, other pathogenic arenaviruses have also been reported to include DCs as important elements of their pathogenesis as well.

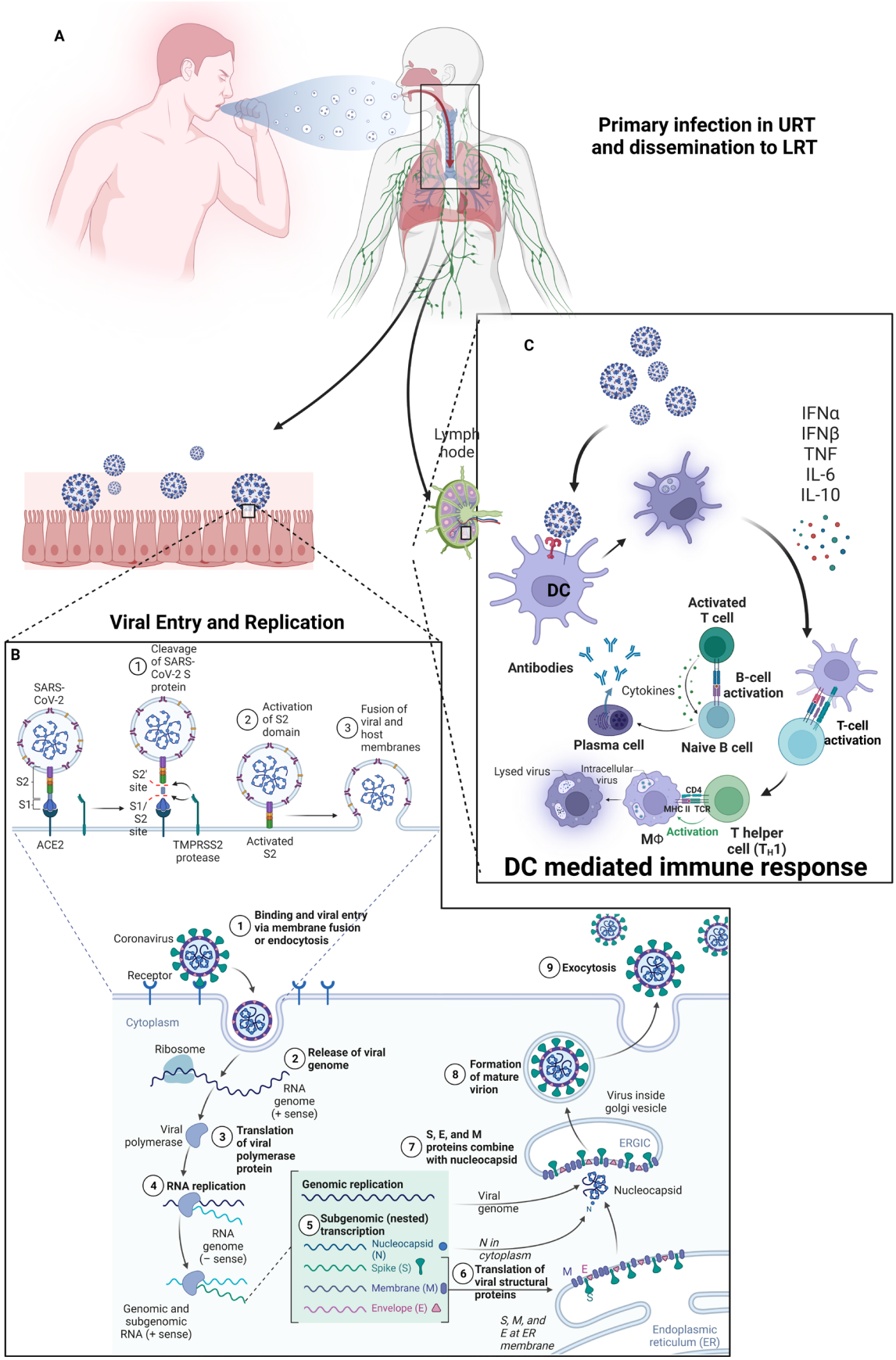

Figure 1.7. SARS-CoV-2 Transmission, viral cycle and DCs role. A. Viral particles from an infected individual enter the respiratory tract and stablish the infection in the URT and LRT. **B.** SARS-CoV-2 attachment to ACE2 on

target cell membrane and activation of the Spike by TMPRSS2 to mediate virus entry into the cell and start the replication cycle, multiplying in the host cell. From Ref[142,143] **C.** DCs SARS-CoV-2 recognition via PRRs and mediation of the immune response. Image created using BioRender (https://biorender.com/). IFN: Interferon; TNF; Tumour Necrosing Factor; IL: Interleukin; ACE 2: Angiotensin-Converting Enzyme 2; TMPRSS 2: transmembrane serine protease 2; URT: Upper Respiratory Tract; LRT; Lower Respiratory Tract.

1.7. Arenavirus

In this thesis we have focused on Junín (JUNV) and Lassa (LASV) arenaviruses, belonging to the New World and Old-World group respectively. JUNV and LASV arenaviruses are highly pathogenic viruses that cause severe haemorrhagic fevers in humans[144]. Infected individuals can experience mild symptoms, but some percentage develops a severe form of the disease that often requires hospitalization and can be fatal[145]. Despite the development of the Candid#1 vaccine for JUNV, there is no other vaccine approved for LASV or other arenaviruses, and there are still no efficient antivirals approved against any of them, leaving populations vulnerable to these deadly infections[146,147]. JUNV and LASV viruses still pose a significant challenge to public health due to their high pathogenicity and ability to evade host immune responses.

1.7.1. Classification and viral structure

Arenavirus family belongs to the order Bunyavirales[148] and are further classified into two main groups based on geographical distribution: Old World arenaviruses, primarily found in Africa and Europe, and New World arenaviruses, prevalent in the Americas[145]. Each group includes several species and strains of viruses, some of which are known to cause severe diseases in humans [146]. Recent discoveries have found that arenavirus do not only infect traditional mammal hosts, but also snakes and fish[146], which contributed to increase the number of genera within the *Arenaviridae* family from one, the original *Mammarenavirus*, to four, adding *Antennavirus*, *Hartmanivirus*, and *Reptarenavirus*[146]. The original and largest genus, *Mammarenavirus*, has also added new viruses isolated from rodents captured in different areas of the Americas, Africa, and Asia[149,150]. This high genetic plasticity could facilitate zoonotic spread and adaptation to new hosts, this finding has significant implications for understanding the epidemiology of these viruses[146].

Arenaviruses have been classified as enveloped, negative, single-stranded RNA virus[150,151]. Their genome consists of two or three single-stranded, usually ambisense RNA segments, named small (S), medium (M) and large (L). The small RNA encodes the nucleoprotein (NP), and in many cases, as it is in the case of Junín and Lassa viruses, the glycoprotein precursor (GPC). The L RNA segment encodes de L protein, and, in some cases, as it is in the case of

Junín and Lassa viruses, the zinc-finger matrix protein (Z). When viral proteins assemble, spherical or pleomorphic shape, 40-200nm in diameter virions are formed. Virion budding occurs from the cellular plasma membrane, thereby providing the virion envelope[150] (**Figure 1.8**).

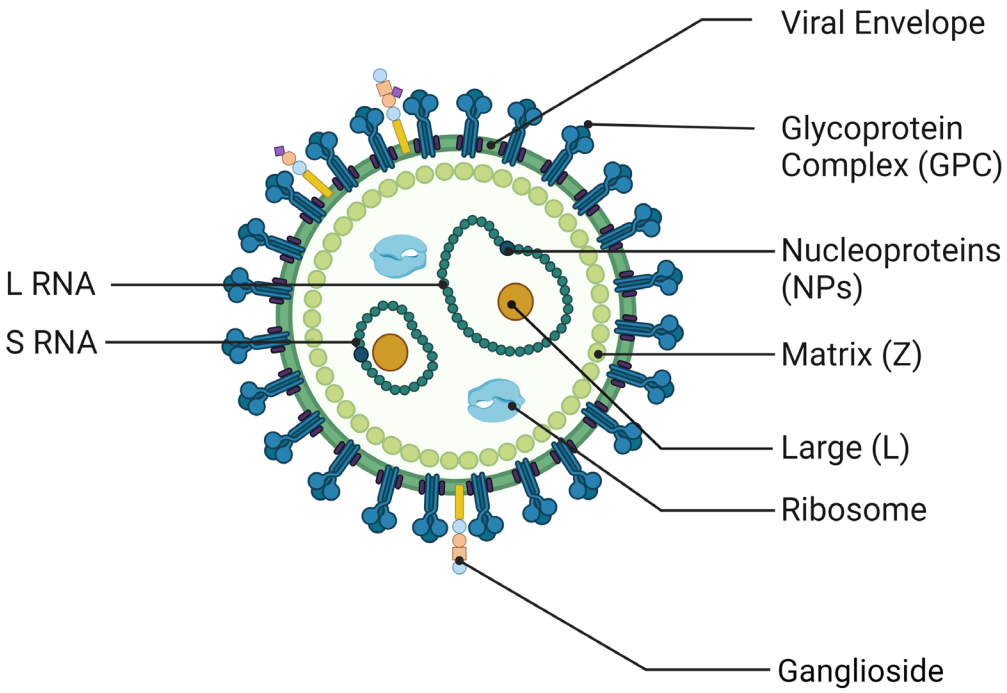

Figure 1.8. Arenavirus structure. The arenavirus virion consists of the following structural proteins: Glycoprotein Complex (GPC), Nucleoproteins (NPs), and Matrix protein (Z). It also incorporates ribosomes, and the Small (S) and Large (L) RNA segments. When budding, it incorporates the viral envelope that could contain gangliosides present in the cell membrane from the host cell which can interact with Siglec-1. Image created using BioRender (https://biorender.com/). RNA; Ribonucleic Acid.

1.7.2. Epidemiology

Argentine Haemorrhagic Fever (AHF), caused by JUNV, was first reported in the mid-1950s and is an endemic disease from Argentina. AHF disease mainly affects rural workers from the agricultural central east Argentina, with annual outbreaks from the end of summer until midwinter, concurrent with the harvest of maize and with the increase in the population of wild rodents[152]. From its first description, annual outbreaks were reported to the point that almost five million individuals were considered to be at risk[153]. After the live attenuated vaccine Candid#1 was approved for endemic use, the incidence of AHF has been greatly reduced[153].

Contrary to AHF, Lassa fever caused by LASV remains a significant public health concern in certain regions of West Africa, particularly in Nigeria, Sierra Leone, Guinea, and Liberia[154–156]. Outbreaks of Lassa fever occur annually, and studies have estimated that as many as 500,000 cases and 5,000 deaths occur yearly in West Africa due to LASV infections[157]. The mortality rate associated with Lassa fever can be as high as 30%[145,156], making it a serious threat to human health. Despite efforts to control the disease, including improved surveillance and healthcare practices, Lassa outbreaks continue to occur[158,159]. In recent years, there have been reports of Lassa fever cases in Europe, highlighting the potential for the virus to spread beyond its endemic regions[157,160]. As Lassa fever outbreaks continue to threaten West Africa, efforts are being made to strengthen surveillance systems, enhance diagnostic capabilities, and improve prevention strategies[156].

Understanding the epidemiology of JUNV and LASV is crucial in elucidating how this virus spreads in populations. Understanding this aspect is essential for comprehending the transmission dynamics and viral life cycle, which together explain how the virus propagates and interacts within its host organisms.

1.7.3. Transmission and viral cycle

The first steps of the viral cycle for Junín and Lassa viruses are very similar, and despite their viral cycles' progression differs, they both cause infection and spread within the human body leading to haemorrhagic fever. The main mode of transmission for arenaviruses is through persistently infected rodent species that serve as primary host for both Junín and Lassa viruses[147,161,162]. The viruses are carried by the *Calomys musculinus* mouse, the main host for JUNV[147], and the *Mastomys natalensis* rat in the case of LASV[163]. Humans usually become infected after close contact with infected rodents (cuts or bites), via inhalation of infectious rodent urine or faeces, or by contaminated harvested grain[147,163–166] (**Figure 1.9A**). People who encounter contaminated grain or inhale aerosolized particles are at risk of infection. In the case of LASV, it has also been documented transmission through ingestion of contaminated food and via person-to-person contact with bodily fluids, such as blood or urine of infected individuals [146,163,167–169]. This often occurs in healthcare settings or during close contact with an infected person[167–169].

Although arenaviruses can enter the organism through different ways, the most common transmission route is inhalation[166,170]. Primary targets in the entry site are URT and LRT resident MΦs and DCs (**Figure 1.9B**). After early viral replication infected cells will, via the

bloodstream, reach the lymph nodes, spleen, and liver, where productive infection will be stablished. Because DCs are APCs, arenaviruses can take advantage of DCs travelling to the lymph nodes to initiate the immune response, infecting more cells and allowing the virus to spread throughout the organism[151,171,172].

JUNV can enter the body via the skin, respiratory tract, or gastrointestinal mucosa[172]. It has been proposed that APCs, more specifically, MΦs and DCs, are early targets for JUNV infections [173,174]. Upon entry, Junín interacts with Transferrin Receptor 1 (hTfR1), which is the main cellular receptor for this virus present in the cellular surface[166,175–178]. Additionally, alternative non-canonical receptors have been also described for JUNV, as is the case of lectin receptors such as DC-SIGN or L-SIGN. JUNV GPC is glycosylated in such a way as to allow its interaction with DC-SIGN and L-SIGN, acting as a non-canonical primary receptor enhancing JUNV infection independently of the canonical hTfR1[179]. The exact mechanism by which DC-SIGN and L-SIGN interact with JUNV GPC has not been described yet, but it has been demonstrated that this interaction not only acts as an attachment and entry receptor, but it also increases the virus yield in infected cells expressing these lectins[179].

Interaction with hTfR1 triggers viral entry. In the case of JUNV, it has been described as a clathrin-mediated endocytosis[166,180] (**Figure 1.9B**). Electron microscopy revealed that JUNV particles localize in plasma membrane invaginations and clathrin-coated pits, and inhibiting clathrin-mediated endocytosis reduced virus internalization without affecting binding[180]. Additionally, studies confirmed the involvement of dynamin II and epidermal growth factor receptor substrate 15 (EPS15), which are associated with the clathrin-coated endocytic pathway, in JUNV entry into host cells[181,182]. JUNV then travels along the endocytic pathway, changing the acidity of the internalized endosome containing JUNV[166]. Previous studies have indicated that acidification of the endosomes is necessary for virus internalization[166] (**Figure 1.9B**). Specifically, cell-cell fusion experiments have shown that an acidic pH of around 5 is optimal for facilitating fusion between the JUNV envelope and the cellular membrane[183]. The viral fusion is mediated by viral protein GP2, which experiences conformational changes in low pH environments, resulting in the exposure of a specific motif that facilitates viral fusion[184–187]. Genome replication and transcription occur in the cytoplasm of the host cell and requires viral proteins to combine with the viral RNA to form ribonucleoprotein (RNP) complexes[172]. After viral proteins have been translated, GP precursor will be processed in the endoplasmic reticulum (ER) and travel as GP1-GP2 protein complex to the be inserted in the cell membrane[172]. The Z protein directs the budding process by interacting with the newly formed nucleocapsid and shaping the membrane where the GP protein complex has been inserted[172]

(**Figure 1.9B**). Z protein has been described to play a major role in viral budding, but additionally, it may also have a regulatory function in cell response[172]. It has been demonstrated that Z protein from JUNV, but not from LASV, binds to RIG-I, resulting in the downregulation of IFNβ response[188].

Curiously, LASV does share an identical replication mechanism, but it follows a different entry pathway. LASV uses α-Dystroglycan (αDG) as primary receptor[189–193] (**Figure 1.9B**). αDG is ubiquitously expressed in multiple cell types, helping link cells to the extracellular matrix[174]. Among these cells, endothelial cells, and APCs, in particular DCs, are the primary target for LASV [194–196]. Interestingly, and similar to what has been described for JUNV, animal studies and human clinical data have shown high viral titters in the liver despite the fact that hepatocytes do not express αDG[174,197]. This suggests that other cellular factors are involved in LASV cell entry. Studies have demonstrated that molecules such as AXL, Tyro3, DC-SIGN and LSECtin play a role in this mechanism[174,198]. Supporting this, studies performed in non-human primates and post-mortem histology analysis did not find correlation between LASV load in organs and tissue distribution of functional αDG[146]. Despite these findings, αDG remains as the main receptor for LASV, and the interaction with viral GP1 initiates the entry mechanism into the cell[199]. Upon binding, a clathrin-independent mechanism internalises the virus into a multivesicular body containing LAV particles[199]. Then, the multivesicular body becomes a late endosome as the pH becomes acidic, triggering a conformational transition of the LASV GP (**Figure 1.9B**). In contrast with JUNV, LASV fusion following endocytosis requires a receptor switch to the lysosome-associated membrane protein 1 (LAMP1)[200,201] that allows the release of viral genome into the cytoplasm[146,199], which is facilitated by this conformational change. After the viral genome is released, replication of LASV follows a similar mechanism as JUNV[174] and in a similar way, LASV Z protein drives viral budding, but has also been demonstrated to inhibit RIG-I, resulting in IFN-I suppression[146].

Overall, and despite the differences in pathogenicity, both JUNV and LASV infect and replicate within APCs, particularly DCs, and interfere with the immune response triggered. The infection of DCs by arenaviruses can have significant implications for viral spread, immune evasion, and immune response to infection. Understanding the viral cycle of JUNV and LASV is crucial for developing better treatments and prevent severe disease outcomes.

1.7.4. Treatment and prevention

There are currently no specific antiviral drugs or biologicals available for the treatment of arenavirus infections[153,202]. Supportive care is the mainstay of management for patients with severe arenavirus diseases. However, there are ongoing efforts to develop vaccines and antiviral therapies to combat these infections[202].

Candid#1 vaccine has been a significant advancement in the control of JUNV, and similar efforts are underway to develop vaccines for Lassa fever[203–209]. JUNV has been effectively controlled in recent years thanks to the use of the Candid#1, a live attenuated vaccine that has been successful in reducing the incidence of Junín fever and preventing outbreaks in areas where the virus is endemic[177,210]. In the case of LASV there are no vaccines approved at this moment[211]. Nevertheless, there are four different vaccines in clinical trials. Three in phase I trials, and the another in phase II trial. One of them is a DNA-based vaccine, while the other three are recombinant viral vector vaccines[211]. The four vaccines aim to build immunity in a similar way as Candid#1, by exposing the immune system to some form of LASV GP or GPC[211].

Additionally, antiviral drugs targeting specific steps of the viral replication cycle are being explored as potential treatment options for arenavirus infections[157,163,212,213]. A small antiviral molecule initially developed for LASV has proven *in-vitro* efficacy on multiple strains of LASV and JUNV as well, by inhibiting GP mediated entry. In addition, a daily oral dose of this treatment protected mice from lethal doses of Tacaribe virus (TACV), another pathogenic arenavirus[212]. At his moment it has proved to be safe in humans after completing phase Ia clinical trials[157]. Another small antiviral molecule targeting GP2 has proven to be effective inhibiting arenavirus fusion, including LASV and JUNV. Furthermore, mice infected with TACV and treated with the antiviral were able to survive and clear the infection[213]. Finally, despite ribavirin has proven ineffective in the late stages of the infection, two LASV patients survived after a combination treatment with ribavirin and favipiravir, a small purine analogue[214].

Despite the efficacy demonstrated by the approved vaccine to protect against JUNV, and antiviral treatments against LASV infection, there is still a risk that JUNV escape variants appear, and a need for protective therapies against LASV. Studying the viral pathogenesis and the cellular components driving the immune response against arenaviruses, might help in the development of new strategies to fight the infection by targeting host cell molecules playing a key role in the viral cycle.

1.7.5. Role of DCs in arenavirus infection

DCs play a crucial role in the immune response against arenavirus[195,199,215] and are among their primary targets in early infection[173]. DCs have been described to facilitate tissue and systemic viral propagation of various viruses, such as HIV-1 or Ebola virus[53,58]. As it happens for Ebola virus[53], JUNV and LASV DCs infect DCs in a productive way[173]. Curiously, it has been reported that Ebola virus and LASV share the same cellular tropism, infecting MΦs, DCs, endothelial cells and the liver[215]. It has been proposed that because αDG is highly expressed in MΦs and DCs, this may explain why these cells are early targets of LASV infection[216]. In the case of JUNV, which uses hTfR1 for cell entry, similar to αDG, is expressed on a wide variety of cell types and would therefore allow pantropic infection[215].

When infected by LASV, DCs are the main targets and have been found to produce significantly more virus compared to MΦs, which are also primary targets for LASV[162]. Despite being primary targets and getting productively infected by LASV, MΦs and DCs fail to become activated upon infection[194] and no increased levels of activating markers or cytokines has been reported[215]. The activation of DCs is critical for developing an effective T-cell response, virus clearance and patient recovery[215]. Experiments in macaques showed that those who survived the infection had activated T-cells, while those who perished displayed low and delayed T-cell activation[215,217]. Curiously, reports from hospitalized patients showed that high levels of IgG or IgM were not associated with the outcome of the disease, however, high viral titres were associated with poor outcome, indicating that the antibody response is not effective controlling viral replication[218].

Opposite to LASV infection, JUNV-infected patients display elevated levels of cytokines such as TNF-α, IFN-α, IL-6 and IL-10[215,219–221] (**Figure 1.9C**). Although JUNV infected patients showed high cytokine levels, *in vitro* experiments showed no increase in cytokine production[222]. In addition, another difference between LASV and JUNV, is that for JUNV infection, antibody response appears to be effective. When plasma from patients previously exposed to JUNV was administered to other JUV infected patients early in the course of infection, the mortality rate was reduced from 16% to 1%[223]. In the case of LASV, neutralizing antibodies from survivors have been tested, but due to genetic diversity of LASV, they only worked on the same lineages that infected the survivor[157].

Despite their differences, JUNV and LASV share a common motif in the NP. Curiously, this motif provides the ability to inhibit type I IFN in LASV infection, but it has no effect in JUNV. This motif has been described to inhibit the translocation of IFN regulatory factor 3 in infected cells[144] and it has been suggested that is able to degrade viral PAMP RANs, thereby preventing pathogen recognition by innate PRRs, leading to the suppression of IFN production[224,225].

Furthermore, Z protein from JUNV has been described to bind RIG-I, resulting in IFN-β response downregulation[188]. On the contrary, LASV Z protein does not bind to RIG-I but inhibits mitochondrial antiviral signalling protein (MAVS) to RIG- I, thus preventing the downstream signalling that would result in production of type I IFN[188].

Given the role of DCs building the antiviral immune response and the mechanisms by which arenavirus interfere with it, there is a need to neutralize these routes. As previously shown *in vitro* for HIV-1 and Ebola viruses, α-Siglec-1 mAbs can effectively decrease viral uptake by DCs[53,68], thus preventing the virus to take advantage of DCs. In the next section we present the evidence that supports the use of these antibodies mAbs as potential antivirals.

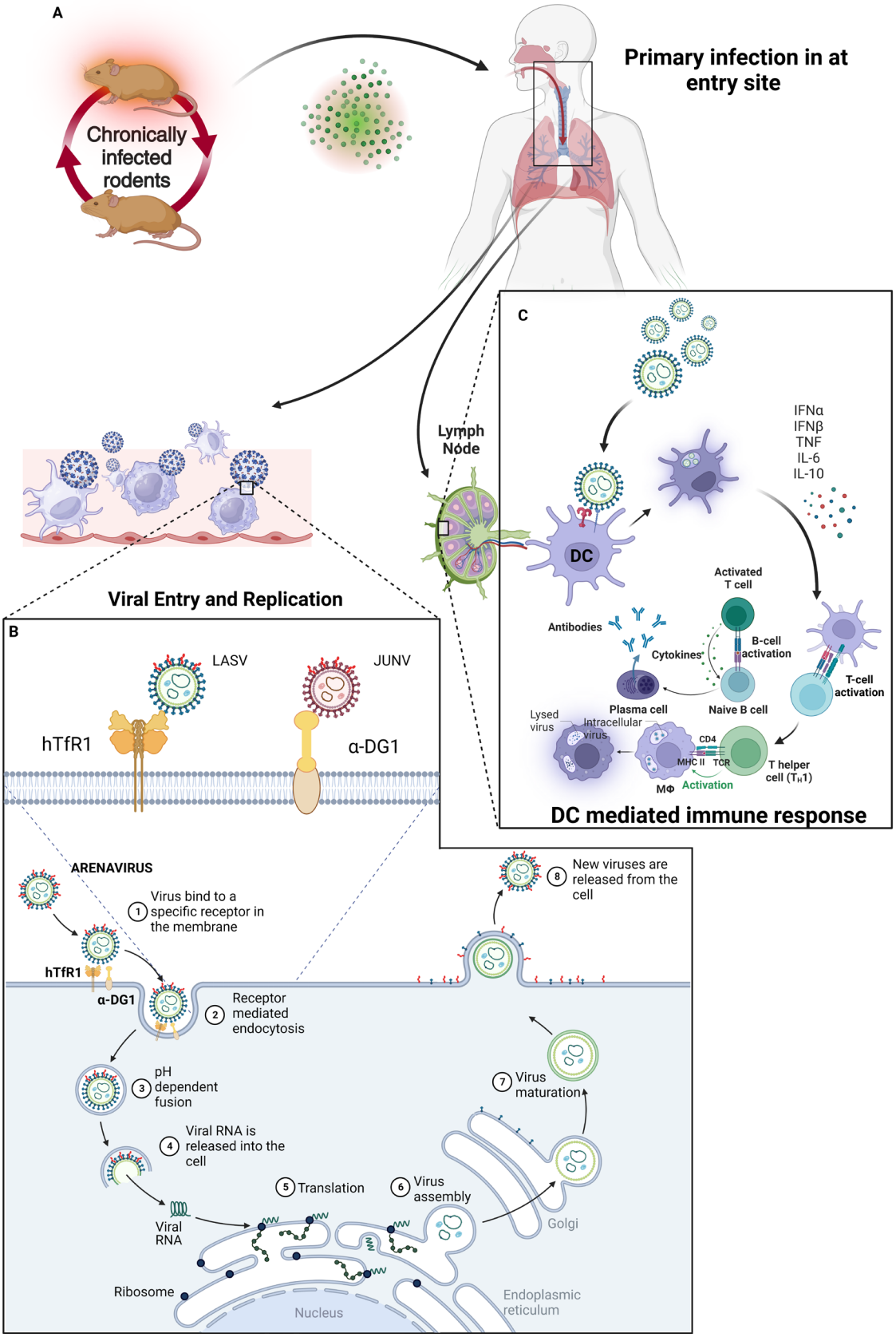

Figure 1.9. Arenavirus **transmission, viral cycle and DCs role. A.** Viral particles from a chronically infected rodents enter the respiratory tract and stablish the infection at the entry site. **B.** Arenavirus enters its primary target via canonical receptors αDG and hTrF1. After being internalized in and endosome, as the pH changes, the viral

RNA is released, and replication cycle begins in the host cell. The assembled virion will bud from the cell incorporating the viral envelope from the host cell membrane. **C.** DCs arenavirus recognition via PRRs and mediation of the immune response. LASV is able to inhibit IFN release, while JUNV increases this response. Image created using BioRender (https://biorender.com/). IFN: Interferon; TNF; Tumour Necrosing Factor; IL: Interleukin; hTRF1: Human Trans-Ferrin Receptor 1; α-DG1: Alpha Dystroglycan 1.

1.8. Antibody-based therapies.

The number of approved antibody therapeutics is rapidly growing every year[124]. As for June 2022, 162 antibody therapies have been approved by at least one regulatory agency in the world, including 115 canonical antibodies, 14 antibody-drug conjugates, 7 bispecific antibodies, 8 antibody fragments, 3 radiolabelled antibodies, 1 antibody-conjugate immunotoxin, 2 immunoconjugates and 12 Fc-Fusion proteins[226]. The medical indications with more approved antibody-based treatments are cancer and immune-related diseases[226]. However, antibody therapies are also employed for a wide range of human maladies related to the fields of haematology, neurology, ophthalmology, metabolic disease, musculoskeletal diseases, transplantation, and infectious diseases[124].

1.8.1. Antibody-based therapies as antiviral treatment

As part of the immune response to pathogens, antibodies are synthesized and possess a crucial role for effectively control and eliminate pathogenic viruses. Antibody therapy covers multiple ways to combat diseases based on the unique and diverse functions of antibodies. On one hand, antibodies can target host factors essential for the pathogen's cycle (**Figure 1.10A**). On the other hand, antibodies can bind to the virus or viral antigen, neutralizing it by impeding cellular infection (**Figure 1.10B**), or activate immune-effector functions, stimulating the patient's host defence mechanisms in a similar way to the antibodies created by the immune system (**Figure 1.10D**). This activation includes pathways like the antibody-dependent cytotoxic pathway and complement-mediated cytotoxicity. antibodies can also be designed to. When directed towards these factors, antibodies can block crucial interactions that facilitate the pathogen's replication cycle, reducing its ability to cause infection[192,193] (**Figure 1.10C**). It is worth noting, that antibody-based therapies, despite taking advantage of the diverse antibody functions, not always use antibodies as the treatment. There are occasions in which antibodies are modified to retain their functions while gaining other properties, such as with antigen-binding fragments (Fabs). It is also possible that instead of a single antibody, a combination of them is used to effectively treat a disease. These are usually obtained from plasma serum, but they are also called antibody cocktails when the antibodies are specifically selected.

Multiple antibody-based antiviral therapies have been approved over the last years due to the advantages offered. Different examples of these therapies can be found in **Table1**.

Therapeutic Area	Name	Target	Format	First global approval
Influenza	C05 [227,228]	Influenza HA receptor binding site	Fab	Pre-clinical
Influenza	Zanamivir (Relenza) [227,228]	Influenza HA	Human	1999 FDA
HIV-1	Ibalizumab [229] (Trogarzo)	CD4	Humanized	US, 2018
SARS-CoV-2	Regdanvimab (Regkirona)	Spike protein	Human	Republic of Korea, 2021
Infectious diseases	Sotrovimab[126] (Xevudy)	Spike protein	Humanized	Australia, 2021
RSV	Palivizumab[230]	RSV G	Recombinant	EU, 1999
Infectious disease	RabiShield[231]	Rabies virus G glycoprotein	Recombinant	India, 2016
Infectious disease	Ormutivimab	Rabies virus surface glyco-protein 4	Human	China, 2022
EBOV	ZMapp [231–233]	EBOV surface proteins	Antibody cocktail	phase II/III

Table 1. Different antiviral therapies based in antibodies against viral and host factors. Among the antibody-based antiviral treatments approved or in ongoing clinical trials, the majority is focused on targeting a viral component.

1.8.2. Antibody-based therapies: advantages and limitations

Among the advantages, antibody-based therapies can be found to be specific for a virus. The same way the immune system generates specific antibodies for each pathogen, these therapies can benefit from the high specificity of antibodies. This feature allows antibody-based therapies to target specific molecules to specifically block the viral cycle at a certain point. For example, targeting the SARS-CoV-2 S protein to block its attachment to target cells (**Table 1**). This high specificity is a double-edged feature, since there is a risk of immune evasion associated with epitope mutation, which is relatively common in antibody-based antiviral therapies or vaccine generated immunity and could reduce its efficacy. A solution to this problem could require a mixture of antibodies corresponding to evolving viral variants or to isolates from different viral outbreaks [231]. The source of the antibody might become another limittion. The first antibody-based therapies were obtained from animal origin, which can be recognized by the human immune system and trigger an immune reaction. This reaction is

called immunogenicity, which is triggered when the human immune system recognizes foreign proteins, animal or even from endogenous human origin, and generates a humoral and/or cellular immune response. Over 90% of the therapeutic proteins cause immunogenicity, with the production of anti-drug antibodies as a result[124]. The risk of immunogenicity is the main reason why antibody-based therapies cannot be used directly to treat humans. In order to avoid risks, antibodies used to treat humans need to be modified to reach the clinic.

The modifications performed to reduce the risk of immunogenicity usually modify the protein structure that conforms the antibody. A mammalian IgG antibody structure is composed of two copies of each of two protein chains: the light chain (~24 kDa) and the heavy chain (~55 kDa). Altogether they fold forming an immunoglobulin protein [227]. They bind together and align to form three structural domains, two Fabs and one constant fragment (Fc), that are linked by a flexible “hinge” region. This hinge can be cleaved to obtain Fab and Fc fragments by proteases[227]. The Fc fragment is a dimer composed by the constant domains that mediate effector function by binding to immunological receptor molecules such as complement proteins and Fc receptors[234]. Fab fragments, in contrast, are a combination of variable light and constant light chains paired with variable heavy and constant heavy segments, forming a mixed light-heavy chain dimer. The Fab fragment recognizes the antigen by using various or all the six complementarity-determining region (CDR) loops (three from each light and heavy chain), which extend out from the structurally conserved framework region[227]. CDRs are responsible for mediating their ability to recognize targets with high specificity[234] and therefore maintaining this part of the antibody is crucial in order to achieve an effective treatment.

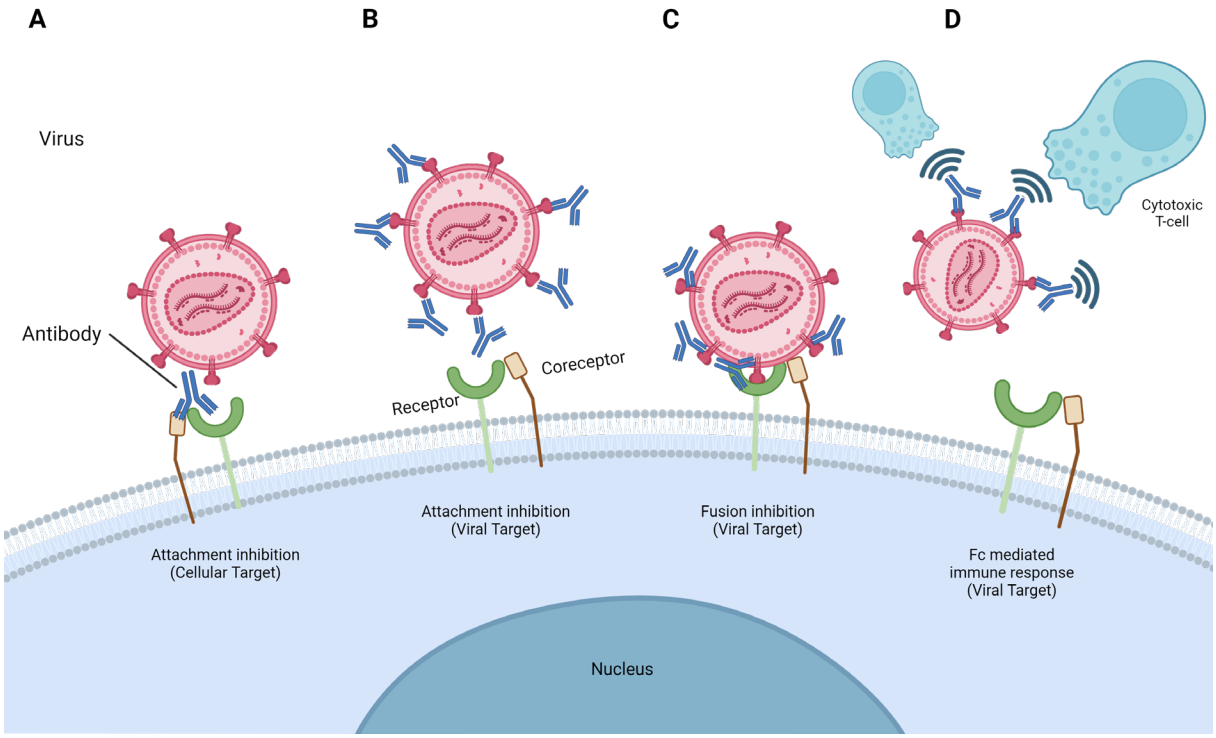

Figure 1.10. Therapeutic mechanisms of monoclonal antibodies to combat viral infections. A. Antibodies targeting host factors, such as the viral receptor, can block cellular infection. **B**. Antibodies directed towards the virus can also block binding to the receptor impeding viral entrance into the target cell. **C.** Antibodies directed towards other viral targets can block crucial interactions that facilitate the pathogen's replication cycle, such as viral fusion despite receptor binding, reducing its ability to cause infection. **D.** Antibodies directed toward the virus can activate immune-effector functions, stimulating the patient's host defence mechanisms. Image created using BioRender (https://biorender.com/).

1.8.3. Antibody modifications to reach the clinic.

Antibodies may face issues related to stability, immunogenicity, or pharmacokinetics that could impede their clinical use. As a result, various modifications have been employed to optimize their performance, enhance therapeutic outcomes, and allow a successful translation from the laboratory to the clinic.

When designing an immune therapy aimed to be used in the clinic, an antibody can be engineered to enhance the efficacy or to avoid other immune reactions that could be developed. Of the approved antibody-based therapies, 39% are fully human, meaning that they only feature human genetic sequences, 51% are humanized, 8% are chimeric and 2% are Fabs[231].Among the possible antibody modifications to reach the clinic, we have explored the use of Fabs and mAb humanization through CDR engraftment.

1.8.4. Fab immunotherapy

Fabs have become a widely used format of immunotherapy in which the variable heavy and light domains, linked by a flexible polypeptide, retain the specific, monovalent, antigen-binding affinity from the parent IgG, while having the Fc region removed. New techniques have allowed Fabs to be generated in bacterial or transiently transfected mammalian cell cultures[235–238], nevertheless, they are usually generated by enzymatic digestion of a complete IgG, using a protease such as papain to remove the Fc region, leaving the Fab as final product[229,239,240] (**Figure 1.11**).

Despite lacking the effector function provided by the Fc region[241,242], Fabs have demonstrated some advantages over mAb treatments. It is precisely the lack of Fc region what reduces Fabs' potential immunogenicity compared to a whole IgG[243]. In addition, Fabs can be easier and less costly to produce than full IgG antibodies due to their relatively small size, the lack of glycosylation and the capability to produce them in bacterial cultures[235,236]. Their smaller size has showed improved pharmacokinetics for tissue penetration and access to less accessible epitotes[239,241]. Fabs neutralize influenza virus through multiple mechanisms, including binding to conserved receptor binding sites on the hemagglutinin surface glycoprotein and inhibiting the conformational rearrangement required for viral fusion. In addition, Fabs can bind target epitopes without cross-linking, and have shown reduced steric effects compared to full-length bivalent antibodies[239].

However, Fabs' shorter half-life is not always an advantage. The Fc region that Fabs lack serves to both stabilize and allow FcR-recycling[235], and therefore, Fabs suffer rapid degradation in the human body, resulting in short half-lives in circulation[235,244]. Several strategies have been developed to counter these problems, such as protein or fatty acid conjugation, PASylation or PEGylation[235,245,246]. Nonetheless, by applying these modifications to Fab production may result in losing manufacturing advantages over full-length antibodies[235]. This instability can also result in increased risk of aggregation during Fab production or purification, which might lead to increased possibility of immunogenicity in patients[235]. Finally, the lack of Fc domain, despite providing the advantage of reduced size and risk of immunogenicity, also results in the most obvious disadvantage: Fabs cannot induce Fc-mediated immune responses such as cell-mediated cytotoxicity or complement dependent cytotoxicity unless they are conjugated to an effector moiety[235,247]. As a result, in cases where an Fc-mediated immune response is necessary, alternative strategies have been developed to address the issue of immunogenicity. Antibody chimerization and humanization to generate humanized mAbs (hu-mAbs) are two examples of these strategies.

1.8.5. Chimeric and Humanized mAbs (hu-mAbs)

The development of hu-mAbs aims to optimize their effector functions and mitigate the immunogenicity associated with rodent antibodies[238,240,248,249]. Hu-mAbs are engineered antibodies that have been modified to possess human-like frameworks while retaining the antigen-binding regions derived from non-human sources, typically mice[238,240,248,249].

Since the first-time antibody humanization was described in the second half of 1980's [248], multiple humanization methods have been described. The process of humanization originated with chimerization[248]. A technique that consists in merging the variable regions of mouse antibodies with the constant regions of human antibodies to create molecules that contained approximately 70% human identity[248] (**Figure 1.11**). Chimeric antibodies effectively kept the specificity of the original mouse antibodies while reducing their immunogenicity in humans. However, they still triggered a response known as human anti-chimeric antibody (HACA) response[248]. An alternative method for humanization of non-human antibodies that avoids this issue is CDR grafting. With this method the CDRs of non-human antibodies are grafted onto the human frameworks[240] (**Figure 1.11**). Typically, human frameworks that closely resemble the framework regions of non-human antibodies are selected as a recipient for CDR grafting[240,250–252]. The process begins by comparing the murine VH and VL chain sequences with the functional human germline[250]. Then the highest homology sequences for each chain from the human germline are selected as acceptor sequences for grafting murine CDRs[250]. Previous studies have demonstrated that direct transplantation onto human framework often results in a loss of affinity and specificity for the target antigen[251,253,254]. To reduce this effect, residues in the framework that are involved in the presentation of the CDR loops must be preserved[250]. The final sequence can then be synthesized and cloned into expression vectors that will express the humanized mAb[250]. This approach has significantly contributed to the current success of therapeutic mAb by effectively minimizing the potential for immune reactions while preserving the therapeutic properties of the original murine version [255,256].

In addition to offering the advantage of minimizing potential adverse immune reactions in patients, hu-mAbs can also exhibit improved binding affinity and specificity or can be engineered to obtain desired effector activity[238]. Additionally, hu.Mabs have shown improved stability and longer half-life circulating the organism than murine origin mAbs, quickly cleared due to the HACA response[237,257,258], or Fabs, less stable due to the lack of Fc region[235,248,259].

However, the production process for humanized mAbs can be complex and costly[238,260]. While manufacture costs are not a big issue, several hundred million dollars are associated with developing hu-mAbs through licensure[260]. The high developing cost leads to higher treatment

costs, which result in limiting their access for some patients and healthcare systems. In addition, there may still be a risk of immunogenicity due to residual non-human sequences [254] and over time, some patients may develop resistance to humanized monoclonal antibodies, reducing their effectiveness[261].

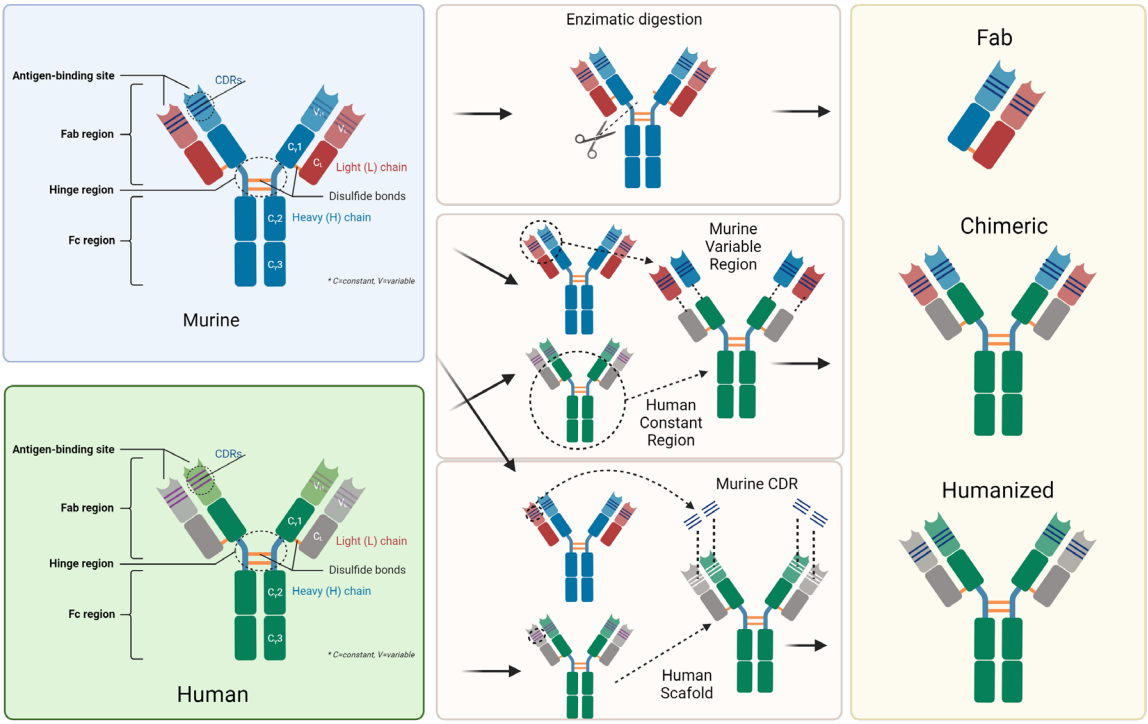

Figure 1.11 Schematic overview of mAb modifications to reach the clinic. Human and murine antibodies include variable regions, also called VH and VL, and the constant region (dark blue and green domain). A Fab consists of the light chain (VL + CL, in red) and the domains of the heavy chain (VH and Cγ1). There are different modifications that can be made to increase the safety of an antibody-based treatment. By enzymatically digesting the di-sulphide bonds from an antibody, a Fab consisting on the VL can be obtained. The chimeric mAb, in which the variable region is of murine origin, and the rest of the chain is of human origin. The humanized mAb only includes the hypervariable segment (CDR) of murine origin and uses a fully human scaffold. Cγ: domains of the constant region of the heavy chain; CL: constant domain of the light chain; VH: variable domain of the heavy chain; VL: variable domain of the light chain. Image created using BioRender (https://biorender.com/).

Taking into account the above-mentioned advantages and disadvantages of modified antibodies, along with the interaction of Siglec-1 with viruses, anti-Siglec-1 antibodies developed by our group could reach the clinic by following these procedures.

1.8.6. Anti-Siglec-1 mAbs

Over the past years, our group has also been exploring the potential use of host-directed mAbs as an antiviral therapy, and we have produced five anti-Siglec-1 clones that bind to different epitopes of the N-terminal region of the receptor, which interacts with sialylated ligands present

in gangliosides anchored to the viral envelope of distinct pathogenic viruses[53]. These mAbs were selected for their capacity to target Siglec-1 with high affinity, below the nanomolar range, and block its interaction with distinct enveloped viruses[53].

Our group has demonstrated the *in vitro* capacity of these mAbs to block Siglec-1 interaction with HIV-1 and Ebola VLPs[53]. Results showed that in DCs, HIV-1 uptake was blocked after pre-incubating the cells with these anti-Siglec-1 mAbs[53]. Furthermore, HIV-1 *trans*-infection to target $CD4^+$ T cells was also reduced[53]. Our group also tested the ability of anti-Siglec-1 mAbs to block Ebola VLP uptake and fusion into DCs. VLP uptake was blocked, and fusion into the cell was significantly reduced by the effect of anti-Siglec-1 mAbs[53]. Since the capture of two distant related viruses such as HIV-1 and Ebola was reduced by anti-Siglec-1 mAbs, it is likely that other enveloped viruses might exploit Siglec-1 on myeloid cells to *trans*-infect or facilitate viral entry[53] (**Figure 1.12**). Thus, anti-Siglec-1 mAbs could become a broad-spectrum therapy for several enveloped viruses.

Yet, because anti-Siglec-1 antibodies generated by our group were from animal origin, they had to be modified to avoid immunogenicity. As previously explained, multiple approaches are available to achieve this, and our group has opted for Fab generation and antibody humanization among them. Since targets such as Siglec-1 may not always be easy to reach, and the antibodies' half-life may not always be long enough to stay in circulation we used antibody engineering to optimize the generated candidates in order to use them as therapies and reach the clinic.

The complex interplay between APCs and viral infections highlights their critical role in determining the immune response to pathogens. Among the various receptors expressed by APCs, Siglec-1 may play a key role, influencing both the modulation of the immune response and the viral pathogenesis. Its ability to facilitate viral spread and evade immune surveillance highlights its potential as a therapeutic target. The development of Fabs and humanized anti-Siglec-1 antibodies is a promising approach to combat viral infections. By understanding the unique properties of Siglec-1 and its immune-virological mechanisms, we can design more effective treatments, which will ultimately help advance medical interventions against a wide range of viral diseases.

A

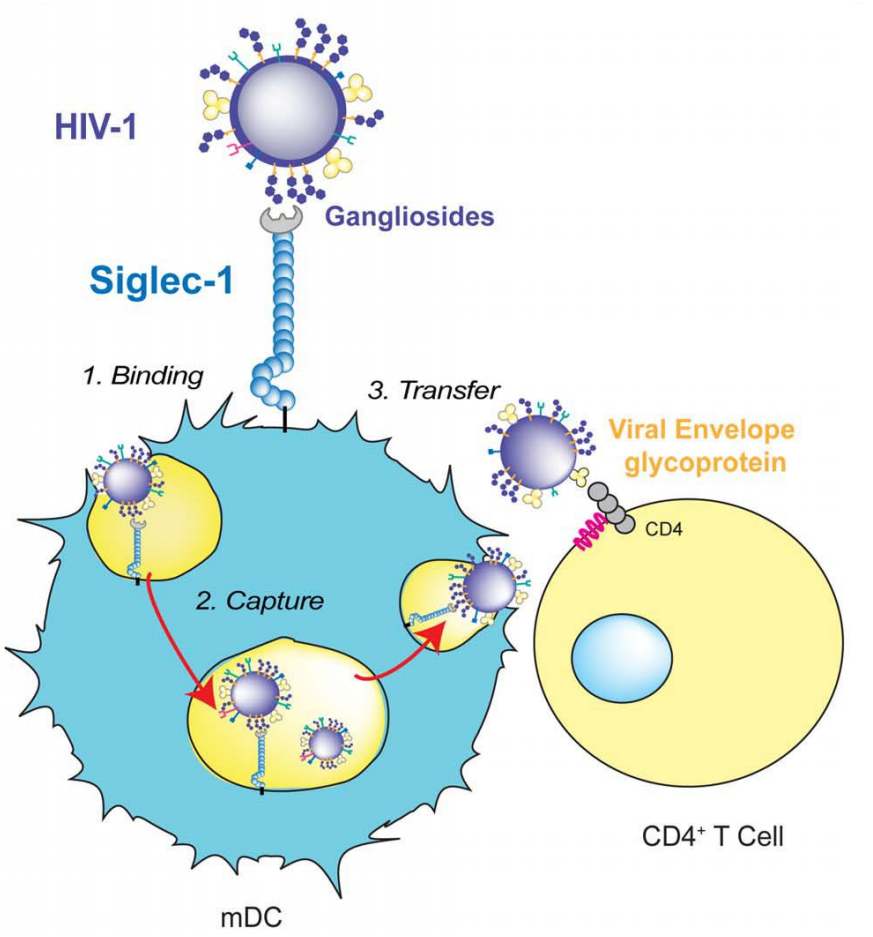

B

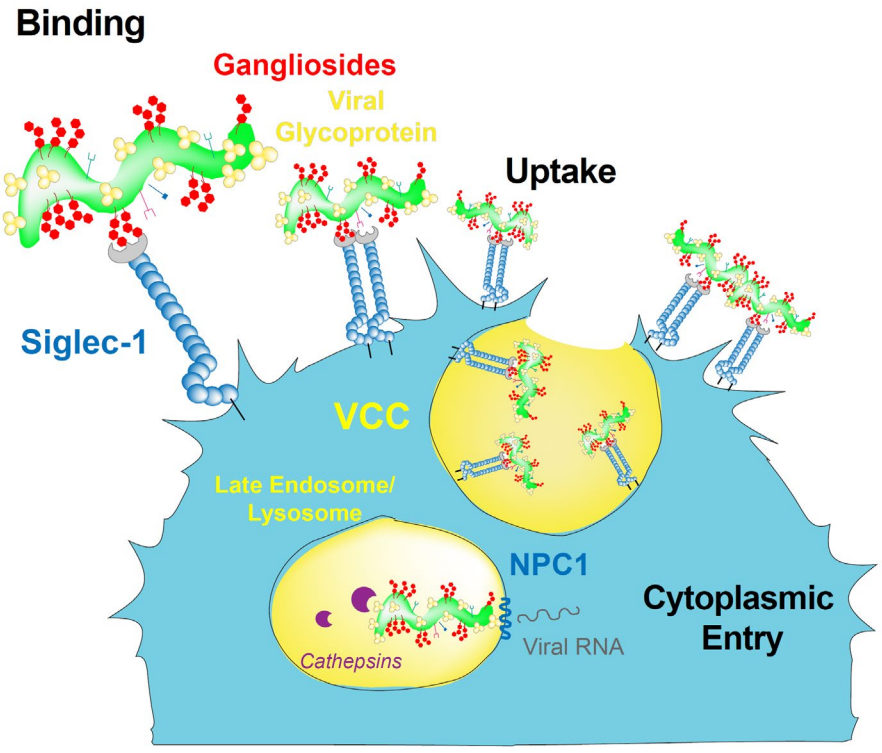

Figure 1.12 Capture overleaf

Figure 1.12 Schematic overview of Siglec-1 mediated viral uptake mechanisms for HIV-1 and EBOV. A. HIV-1 binds to Siglec-1 through viral membrane gangliosides. Viral capture is followed by accumulation in a storage compartment until virus is released to infect a contacting $CD4^+$ T cell via viral envelope glycoprotein and CD4/ coreceptor interactions. From Ref[262]**. B**. Siglec-1 recognition of sialylated gangliosides such as GM1 on the membrane of Ebola virus (shown in red) modulates the binding, uptake and trafficking of viral particles to a sac-like virus-containing compartment (VCC) continuous with the plasma membrane. Viruses stored on VCCs can be redirected into the classical internalization pathway and facilitate viral entry into the cytoplasm. NPC1, Niemann-Pick C1 receptor. From Ref[53]. VCC: Virus-Containing Compartment; NPC1: Niemann-Pick C1 Protein; mDc: mature Dendritic Cell.

Chapter 2 – Hypothesis and Aims

Upon viral infection APCs are the first cellular line of defence. APCs will sense the invading pathogen via PRR triggering an immune response against it. Some viruses have acquired APCs as targets in the early stages of infection, disrupting the immune response. Among the PRRs able to interact with invading pathogens, Siglec-1 is a molecule present in myeloid cells that can recognize sialylated motifs from gangliosides present in viral membranes. Previous work has demonstrated that enveloped viruses such as HIV-1 and Ebola not only interact with Siglec-1 in APCs, but are aided by this receptor, facilitating *trans*-infection to target cells in the case of HIV-1 or acting as an auxiliary receptor for Ebola virus. SARS-CoV-2, another enveloped virus, might also be recognized by Siglec-1, and since has been demonstrated that cannot productively infect APCs, it might follow the same *trans*-infection mechanism seen for HIV-1. Arenaviruses, in a similar way to Ebola virus, target MΦs and DCs in the early stages of the infection. As enveloped viruses, they might also be recognized by Siglec-1 and therefore aided by this auxiliary receptor that could enhance APC infection.

Our group has developed anti-Siglec-1 murine mAbs that block viral uptake and *trans*-infection in activated myeloid DCs. These Anti-Siglec-1 mAbs block HIV-1 uptake and *trans*-infection, as well as EBOV uptake and fusion. Antibodies are effective antiviral therapies to block viral infection, but to become a real-world therapy, our murine anti-Siglec-1 mAbs need to be humanized to reach clinical stages.

We hypothesize that Siglec-1 can play a key role in the dissemination and pathogenesis of other enveloped viruses aside from HIV-1 and EBOV, either facilitating *trans*-infection or aiding viral entry, and contribute to viral dissemination. If that is the case, anti-Siglec-1 mAbs may have the therapeutic potential to be used as broad-spectrum antiviral treatments for distinct enveloped viruses, reducing or preventing viral propagation.

The aims of this thesis are the following:

1. To test if Siglec-1 interacts with other enveloped virus such as SARS-CoV-2 and favour viral spreading.
2. To determine if Siglec-1 can act as an attachment receptor for distinct arenaviruses.
3. To produce Fabs and humanize anti-Siglec-1 antibodies and test their capacity to block the interaction with different enveloped viruses to determine their capacity as a future treatment to combat or prevent viral infections.

Chapter 3 – Results I: SARS-CoV-2 interaction with Siglec-1 mediates *trans*-infection by dendritic cells.

The results included in this chapter are part of:

Perez-Zsolt, D., Muñoz-Basagoiti, J., Rodon, J., Elosua-Bayes, M., Raïch-Regué, D., Risco, C., Sachse, M., Pino, M., Gumber, S., Paiardini, M., Chojnacki, J., Erkizia, I., Muñiz-Trabudua, X., Ballana, E., Riveira-Muñoz, E., Noguera-Julian, M., Paredes, R., Trinité, B., Tarrés-Freixas, F., Blanco, I., Guallar, V., Carrillo, J., Blanco, J., Telenti, A., Heyn, H., Segalés, J., Clotet, B., Martinez-Picado, J.*, Vergara-Alert, J.* and Izquierdo-Useros, N.*, 2021. **SARS-CoV-2 interaction with Siglec-1 mediates trans-infection by dendritic cells**. Cellular & Molecular Immunology, 18(12), pp.2676-2678.

*Senior and corresponding authors

Author's contribution: The author of this thesis contributed to the current work by measuring lectin expression in cell lines by FACS used to assess the interaction between SARS-CoV-2 and Siglec-1. The author also contributed by generating high-resolution microscopy images and videos demonstrating VCC formation where the virus and the receptor accumulated.

2.1. Introduction

Over the last years, SARS-CoV-2 has caused a worldwide pandemic that prompted a quick response by generating vaccines and treatments against the virus[263]. These vaccines have proven to be effective against severe disease associated with multiple SARS-CoV-2 variants that have aroused during this period. Yet, new viral variants are showing progressive levels of humoral immune escape and it is possible that in the near future other viruses with similar outbreak potential could also escape these strategies and require treatments that have not been developed yet. These treatments are particularly relevant as SARS-CoV-2 infection can lead to severe COVID-19, which can also cause admission into the intensive care units in the worse scenarios. Severe COVID-19 has been associated with acute respiratory distress syndrome[264] and with a disproportionate inflammatory response characterized by a cytokine storm-like syndrome[265–268].

Global immunization campaigns are still ongoing, and despite the efforts, vaccines have not reached the entire world population, increasing the chances of new escape variants arousing. Therefore, there is an urgent need to find effective therapeutic treatments to reduce the mortality associated with COVID-19. The respiratory illness caused by SARS-CoV-2 leads to hospitalization in 10-30% of the infected individuals and, eventually, the admission into the intensive care unit[91,269,270]. Severe COVID-19 is associated with pneumonia, dyspnoea, hypoxemia and lymphopenia, and can rapidly progress to respiratory failure[264]. Acute respiratory distress syndrome (ARDS) is also a common complication and is associated with a disproportionate inflammatory response to SARS-CoV-2, characterized by a cytokine storm-like syndrome [265–268]. Of note, mortality rate in COVID-19-associated ARDS is 45%, and the incidence of ARDS among non-survivors of COVID-19 is 90%[271].

Earlier studies have highlighted the paramount role of myeloid APCs, such as MΦs and DCs, in mediating an antiviral inflammatory response, which is exacerbated in severe COVID-19 cases[137,138]. A critical role of lung macrophages in inducing the inflammation associated with the pathologic sequelae of SARS-CoV-2 infection has been confirmed also in non-human primates (NHP)[272]. At the moment of doing this work, whether these cells effectively trap and process SARS-CoV-2, was yet to be elucidated. Myeloid APCs might contribute to viral pathogenesis if they are susceptible to infection, or able to capture and transfer infectious viruses to bystander target cells, thereby favouring viral spread to other tissues[69,273,274]. Indeed, viral dissemination mediated by APCs is a common pathway co-opted by different types of viruses to evade immunity, as it is the case of the HIV-1, which is effectively transferred to target cells via a mechanism known as *trans*-infection[67,273]. For other viruses, such as Ebola

virus, productive infection of APCs is critical in determining host susceptibility and viral dissemination to distant tissues[70,275].

Early interactions between viruses and macrophages or DCs are critical to either trigger immune responses or favour viral dissemination. For SARS-CoV-2, the outcome of such interactions was not fully explored, although it could impact the progression of COVID-19 severity. Thus, elucidating the initial steps of viral interaction with myeloid APCs was essential for the design of new therapies to increase protection of exposed individuals. Several lectin receptors are critical for initial viral recognition on APCs. C-type lectins such as DC-SIGN mediate the attachment of several viruses such as HIV-1 or Ebola virus via viral glycoprotein recognition[76,273,276,277], being also the case for SARS-CoV-2[278]. The sialic acid-binding lectin Siglec-1 is an interferon inducible receptor expressed on activated myeloid cells[51,58,279] whose expression is up-regulated on APCs in SARS-CoV-2 infected individuals[54]. Siglec-1 is implicated in the binding of HIV-1 and Ebola virus via the recognition of sialylated ligands exposed on the lipid membranes of these viruses. The V-set domain of Siglec-1 interacts with sialyllactose on viral membrane gangliosides [64,65,68], which HIV-1, Ebola virus and other enveloped viruses incorporate during the budding from the membranes of infected cells[65,78,280–282]. However, a general role for Siglec-1 in facilitating SARS-CoV-2 uptake and *trans*-infection to pulmonary target cells such as pneumocytes or respiratory ciliated cells remained largely unexplored, despite being one of the lectins that are highly expressed on pulmonary macrophages.

Here we show that, although being largely resistant to SARS-CoV-2 infection, myeloid cells effectively capture and trap incoming viruses in internal compartments connected with the plasma membrane, eventually leading to viral degradation overtime. We also show that Siglec-1 mediates SARS-CoV-2 recognition of different viral variants of concern via interaction with sialylated ligands, such as the ganglioside GM1 identified on SARS-CoV-2 membrane. Also, immunohistochemistry of pulmonary tissues of SARS-CoV-2 infected NHP corroborated, directly *in vivo*, the presence of Siglec-1 on myeloid cells containing viruses. Siglec-1 capacity to bind SARS-CoV-2 was more relevant than other well-known attachment receptors, such as DC-SIGN, and more effective at mediating transfer of viruses to susceptible target cells via *trans*-infection. Notably, since anti-Siglec-1 mAbs blocked SARS-CoV-2 *trans*-infection on DCs, targeting Siglec-1 could offer cross-protection against different SARS-CoV-2 variants and other enveloped viruses that exploit APCs for viral dissemination.

2.2. Methods

2.2.1. Biosafety statement

The institutional review board on biomedical research from Hospital Germans Trias i Pujol (HUGTiP) approved this study. The biologic biosafety committee of the Research Institute Germans Trias i Pujol approved the execution of SARS-CoV-2 experiments at the BSL3 laboratory of the Center of bioimaging and comparative imaging (CMCIB).

2.2.2 Raji R116A stable cell line generation

Raji B cells were used to develop a stable cell line expressing Siglec-1 with a point mutation generated by changing (Arg → Ala) at 116 (R116A) by Blue Heron Biotech (Raji R116A). We chose a Raji B cell line because it lacks endogenous expression of these lectins and can be transfected without unspecific upregulation of Siglec-11. Raji B cell line was transfected with the plasmid encoding Siglec-1 with R116A mutation using Amaxa nucleofector (Lonza) and following the manufacturer's instructions. Transfected cells were maintained in RPMI with 1mg ml-1 geneticin (Invitrogen) for selection of a stable clone with high Siglec-1 expression. Expression of Siglec-1 was periodically checked by cytometry with anti-Siglec-1-PE 7-239 mAb (AbD Serotec) at RT for 15 min. 1 month after transfection cells were sorted to obtain clones with the highest expression using FACSAria II (BD Biosciences). Selected clones were grown for another month and the cell sorting process was repeated. Obtained clones were grown for a month, then Siglec-1 expression was checked for each clone and the two with the highest expression were selected, expanded, and stored.

2.2.3. Cell lines

Vero E6 cells (ATCC CRL-1586) were cultured in Dulbecco's modified Eagle medium, (DMEM; Lonza) supplemented with 5% fetal bovine serum (Invitrogen), 100 U/mL penicillin, 100 µg/mL streptomycin, and 2 mM glutamine (all ThermoFisher Scientific). HEK-293T (ATCC repository) were maintained in DMEM with 10% fetal bovine serum, 100 IU/mL penicillin and 100 µg/mL streptomycin (all from Invitrogen). Raji B lymphocyte, Raji DC-SIGN (kindly provided by Y. Van Kooyke) and Raji R116A cell lines were maintained in Roswell Park Memorial Institute medium (RPMI; Invitrogen) or RPMI plus 1 mg/mL geneticin (Invitrogen). Generation and maintenance of Raji Siglec-1, Raji Siglec-5 and Raji Siglec-7 has been described[53]. HEK-293T overexpressing the human ACE2 were kindly provided by Integral Molecular Company and maintained in DMEM with 1 µg/mL of puromycin (Invitrogen). TMPRSS2 human plasmid (Origene) was transfected using X-tremeGENE HP Transfection Reagent (Merck) on HEK-293T overexpressing the human ACE2 and maintained in the previously described media containing 1 mg/mL of geneticin (Invitrogen) to obtain TMPRSS2/ACE2 HEK-293T cells. All

media contained 10% fetal bovine serum, 100 IU/mL penicillin and 100 µg/mL streptomycin (all from Invitrogen).

2.2.4. Primary Cell Cultures

Peripheral blood mononuclear cells were obtained with a Ficoll- Hypaque gradient (Alere Technologies AS) from blood donors and monocyte populations (>90% $CD14^+$) were isolated with CD14-negative selection magnetic beads (Miltenyi Biotec). Macrophages were obtained culturing these cells in the presence of 100 µg/mL of macrophage colony-stimulating factor (M-CSF) for seven days and replacing media and cytokines every 2 days. DCs were obtained culturing these cells in the presence of both 1,000 IU/mL of granulocyte-macrophage colony-stimulating factor (GM-CSF) and interleukin-4 (IL-4; both from R&D) for seven days and replacing media and cytokines every 2 days. Activated cells were differentiated by culturing myeloid cells at day five for two more days in the presence of 1,000 IU/mL of interferon-alfa (IFNα; Sigma-Aldrich) or 100 ng/mL of lipopolysaccharide (LPS, Sigma-Aldrich).

2.2.5. Virus Isolation, Titration, and Sequencing

Unless otherwise specified, SARS-CoV-2 used was the virus isolated in March 2020 from a nasopharyngeal swab as described in (Rodon, 2021). The virus was propagated for two passages and a virus stock was prepared collecting the supernatant from Vero E6. Genomic sequence was deposited at GISAID repository (http://gisaid.org) with accession ID EPI_ISL_510689. Compared to the Wuhan/Hu-1/2019 strain, this isolate has the following point mutations: 376 D614G (Spike), R682L (Spike), and C16X (NSP13). The SARS-CoV-2 B.1.1.7 variant (originally isolated from the UK), the P.2 ZETA variant (originally isolated from Brazil) and the B.1.351 variant (originally isolated from South Africa) were identified during routine sequencing of a clinical nasopharyngeal swabs in Spain during January- February 2021 and subsequently isolated on Vero E6 cells. These sequences are deposited at GISAID database with accession numbers EPI_ISL_1663567; EPI_ISL_1831696 and EPI_ISL_1663571 for B.1.17, P.2 ZETA and B.1.351, respectively. Genomic sequencing was performed from viral supernatant by using standard ARTIC v3 based protocol followed by Illumina sequencing[283]. Raw data analysis was performed by viralrecon pipeline[284] while consensus sequence was called using samtools/ivar at the 75% frequency threshold.

2.2.6. Pseudovirus production

HIV-1 reporter pseudoviruses expressing SARS-CoV-2 Spike protein and luciferase were generated using two plasmids. pNL4-3.Luc.R-.E- was obtained from the NIH AIDS repository. SARS-CoV-2.SctΔ19 was generated (Geneart) from the full protein sequence of SARS-CoV-

2 spike with a deletion of the last 19 amino acids in the C-terminal, human-codon optimized and inserted into pcDNA3.4- TOPO[285]. Spike plasmid was transfected with X-tremeGENE HP Transfection Reagent (Merck) into HEK-293T cells, and 24 h post-transfection, cells were transfected with pNL4-3.Luc.R-.E-. VSV-G plasmid (kindly provided by A. Cimarelli) was used to equally pseudotype pseudoviruses. Supernatants were harvested 48 h later, filtered with 0.45 µM (Millex Millipore) and stored at -80ºC until use. Viruses were titrated in HEK-293T overexpressing the human ACE2.

2.2.7. Pseudoviral fusion assay

Macrophages or DCs activated or not with IFNα as previously described along with HEK-293T ACE2 cells were exposed to equivalent MOI of VSVg or SARS-CoV-2 spike pseudotyped lentiviruses. To block ACE2 dependent viral fusion, some wells had 20 µg/mL of human ACE2-murine Fc fusion protein. Two days post-infection, cells were lysed with the Glo Luciferase system (Promega). Luminescence was measured with an EnSight Multimode Plate Reader (Perkin Elmer).

2.2.8. Construction of a human-ACE2 murine-Fc-fusion protein (ACE2-mFc)

Expression vector was generated with the Geneart service (Thermofisher Scientific). Coding sequence included the first 615 amino acids from the Human ACE2 sequence, with H345A and H505A mutations to inactivate the catalytical sites, followed by the constant region of the heavy chain of the murine IgG1. For protein production, Expi293F cells (Thermofisher Scientific) were transfected with ACE2-mFc vector at a density of 2.5 x 106 cells/mL using Expifectamine (Thermofisher Scientific). Enhancers 1 and 2 (Thermofisher Scientific) were added to the culture 18 h post-transfection. Cells were incubated for 5 days and supernatants were harvested and passed through a 0.22 µm PVDF filter. For purification, supernatants were loaded into a 5 mL SepFast Ø11mm (Quimigen) packed with CaptureSelect™ IgG-Fc (ms) affinity resin (Thermo Scientific) connected to an Äkta Start Chromatograph (Cytiva). The column was washed with 5 column volumes (CV) of PBS and ACE2-mFc was eluted with 2 CV of 0.1M Glycine at pH=3.5. The sample was concentrated with a 30kDa Amicon Centrifugal Concentrator at 3000 x g. ACE2-mFc concentration was determined by sandwich ELISA using a goat anti-mouse IgG Fc (Jackson Immunoresearch, 115-006-071) for capture, a horseradish peroxidase (HRP) labelled F(ab)2 Goat anti-mouse IgG Fc (Jackson immunoresearch, 115-036-071) as secondary antibody, A purified mouse IgG (D50, NIH AIDS Reagent Program) as standard and o-phenylenediamine dihydrochloride (Sigma-Aldrich, #P8787-100TAB) as substrate. Light absorbance was measured at 492/620 nm on EnSight Multimode Plate Reader

(Perkin Elmer). ACE2-mFc inhibitory capacity was tested in a SARS-CoV-2 neutralization assay as described previously[286].

2.2.9. SARS-CoV-2 Uptake and Degradation Assays

Uptake experiments with SARS-CoV-2 were performed pulsing 0.5 x 106 Raji or 1 x 106 myeloid cells at a rate of 70 ng of Nucleocapsid at 37ºC for the indicated timepoints. For blockade, cells were preincubated for 15 min at RT with 10 µg/mL of mAbs α-Siglec-1 7–239, or IgG1 isotype control (BD Biosciences), or left untreated before viral exposure. After extensive washing, cells were lysed at a constant concentration of 1x106 cells/mL, centrifuged to remove cellular debris and assayed with a SARS-CoV-2 Nucleocapsid protein (NP) High-sensitivity Quantitative ELISA (ImmunoDiagnostics). For degradation experiments, myeloid cells were exposed to SARS-CoV-2 for 4h, extensively washed, and left in culture for the indicated timepoints until cell associated viral content and viral release to the supernatant were measured with the indicated ELISA kit.

2.2.10. Electron microscopy of myeloid cells

10 x 106 myeloid cells (macrophages or DCs activated with LPS) were exposed to SARS-CoV-2 with an MOI of 1 for 24h, fixed with paraformaldehyde (PFA) at 4% (Biotium) and glutaraldehyde 1% (Sigma Aldrich/Merck) for one hour at room temperature (RT) and processed for embedding in resin, ultramicrotomy and transmission electron microscopy as previously described[287]. Briefly, after fixation the samples were washed three times with PBS and cells were gently scraped with a rubber policeman. Cell pellets were postfixed with 1% osmium tetroxide + 0.8% potassium ferrocyanide in water for 1h on ice. The samples were dehydrated on ice with a gradual series of acetone and infiltrated at RT with epoxy resin. After heat polymerization the samples were sectioned with a UC6 microtome with a nominal feed of 70 nm. Sections were collected on 300 mesh bare copper grids and contrasted with 4% aqueous uranyl acetate, followed by Reynold´s lead citrate. Images were taken either using a Jeol 1011 run at 100 kV equipped with a Gatan ES1000W camera or a Jeol 1400 run at 80kV with a Gatan Oneview camera.

2.2.11. Activation of myeloid cells

Myeloid cells were left untreated activated for 48h with SARS-CoV-2 at a MOI of 0.1 and compared to cells treated with IFNα or LPS as previously described. Cells were blocked with 1 mg/mL human IgG (Privigen, Behring CSL) and stained with anti-Siglec-1-PE 7-239 mAb (AbD Serotec), anti-DC-SIGN-PE DCN46 mAb, anti-HLA-DR-PerCP L243 mAb, anti-CD86-FITC 2331 (FUN-1) mAb, anti-CD83-FITC HB15e mAb and anti-CD14-PerCP MφP9 mAb (all from BD Biosciences) at 4 °C for 30 min. Mouse IgG1-PE (AbD Serotec) was included as

isotype control. Samples were analysed with FACS Canto (BD Biosciences) using FlowJo software to evaluate collected data.

2.2.12. Confocal Microscopy analyses

LPS-treated DCs were pulsed with SARS-CoV-2 with an MOI of 1 for 4 h at 37 °C. After extensive washing, cells were fixed and permeabilized (Fix & Perm, Invitrogen) and stained with anti-rabbit nucleocapsid pAb (GeneTex) revealed with a Goat pAb Anti-Rabbit IgG Alexa 488 (Abcam) and an anti- Siglec-1 7-239 Alexa 647 mAb (Biolegend). Cells were cytospun into coverslips, covered with DAPI-containing Fluoroshield mounting medium (Sigma-Aldrich) and analyzed with a Dragonfly (Andor) 505 multimodal confocal microscope with GPU driven deconvolution to maximize resolution.

2.2.13. Super-resolution analysis of SARS-CoV-2

For super-resolution detection of nucleocapsid and Spike proteins and GM1 gangliosides, SARS-CoV-2 particles were adhered to poly-L coated coverslips for 15 min at RT and fixed in 4 % PFA/PBS for 30 min. Fixed and inactivated virus samples were permeabilized and blocked using 0.1 % saponin /0.5 % BSA/PBS. Virus particles were immunostained with rabbit anti-SARSCoV- 2 N protein (Sino Biological) or rabbit anti-GM1 Ab (Abcam) followed by antirabbit Abberior STAR RED (Abberior GmbH) Fab fragments. SARS-CoV-2 Spike protein was detected with an ACE2- mAb Fc recombinant protein and anti-mouse Abberior STAR 580 (Abberior GmbH) Fab fragments. SARS-CoV-2 Spike protein was detected with an ACE2-mAb Fc recombinant protein and anti-mouse Abberior STAR RED conjugated Fab fragments. Following immunostaining, all samples were overlaid with SlowFade Diamond mounting medium (ThermoFisher Scientific, USA) and imaged using STED microscopy. Super-resolution analysis of SARS-CoV-2 virus particles was performed using Leica SP8 STED 3X microscope (Mannheim, Germany) equipped with a 100×/1.4 NA oil immersion STED objective. STED images of N protein, GM1 (Abberior STAR RED) and S-ACE2 protein complexes (Abberior STAR 580) signals were acquired sequentially for each channel using 637 nm and 587 nm lines from the white light laser. Abberior STAR RED and Abberior STAR 580 signal was depleted with a donut-shaped 775-nm pulsed STED laser. STED depletion conditions were tuned to achieve 40 nm lateral resolution (full-width-at-half-maximum, FWHM) as estimated from fluorescent bead and single fluorescent antibody molecule measurements. STED images were acquired with following parameters: pinhole size: 1.03 Airy; dwell time: 2 µs/pixel and XY pixel size: 20 nm. Acquired STED images were thresholded and filtered using Gaussian filter (Sigma (Radius) = 0.75) using Fiji (ImageJ distribution) software.

2.2.14. Trans-infection Assay

HEK-293T overexpressing the human ACE2, or both ACE2 and TMPRSS2 were used to test if SARS-CoV-2 pseudotyped viruses can fuse with these receptors via trans-infection. A constant pseudoviral titer was used to pulse cells in the presence of the indicated mAbs for 2 h at 37ºC. Cells were extensively washed and cocultured with or without target cells at a ratio 1:1. Two days post-infection, cells were lysed with the Glo Luciferase system (Promega). Luminescence was measured with an EnSight Multimode Plate Reader (Perkin Elmer). Vero E6 cells were used to test if SARS-CoV-2 can be trans-infected. A constant MOI of SARS-CoV-2 from B.1.1.7 variant was used to pulse Raji cells for 4 h at 37ºC. Cells were extensively washed and co-cultured with or without target cells at the indicated ratios. One duplicate was co-cultured in the presence of 10 µM of Remdesivir to block viral replication. Cells not exposed to the virus were equally co-cultured with Vero E6 cells and used to set 100% of cell viability for each condition. Two days post-infection, cells were lysed with the Cell Titter Glo viability system (Promega). Luminescence was measured with a Luminoskan (ThermoScientific).

2.2.15. Immunohistochemical staining on sections of SARS-CoV-2

The paraffin-embedded sections of SARS-CoV-2 infected lungs from a previous study with Rhesus macaques [272] were subjected to deparaffinization in xylene, rehydration in graded series of ethanol, and rinsed with double distilled water. Antigen retrieval was performed by immersing sections in DIVA Decloaker (Biocare Medical) at 125°C for 30 seconds in a steam pressure decloaking chamber (Biocare Medical) followed by blocking with SNIPER Reagent (Biocare Medical) for 10 min. The sections were incubated with SARS Nucleocapsid Protein Antibody (Rabbit polyclonal; Novus Biologicals, NB100-56576SS) and rabbit anti-human Anti-Sialoadhesin/CD169 antibody (clone SP216, Abcam, ab183356) for 1 h, followed by a double detection polymer system (Mach 2 Double Stain 2, Biocare Medical). Labelled antibodies were visualized by development of the chromogen (Warp Red and/or Vina Green Chromogen Kits; Biocare Medical). Digital images of lung were captured at 100×, 200× and 400× magnification with an Olympus BX43 microscope equipped with a digital camera (DP27, Olympus) and evaluated using Cellsens Standard digital imaging software 2.3 (Olympus).

2.2.16. Statistical analysis

Statistical differences from 100% of viability were assessed with a one-sample t-test. Statistical differences were also assessed with a Mann Whitney t test, a Wilcoxon matched paired t test and a paired t test. Comparisons were performed with Graph Prism 9.

2.3. Results

2.3.1. Myeloid cells are not productively infected by SARS-CoV-2 but capture and degrade trapped viruses.

Preliminary reports indicate that myeloid cells such as monocyte-derived macrophages and DCs are highly resistant to coronavirus infection[288–290]. In line with these findings, we observed a reduction above 50% in the viability of susceptible Vero E6 cells 3 days post SARS-CoV-2 infection, that was not observed for monocyte-derived myeloid cells (**Figure 3.1A**). Of note, upon SARS-CoV-2 invasion, myeloid cells responded to activating signals that initiate antiviral responses, such as the release of type I interferon-α (IFN-α), or to the presence of bacterial lipopolysaccharide (LPS), which are increased throughout the course of SARS-CoV-2 infection[291]. Thus, we tested the fusion capacity of SARS-CoV-2 spike on myeloid cells activated or not in the presence of IFN-α. Reporter pseudoviral vectors expressing VSV glycoprotein effectively fused with both macrophages and DCs, although it decreased on IFN-α treated myeloid cells (**Figure 3.1B**). However, fusion was always negligeable when pseudo viruses were pseudo typed with SARS-CoV-2 spike. Of note, both pseudo viruses effectively fused with HEK-293T cells expressingACE2. For SARS-CoV-2 spike pseudo virus this was specifically blocked by a human ACE2-Fc fusion protein, which was not active on myeloid cells (**Figure 3.1B**).

Next, we compared the capacity of myeloid cells activated or not in the presence of IFN-α to capture SARS-CoV-2 by an ELISA measuring the amount of cell-associated virus. We followed the fate of these viruses for two days, assessing the amount of cell-associated virus captured overtime while measuring the amount of virus remaining in the supernatant (**Figure 3.1C**). Maximal viral uptake on cells was detected 4 h post viral addition, and decreased overtime for activated and non-activated myeloid cells, indicating that APCs were effectively processing captured viruses, since SARS-CoV-2 detected in the supernatant also diminished over time (**Figure 3.1C**). After extensive cellular washing, degradation of viruses trapped for 4 h was also assessed on macrophages and DCs previously activated or not with IFNα (**Figure 3.1D**). Cell-associated viruses detected at 4 h were quickly degraded after 24 h of culture, confirming that APCs were effectively processing captured viruses (**Figure 3.1D**). This was not due to the release of bound viruses to the supernatant, where no SARS-CoV-2 accumulation could be detected over time (**Figure 3.1D**). Moreover, the absence of viral secretion to the media confirmed the inefficient viral replication of SARS-CoV-2 in myeloid cells regardless of their activation status (**Figure 3.1D**). In agreement with these results, electron microscopy micrographs of myeloid DCs showed SARS-CoV-2 on large membranous compartments

resembling degradative structures, where damaged viral particles were observed (**Figure 3.1E**, first image). On Macrophages we also found viruses in vesicles filled with material that marks them as endocytic structures (**Figure 3.1E**, last two images). Hence, viruses were effectively captured by APCs, especially upon cellular activation, that were in any case effectively processed by all APCs.

We then wanted to assess if SARS-CoV-2 could induce activation of myeloid cells. We pulsed DCs and MΦs for 48h with SARS-CoV-2, LPS or IFN-α. Siglec-1 mRNA induction was always more potently triggered by IFN-α than by SARS-CoV-2, which correlated with Siglec-1 expression on the cellular surface, both on DCs and macrophages (**Figure 3.1F**). These results indicate that direct exposure to SARS-CoV- 2 does not activate DCs as potently as LPS or IFN-α. Yet, these bystander activation stimuli released throughout SARS-CoV-2 infection can induce Siglec-1 expression on APCs, especially on DCs (**Figure 3.1F**, histograms).

Overall, these results show that APCs capture SARS-CoV-2 but do not get productively infected, while at the same time display a slight increase in Siglec-1 expression. It is possible that this activation is due to SARS-CoV-2 despite not being as high as IFN-α activation. It has been reported that DCs can mediate HIV-1 uptake via Siglec-1 without productive infection[58,262], and therefore, we next wanted to address if Siglec-1 expressed in APCs could also play a role in SARS-CoV-2 uptake in myeloid cells.

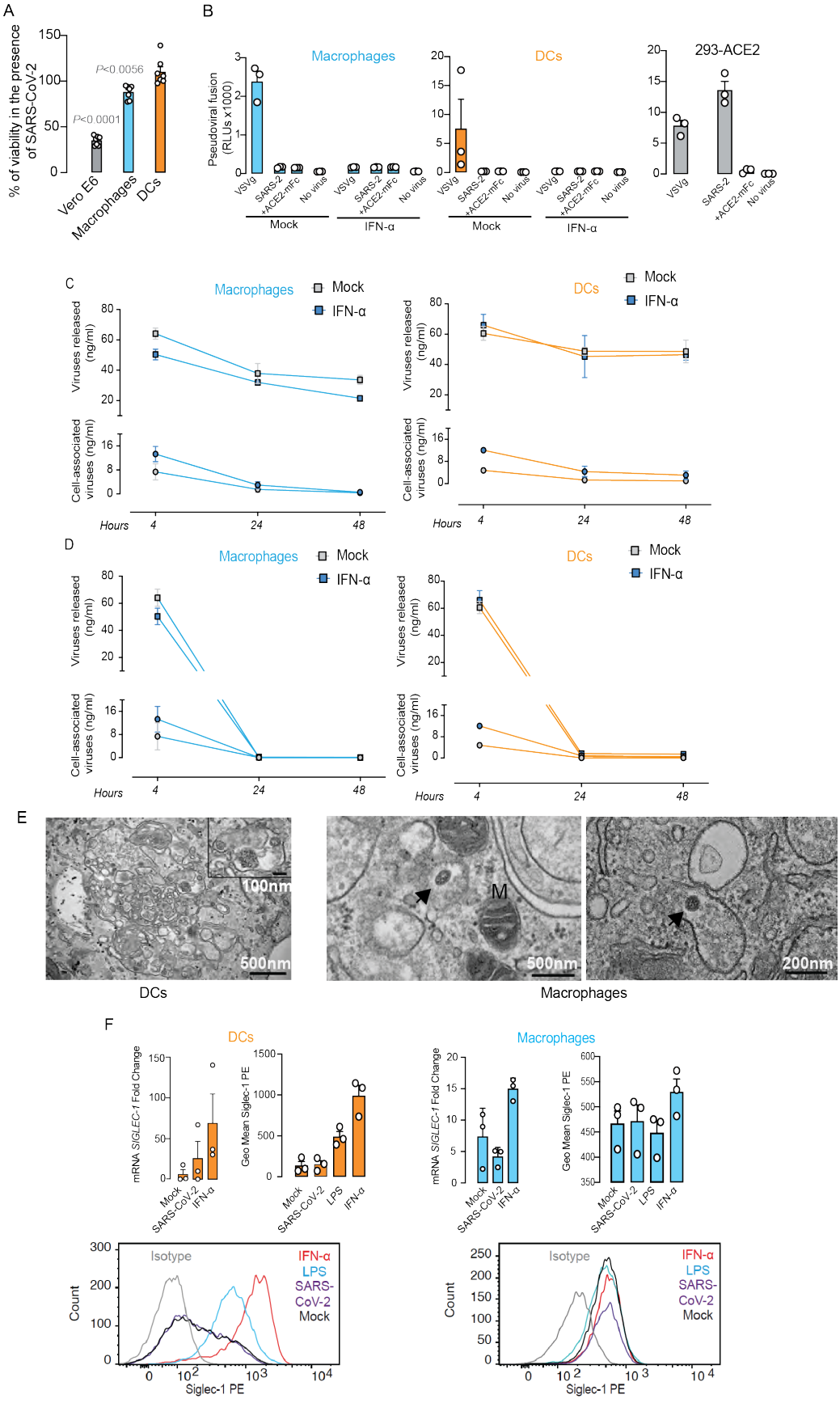

Figure 3.1 Caption overleaf

Figure 3.1 Myeloid cells are not productively infected by SARS-CoV-2 but these APCs capture and degrade trapped viruses. A. Percentage of cellular viability 3 days post infection with SARS-CoV-2 at a MOI of 0.1 in Vero E6 cells, macrophages and DCs. Values from 2 replicates and four experiments. Statistical differences from 100% of viability were assessed with a one-sample t-test. **B**. Fusion of HIV-1 luciferase reporter viruses lacking the envelope glycoprotein pseudotyped with VSV glycoprotein or SARS-CoV-2 Spike in macrophages and DCs stimulated or not with IFN-α and in ACE2 expressing HEK-293T cells. ACE2-mFc fusion protein was used to block ACE2- dependent viral fusion. Values from 2 replicates and one experiment. **C**. Uptake of SARS-CoV-2 by macrophages (left graph) and DCs (right graph) activated or not with IFN-α that were pulsed for 4 h, 24 h and 48 h at 37 °C with the virus, to assess the amount of virus present in the supernatant (squares) and the amount of cell-associated viral nucleocapsid detected on cellular lysates after extensive washing (circles) by ELISA. Data from one representative experiment out of two shows means and SEM and from 3 different donors. **D**. Kinetics of SARS-CoV-2 degradation after 4 h of viral exposure and extensive washing by macrophages (left graph) and DCs (right graph) activated or not with IFN-α. The amount of virus present in the supernatant (squares) and the amount of cell-associated viral nucleocapsid detected on cellular lysates after extensive washing (circles) was measured by ELISA. Data from one representative experiment out of two shows means and SEM from 3 different donors. **E**. Electron microscopy images of Macrophages and LPS DCs exposed first to SARS-CoV-2 at an MOI of 1. Arrows indicate individual viral particles, M, mitochondrion. Data from 2 donors and 2 experiments. **F**. Fold change on SIGLEC1 mRNA induction after 24h of exposure to IFN-α or SARS CoV-2 (MOI=0.01) and representative Siglec-1 surface staining of myeloid cells equally activated and also exposed to LPS analysed by FACS. Results from six independent biological replicates and two experiments.

2.3.2. Siglec-1 receptor binds SARS-CoV-2 variants via sialic acid recognition present on viral membrane gangliosides and mediates SARS-CoV-2 uptake in myeloid cells.

Siglec-1 is upregulated on myeloid cells upon SARS-CoV-2 infection[54], and it is involved in the uptake by APCs of different viruses (including HIV-1 and Ebola virus) via recognition of syalilated gangliosides anchored on the viral membranes[65,78,280,281,292,293]. We therefore tested if Siglec-1 could recognize and capture SARS-CoV-2 by assessing viral uptake in two complementary cellular models. First, we used the antigen presenting Raji B cell line transfected with different lectins, whose level of expression is shown in (**Figure 3.2A**) and measured the capacity of these cells for SARS-CoV-2 uptake. All Raji cells were pulsed with equal amounts of SARS-CoV-2, extensively washed, lysed, and assessed by ELISA to measure the amount of viral nucleocapsid protein. While Raji Siglec-1 cells effectively captured SARS-CoV-2, Raji cells transfected with Siglec-5, Siglec-7, DC-SIGN or devoid of any of these lectins did not (**Figure 3.2B**). We next tested if Siglec-1 uptake of SARS-CoV-2 relied on the recognition of sialylated ligands, which most likely are gangliosides exposed on viral membranes, as previously described for HIV-1 and Ebola virus[53,58,64,65,68]. This was confirmed using a Raji cell line transfected with the Siglec-1 mutant R116A, which contains a mutation critical for sialic acid recognition[51,58] that did not trap SARS-CoV-2 (**Figure 3.2B**), as previously shown for other viruses[53,58]. To further confirm if SARS-CoV-2 interaction was mediated bySiglec-1, we pre-treated Raji cells with an α-Siglec-1 mAb 7-239 previously shown to decrease HIV-1 and Ebola virus uptake[53,58,68]. While isotype mAb had no inhibitory effect, pre-treatment with 7-239 mAb clearly reduced SARS-CoV-2 uptake (**Figure 3.2C**). Of note, distinct SARS-CoV-2 variants (D614G, B.1.1.7 first identified in UK, P.2 Zeta first identified in Brazil, and the B.1.351 first identified in South Africa) were equally trapped via Siglec-1 receptor but

were not captured by the mutated Siglec-1 R116A, indicating that sialic acid recognition is critical for viral trapping (**Figure 3.2D**).

We also used a second cellular model of monocyte-derived macrophages and DCs to verify the role of Siglec-1 receptor on primary cells. Myeloid cells previously treated or not with IFN-α were pulsed with SARS-CoV-2, washed, and assayed by ELISA as described for Raji cells. It is worth noticing that all myeloid cells trapped SARS-CoV-2 but IFN-α activated APCs, which display higher amounts of Siglec-1 (**Figure 3.1G**), were the cells with higher uptake capacity (**Figure 3.2E**). To further investigate whether SARS-CoV-2 viral interaction was mediated by Siglec-1, we used the anti-Siglec-1 mAb 7-239. While isotype mAb had no inhibitory effect, pre-treatment with 7-239 blocked SARS-CoV-2 uptake (**Figure 3.2F**), and this Siglec-1 dependency was higher for IFN-α activated APCs.

In addition, using super resolution microscopy of SARS-CoV-2 viral particles stained for the Spike using an ACE2-mFc fusion protein, we confirmed that GM1, one of the sialyllactose-containing gangliosides interacting with Siglec-1[65], was detected on 74% of viruses binding the ACE2-mFc fusion protein (**Figure 3.2G**). Once Siglec-1 binds HIV-1 or Ebola viruses, this receptor polarizes and engulfs viral particles within VCCs which are continuous with the plasma membrane and connected to the extracellular space[81,82]. To elucidate whether the Siglec-1 receptor also recruits SARS-CoV-2 to these compartments, we investigated viral uptake by confocal microscopy. LPS-activated DCs exposed to SARS-CoV-2 showed a Siglec-1 positive VCC containing viral particles attached to the membrane of the compartment (**Figure 3.2H**). Supporting these results, electron microscopy micrographs of DCs showed SARS-CoV-2 particles associated with sack-like structures resembling viral containing compartments (VCC) (**Figure 3.2I**), as already described for other viruses[53,81]. We found extracellular viruses attached to invaginations of the plasma membrane or VCCs that appear also as vacuoles. These structures were however connected to the plasma membrane. Moreover, immunohistochemistry analysis of the pulmonary tissue of a SARS-CoV-2 infected rhesus macaque from a previous study[272] collected at 10 dpi, confirmed at the protein level the co-expression of Siglec-1 and SARS-CoV-2 nucleocapsid in cells with a typical myeloid cell morphology (**Figure 3.2J**).

Thus, the complementary approaches of Siglec-1 *de novo* expression on Raji cells, combined with the blocking effect of specific mAbs on primary myeloid cells, along with the detection of Siglec-1 interacting GM1 ligands on SARS-CoV-2 particles and accumulation into VCCs, supports that Siglec-1 is a central molecule mediating SARS-CoV-2 uptake via sialic acid recognition in myeloid cells.

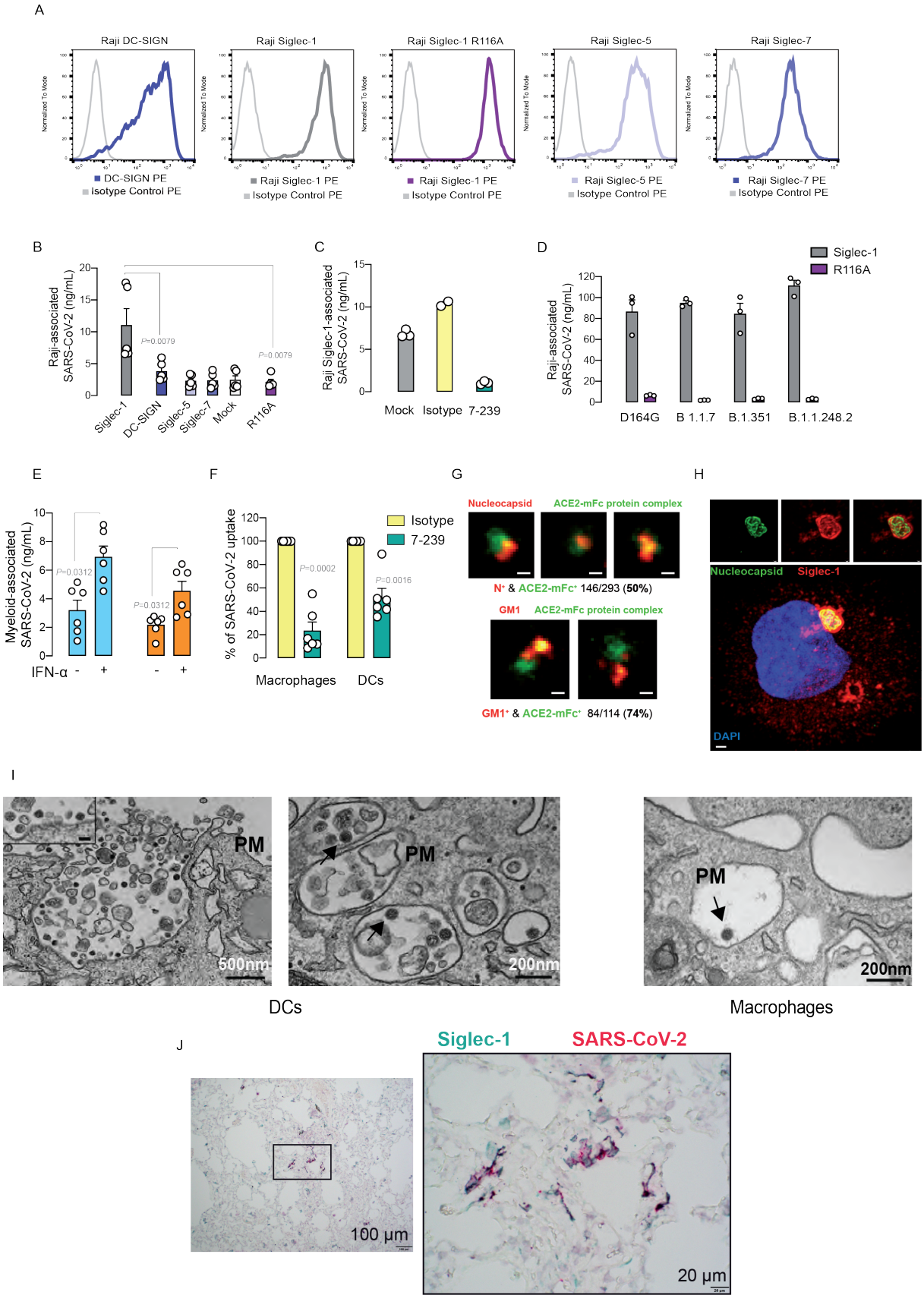

Figure 3.2 Caption overleaf

Figure 3.2 Siglec-1 receptor binds SARS-CoV-2 variants via sialic acid recognition present on viral membrane gangliosides. **A**. Representative surface staining of the different lectins expressed on transfected Raji cell lines analyzed by FACS. **B**. Comparative uptake of SARS-CoV-2 by distinct Raji B cells, that were pulsed for 2 h at 37°C, washed and lysed to assess the amount of cell-associated viral nucleocapsid by ELISA. Values from five replicates and two experiments. Statistical differences were assessed with a Mann Whitney t test. **C**. Uptake of SARS-CoV-2 by Raji Siglec-1 pre-incubated with α-Siglec-1 mAb 7239 or the corresponding isotype control processed as in A. Values from three replicates and one experiment. **D**. Comparative uptake of 4 different variants of SARS-CoV-2 by Raji Siglec-1 and Raji R116A Siglec-1 B cells that were processed as in A. **E**. Uptake of SARS-CoV-2 by macrophages and DCs activated or not with IFNα for 4 h and then processed as in A. Values from at least three donors and two experiment. Statistical differences were assessed with a Wilcoxon matched paired t test. **F**. Percentage of viral uptake inhibition of macrophages and DCs activated IFNα that were pre-incubated with 10 µg/mL of the indicated mAbs and pulsed with SARS-CoV-2 (MOI=0.1). **G**. **H**. Confocal microscopy image of an LPS-treated DC exposed to SARS-CoV-2 at a MOI of 1 showing a 3D reconstruction of the VCC and the whole cell (Scale bars 0,2 µM and 1 µM, respectively). Cells were stained with anti-nucleocapsid pAbs (green), anti-Siglec- 1 mAb (red) and Dapi (blue) to stain the nucleus. See also supplementary movie 1. **I**. Super resolution microscopy of SARS-CoV-2. Top images: viruses stained with anti-nucleocapsid Abs (red) and ACE2-mFc fusion protein that interacts with the Spike of SARS-CoV-2 (green). Bottom images: viruses stained with anti-GM1 Abs (red) and ACE2-mFc fusion protein that interacts with the Spike of SARS-CoV-2 (green). Percentage of co-staining for each is shown. Scale bar: 100 nm. **J**. Immunohistochemistry of a pulmonary tissue from an infected Rhesus Macaque co-stained with Siglec-1 and SARS-CoV-2 nucleocapsid antibodies. Right panel zooms into the highlighted box.

2.3.3. Siglec-1 facilitates SARS-CoV-2 trans-infection to target cells.

Siglec-1 has a dual role enhancing infectivity of various viruses, either facilitating fusion on APCs, as is the case for Ebola virus, or mediating transmission to other target cells, as is the case for retroviruses. This later mechanism is relevant when APCs are not directly susceptible to infection, as it has been reported for HIV-1 on DCs[63]. The inefficient support of SARS-CoV-2 replication on APCs (**Figure 3.1**) would suggest that Siglec-1 could mediate SARS-CoV-2 transmission to target cells in the context of coronavirus infection. Therefore, we next assessed the relevance of *trans*-infection for SARS-CoV-2 bound via Siglec-1. We pulsed distinct Raji cells with equal amounts of SARS-CoV-2. Pulsed Raji cells were extensively washed and co-cultured with target cell lines expressing ACE2. Raji Siglec-1 cells effectively transferred SARS-CoV-2 to cellular targets expressing ACE2 (**Figure 3.3A**). Moreover, *trans*-infection relied on Siglec-1 uptake of SARS-CoV-2 via recognition of sialylated ligands, as the Siglec-1 mutant R116A did not *trans*-infect SARS-CoV-2 (**Figure 3.3A**). No direct infection of Raji cells was detected, as seen when assessing pulsed cells in the absence of ACE2-expressing cellular targets. We also tested primary monocyte-derived myeloid cells activated with IFNα to up-regulate Siglec-1 expression and found that DCs where much more efficient at transmitting SARS-CoV-2 when compared to macrophages (**Figure 3.3B**). We used the α-Siglec-1 mAb 7-239 to explore whether SARS-CoV-2 *trans*-infection could be blocked with this antibody. While isotype mAb had no inhibitory effect, pre-treatment with 7-239 blocked SARS-CoV-2 pseudovirus *trans*-infection to target cells mediated by IFNα-activated DCs (**Figure 3.3C**). No direct infection of DCs was detected, as seen when assessing pulsed cells in the absence of ACE2-expressing targets. Thus, SARS-CoV-2 retention via Siglec-1 allows *trans*-infection of cells expressing ACE2 and TMPRSS2 receptors, especially by DCs.

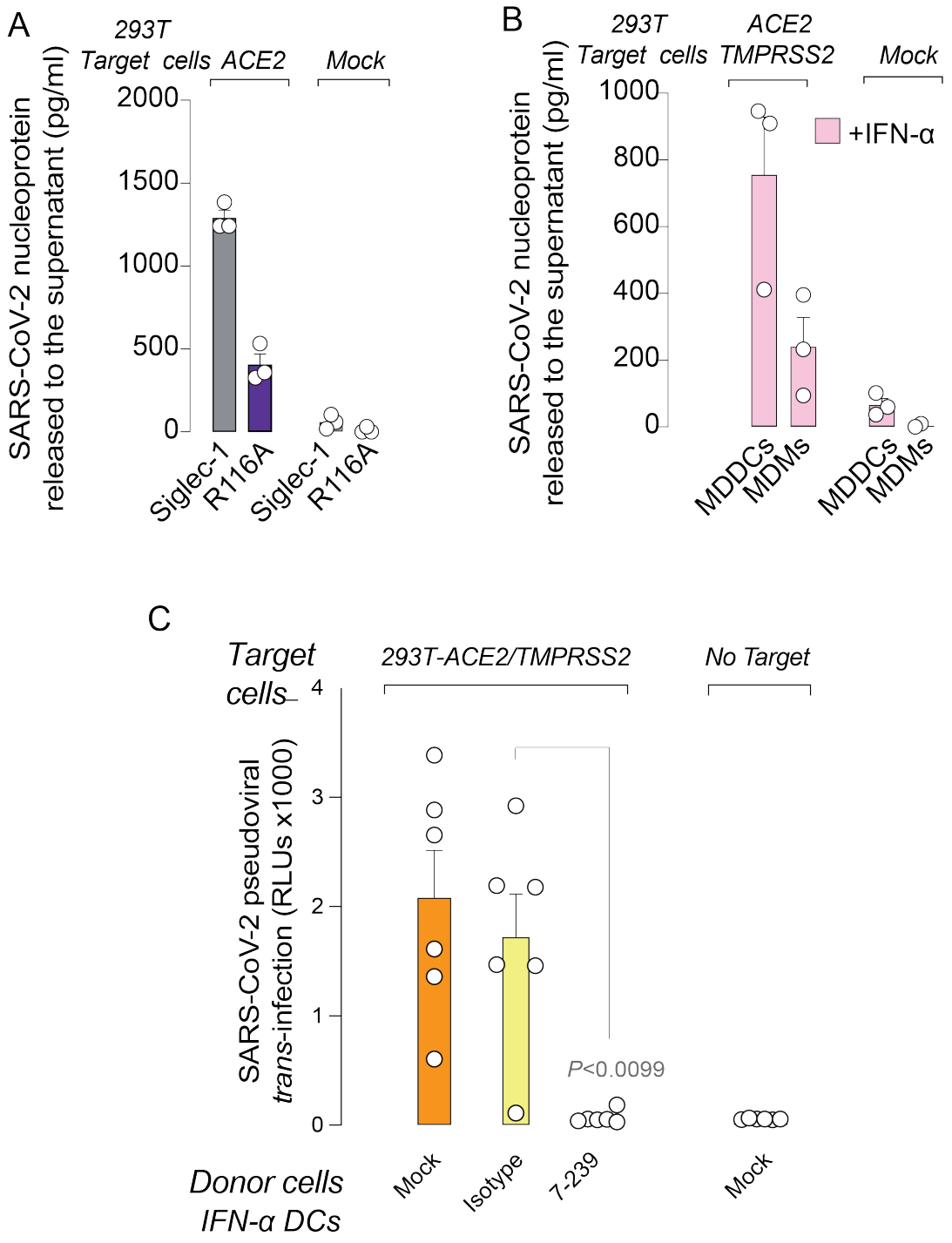

Figure 1.3 A, B Transmission of SARS-CoV-2 by indicated cells. APCs exposed to SARS-CoV-2 were cocultured with HEK-293T cells expressing ACE2 or not. Viral release from one experiment was measured with an ELISA. **C**. Transmission of SARS-CoV-2 pseudoviruses from IFN-α activated DCs to HEK 293T cells expressing ACE2 and TMPRSS2. Cells were pre-incubated with the indicated mAbs and exposed to SARS-CoV-2 before assessing trans-infection. No viral fusion was detected on DCs not co-cultured with SARS-CoV-2 target cells. Data show mean values and SEMs from two experiments including cells from six donors. Statistical differences were assessed with a paired t test. **A, B** show mean values and SEMs.

2.4. Conclusions

These results demonstrate that SARS-CoV-2 can be recognized by APCs expressing Siglec-1. Furthermore, the data presented suggests that Siglec-1 is able to interact with SARS-CoV-2 and might have a key role in the early stages of the infection. The interaction between Siglec-1 and SARS-CoV-2 follow the same pathway previously reported by our group, in which HIV-1 and Ebola virus were recognized via Siglec-1 and accumulated in a VCC[53,68,279].

It is possible that as previously described for HIV-1 and Ebola virus, this interaction favours viral uptake and spread at the early stages of the infection. Since SARS-CoV-2 does not productively infect APCs, it might be following a *trans*-infection mechanism similar to HIV-1. Targeting Siglec-1 with mAbs in the early stages of the infection, to block the interaction with the virus could decrease early SARS-CoV-2 dissemination and the pathogenesis associated with severe COVID-19. Our work has proven that Siglec-1 is interacts with multiple enveloped viruses which are not closely related. Therefore, it might be possible that other enveloped viruses might as well interact with Siglec-1 and follow mechanisms similar to the ones described for HIV-1, Ebola or SARS-CoV-2. We believe that because this receptor could be involved in multiple viral interactions, it has the potential to become a therapeutic antiviral target.

Chapter 4 – RESULTS II: Siglec-1 Functions as an Attachment Receptor for Arenavirus Uptake via Sialylated Ganglioside Recognition

The results included in this chapter are part of:

Xabier Muñiz-Trabudua, Itziar Erkizia, Cristina Borio, Marcos Bilen, Jakub Chojnacki, Patricia Resa-Infante*, Nuria Izquierdo-Useros* and Javier Martinez-Picado*, **Siglec-1 Functions as an Attachment Receptor for Arenavirus Uptake via Sialylated Ganglioside Recognition.** Submitted to Frontiers in Immunology.

*Senior and corresponding authors

Author's contribution: The author of this thesis contributed to the current work by generating arenavirus VLP stocks, analyzing GM1 incorporation by confocal microscopy in arenavirus VLPs, analyzing viral protein expression by Wester-Blot, measuring Siglec-1 surface expression by FACS, and performing VLP capture assays. The author also contributed to the design of the experiments, analysis and interpretation of the results.

4.1. Introduction

Arenaviruses are enveloped viruses with a negative-stranded RNA genome that are associated to rodent-borne diseases that cause rare but often serious illnesses in humans, such as haemorrhagic fevers[1]. Among them, Junín and Lassa viruses are of particular concern due to their potential for outbreaks, their high mortality rates, and limited treatment options[294,295]. Junín virus is the causative agent of Argentine haemorrhagic fever, mainly found in South America[296]. The severity and impact of continuous outbreaks caused by Junín virus over the years underscore the urgent need for effective therapeutic interventions[295]. Despite progress in vaccine development and antibody research against Junín virus, comprehensive antiviral strategies to cover all potential outbreak-causing arenaviruses are still lacking[210,295]. Likewise, Lassa virus poses a significant public health threat, particularly in West Africa, where it is responsible of Lassa fever[156,297]. The limited availability of vaccines and specific treatments for Lassa virus highlights the need to better understand how this virus interacts with the host immune system to prevent infection[298].

Studies that focus on cellular viral entry are crucial for the development of effective therapies against Junín and Lassa viruses. Myeloid antigen-presenting cells, such as dendritic cells (DCs), play a key role in initiating immunity but can also serve as targets for arenavirus infection[145,194–196,299]. Therefore, elucidating the specific mechanisms by which Junín and Lassa viruses enter DCs is essential for the design of successful antiviral treatments and prevention strategies. Certain receptors expressed on DCs, such as C-type lectins and TIM/TAM molecules, are involved in the attachment and entry of arenaviruses into these cells[189]. Upon binding and internalization, the viral glycoprotein of these arenaviruses undergoes a conformational change due to the pH acidification, enabling recognition by endosomal receptors and facilitating viral entry into the cytoplasm[145,300,301]. These viral-host interactions ultimately determine the susceptibility of DCs to Junín and Lassa virus infection. Understanding these early interactions is crucial to design future interventions aimed at decreasing host susceptibility to infection and disease progression.

DCs can facilitate tissular and systemic viral propagation in various infections -such as HIV-1, Ebola virus and SARS-CoV-2 [53,58,302] - given the unique capacity of this cells to favour viral retention and their susceptibility to certain infections. Particular interactions of specific receptors expressed on DCs with key viral components may contribute to viral spread within the host. Identifying and studying these receptors and their ligands could offer potential novel therapies for combating arenavirus infection. An example of such receptor is Siglec-1

(CD169), a I-type lectin expressed on DCs [61,302] that interacts with sialylated gangliosides anchored to the lipid membrane of different enveloped viruses[45]. This receptor mediates viral dissemination via transmission of infectivity to bystander target cells, as is the case of HIV-1 and SARS-CoV-2[58,302], or by favouring productive infection, as it happens for Ebola virus[53].

Here, we report that Siglec-1 mediates arenavirus recognition via interaction with the sialylated ganglioside GM1 identified on the membrane of Junín and Lassa VLPs. Furthermore, we show that DCs can capture and trap Junín or Lassa VLPs via Siglec-1, guiding viral particles into a virus containing compartment that follows the same entry mechanism of HIV-1, Ebola virus and SARS-CoV-2. Specific antibodies against Siglec-1 inhibited Junín or Lassa VLP entry, offering a new target to limit arenavirus dissemination. Identifying and studying host receptors such as Siglec-1 could offer novel therapeutic approaches for combating viral infections.

4.2. Methods

4.2.1. Cell lines

HEK293T, Raji B lymphocyte, Raji R116A and Raji Siglec-1, were maintained as previously described (Chapter 3, Material & Methods 2.3).

4.2.2. Primary cell cultures

Peripheral blood mononuclear cells were obtained with a Ficoll-Hypaque gradient (Alere Technologies AS) from blood donors, and monocyte populations (>97% $CD14^+$) were isolated with CD14 positive selection magnetic beads (Miltenyi Biotec). DCs were obtained as previously described (Chapter 3, Material & Methods 2.4).

4.2.3. Junín and Lassa VLP generation

Junín Z-eGFP VLPs (JUN_{ZeGFP}) and Lassa Z-eGFP VLPs (LAS_{ZeGFP}) were generated transfecting HEK-293T cells with the molecular clone pZ-eGFP and pZ-LASV-eGFP respectively[303]. We generated Junín and Lassa fluorescent VLPs to study the role of Siglec-1 in their viral cycle. We followed a VLP generation protocol similar to the one described by Dr Borio[303]. We adapted the protocol and avoided the last ultracentrifugation step because we performed experiments using primary DCs and we wanted to avoid any additional compounds that could interact with the cells and possibly trigger their activation. HEK-293T cells were transfected using X-tremeGENE 9 DNA Transfection Reagent (Merck) in T75 flasks using a total of 20µg or 30µg of plasmid DNA (Lassa and Junín respectively) at day 0 and 24h later. Supernatants were harvested 72h after the second transfection, cleared of cellular debris by centrifugation, filtered through a 40µm pore cut-off, concentrated at 2000 xg using a centrifugal device with 100 kDa pore size (Makrosep 100 kDa, Pall) and frozen at -80ºC until use. The VLP concentration was determined by an eGFP ELISA kit (Abcam) to detect the eGFP concentration in harvested supernatants and assessed on an EnSight Multimode Plate Reader (Perkin-Elmer).

4.2.4. Junín and Lassa VLP uptake assays

Junín and Lassa VLP uptake experiments were performed pulsing $0.25x10^6$ DCs with a constant amount of 120 ng of eGFP per condition 4h at 37ºC. For blockade, cells were pre-incubated for 15 min at RT (~24ºC) with 10µg/ml of anti-Siglec-1 mAb 7-239 (Abcam), an IgG1 isotype control (BD Biosciences) or left untreated before viral exposure. After extensive washing, cells were acquired with a FACSCelesta or Calibur (BD) and the frequency of positive cells was determined using FlowJo software (TreeStar). Forward-angle and side-scatter light

gating were employed to exclude dead cells and debris from all analysis. Alternatively, 0.25 × 10^6 Raji Siglec-1 cells transfected with WT Siglec-1 plasmid were pulsed with 120 ng of eGFP 1h at 37ºC. Non-transfected and Raji R116A cells were used as internal controls to assess only Siglec-1-dependent viral uptake. To measure Siglec-1 expression, cells were labelled with anti-Siglec-1-PE 7-239 mAb or isotype control and acquired with Calibur (BD).

4.2.5. Spinning disc confocal microscopy analysis of VLP capture

1x10^6 LPS stimulated DCs were pulsed with 200-250ng of eGFP measured by ELISA per condition of JUN $_{ZeGFP}$ or LAS $_{ZeGFP}$ VLPs for 4h at 37ºC. After extensive washing, cells were fixed and permeabilized via Fix&Perm kit following manufacturer's instructions (Life Technologies). Cells were stained with anti-Siglec-1-PE 7-239 mAb and CellTracker™ Red Far-Red Dye (Invitrogen Ref: C34564) following the manufacturer's instructions. Cells were washed, resuspended in 100µl of 1% Formaldehyde and cytospun (Thermo Shandon Cytospin 4). Round coverslips (No.1.5) (VWR) were mounted on each sample using ProLong™ Glass Antifade Mountant with NucBlue™ stain (Life Technologies). Sample analysis was performed using Andor Dragonfly 505 High Speed Confocal Microscope System at Molecular Imaging Platform the IBMB-PCB. Pictures were taken using a 100x oil immersion objective with following parameters: pinhole = 40µm, exposure time: NucBlue = 202.5 ms, eGFP = 202.5 ms, anti-Siglec-1-PE = 112.5 ms, CellTracker™ Red Far-Red Dye = 350 ms, XY pixel size: 51.2 nm/px and analysed with Imaris Viewer software.

4.2.6. Spinning disc confocal microscopy Super-resolution Radial Fluctuations (SRRF) analysis of Junín and Lassa VLPs

VLPs were adhered to poly-l-coated coverslips, fixed in 3% paraformaldehyde, blocked with 0.5% bovine serum albumin (BSA). VLPs were immuno-stained at 4ºC ON with rabbit anti-GM1 pAb and detected by anti-rabbit IgG Fab fragments (Jackson ImmunoResearch) coupled to Star Red dye (KK114, Abberior) using Fix&Perm kit (Life technologies). Samples were acquired using Andor Dragonfly 505 High Speed Confocal Microscope System at Molecular Imaging Platform the IBMB-PCB using SRRF technique. The following parameters were applied for SRRF analysis: exposure time: eGFP = 50 ms, Star Red dye = 90 ms, XY pixel size:51.2 nm/px, Radiality Magnification = 5, Frame Count = 100, Ring Radius = 1.5. Pictures were taken using a 100x oil objective and analysed with Imaris Viewer software.

4.2.7. Western Blot analyses

eGFP and viral protein presence was determined by WB analysis. VLP samples, recombinant soluble Lassa Z protein (Gentaur, 0508-001) and recombinant *A. victoria* GFP protein (Abcam, ab84191) used as controls were diluted in 4x Laemmli Sample Buffer for SDS-PAGE (BioRad,

1610747) with Dithiothreitol (DTT) (BioRad, 1610610) 50mM final concentration, and then boiled 10min at 70ºC. Then samples were loaded in a 4-20% Mini-PROTEAN®TGX™ Precast Protein Gels, 15-well (BioRad #4561096) and run for 18min at 300 V. Protein from the gel was transferred to an ethanol-pre-activated PVDF membrane (BioRad, 1704156) with BioRad precast TRANS-BLOT TURBO system. Membrane was blocked for 30min with StartingBlock™ (TBS) Blocking Buffer (Invitrogen, 37542). After this, membrane was incubated ON at 4ºC with rabbit anti-LASV Z pAb (Gentaur, 0307-002) and mouse monoclonal [LGB-1] to GFP (Abcam, ab291). Following this incubation, membrane was washed with PBS 1x Buffer + 0.1% Tween 20 (Sigma), and then incubated at RT (~24ºC) for 1h with StarBright Blue 700 Goat Anti-Rabbit IgG (Bio-Rad, 12004162) and IRDye 800Cw Conjugated Goat Anti Mouse IgG (LiCor, 926-32210). After this, membrane was washed 3 more times and developed using BIO-RAD Chemidoc Imaging System.

4.2.8. Statistical analyses

We analysed mean changes using Wilcoxon test. Significant mean changes from 100% of the data normalized to percentages were assessed with a one-sample Wilcoxon test. All values of $P<0.05$ were considered significant. All analyses and figures were generated with GraphPad Prism v.8.0 b software.

4.3. Results

4.3.1. Arenavirus VLPs contain GM1 on their membranes that is recognized by Siglec-1

Arenaviruses that cause haemorrhagic fever in humans require biosafety level 4 laboratories to safely study infection [203]. Viral like particles (VLPs) are a non-infectious alternative to study these types of highly pathogenic viruses without the need of high containment biosafety facilities[304]. Arenavirus VLPs can be a useful tool to research arenavirus life cycle[296,303,305–309], and given their similar budding process as compared to infectious viruses they could also be helpful to understand the interplay with Siglec-1 receptor. We therefore studied Junín and Lassa viruses using VLPs in our experiments.

We first wanted to address if arenaviruses displayed sialylated gangliosides on their membranes which could serve as ligands for Siglec-1 receptor, as previously described for other viruses[58,302]. We used anti-GM1 antibodies to analyse the presence of this ganglioside on eGFP-containing arenavirus VLPs by super resolution confocal microscopy. We performed *in vitro* experiments with fluorescent VLPs generated by transfecting the Junín or Lassa protein Z fused to eGFP to generate $JUN_{Z\text{-}eGFP}$ VLPs or $LAS_{Z\text{-}eGFP}$ VLPs. By these means we detected one of the sialyllactose-containing gangliosides that serves as a ligand of Siglec-1[65] on the surface of both Junín (**Fig. 4.1A**) and Lassa (**Fig. 4.1B**) VLPs tagged with eGFP. GM1 was present on 68% of Junín and 12% of Lassa VLPs analysed with this technique. These results indicate that arenaviruses display GM1 on their surface and could therefore interact with Siglec-1.

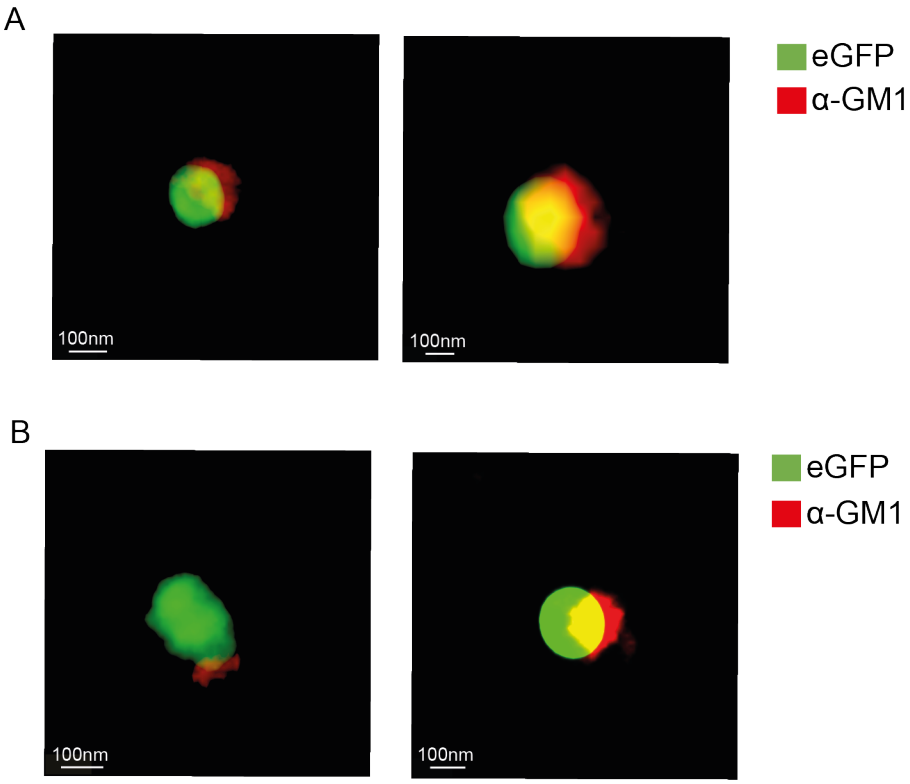

Figure 4.1. VLP arenaviruses contain GM1 on their membranes. A. Representative examples of JUNZ-eGFP VLPs immunostained for GM1 (in red) assessed by super resolution microscopy. **B**. Representative examples LASZ-eGFP VLPs immunostained for GM1 (in red).

4.3.2. Junín VLP uptake relies on Siglec-1 recognition

To test if arenavirus VLPs were able to interact with Siglec-1, we performed viral uptake experiments. Raji Siglec-1 cells showed a VLP uptake in 80% of the cells, which was significantly higher than that exhibited by Raji WT cells (**Fig. 4.2A**). Yet we still detected a 34% capture levels in Raji WT cells, which do not express the receptor, and a 15% in Raji R116A cells, which express a Siglec-1 receptor with a particular mutation that abrogates the recognition of sialylated ligands key for ligan bindign[51]. These results showed that $JUN_{Z\text{-}eGFP}$ VLP uptake was increased when active Siglec-1 was present. To confirm that $JUN_{Z\text{-}eGFP}$ VLPs could be captured via Siglec-1, we also performed uptake experiments with primary DCs, which play a key role in early stages of the infection of distinct viruses[66,310]. As previously reported[53], IFNα and LPS triggered Siglec-1 expression on DCs (**Fig. 4.2B**). This expression was correlated with the uptake of Junín VLP. iDCs showed the lowest VLP uptake, while in DCs stimulated with IFNα or LPS, which express higher levels of Siglec-1, uptake was increased (**Fig. 4.2C**). Yet, when we compared the uptake of $HIV\text{-}1_{Gag\text{-}eGFP}$ VLP with $JUN_{Z\text{-}eGFP}$ VLP in DCs activated with LPS, the highest Junín uptake only reached 15% compared to the 70% reached by $HIV\text{-}1_{GageGFP}$ (**Fig. 4.2D**).

These findings suggested that Siglec-1 mediated Junín VLP uptake, but as opposed to other VLP systems from HIV-1 or Ebola virus[53,262], it also showed a Siglec-1-independent uptake both in Raji WT and Raji R116A cells and a higher detection range in primary immature DCs. We therefore sought to optimize our method for detecting $JUN_{Z\text{-}eGFP}$ VLP uptake to rule out any possible methodological interference.

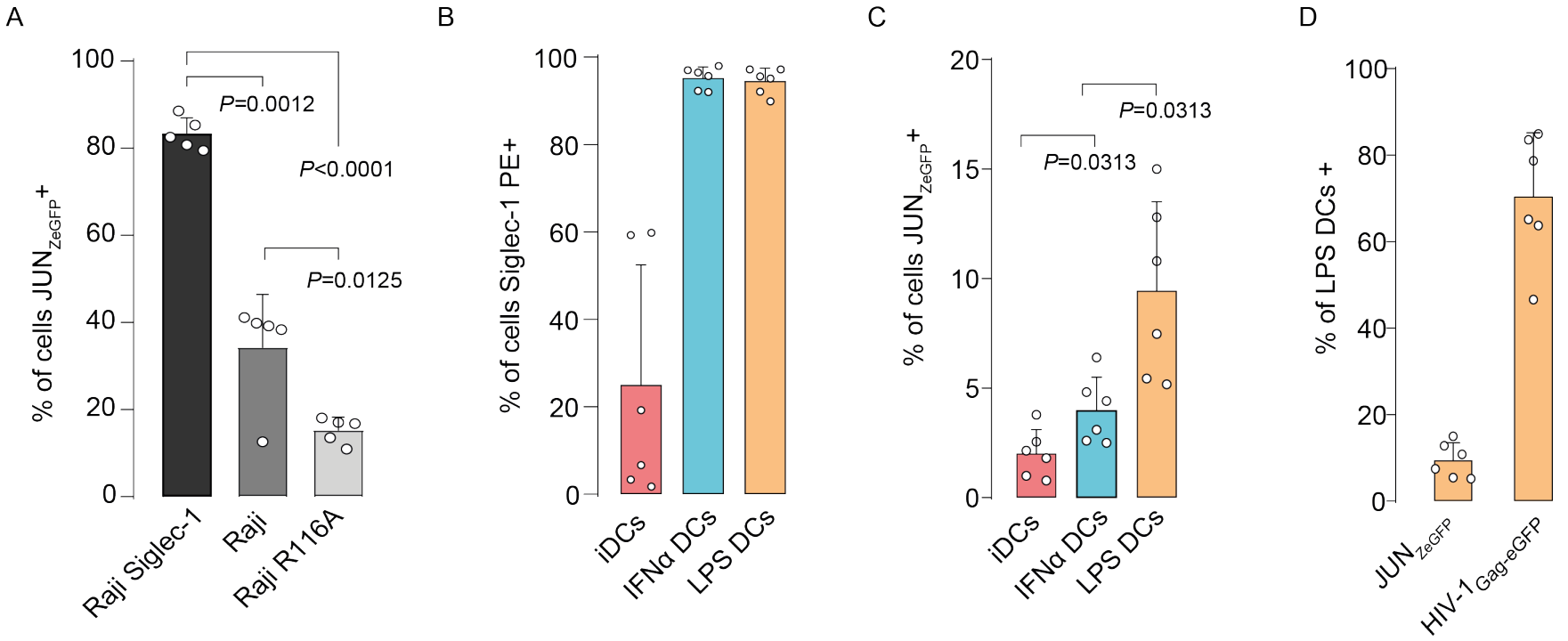

Figure 4.2. **Junín VLP uptake relies on Siglec-1 recognition A.** Comparative uptake of $JUN_{Z\text{-}eGFP}$ VLPs by distinct Raji B cells pulsed for 1 h at 37°C and assessed by FACs. Values from five replicates and two experiments. Statistical differences were assessed with a Wilcoxon non-parametric test. **B.** Siglec-1 surface staining of non-activated DCs, or cells exposed to IFNα or LPS analysed by FACS. Results from six independent biological donors and two experiments. **C.** Comparative uptake of $JUN_{Z\text{-}eGFP}$ VLPs by DCs pulsed for 4 h at 37°C analysed by FACs. Values from six donors and two experiment. **D.** Comparative uptake of $JUN_{Z\text{-}eGFP}$ VLP and HIV-$1_{Gag\text{-}eGFP}$ in LPS activated DCs measured by FACS. Results from six independent donors and two experiments. Statistical differences were assessed with a Wilcoxon non-parametric test.

4.3.3. JUNZ-eGFP VLP filtration confirms Siglec-1 recognition capacity

To increase the eGFP signal, we first tried an indirect immuno-fluorescent labelling of eGFP to enhance the detection range of the assay. For DCs stimulated with LPS, the detected percentage of positive cells significantly increased from 7% to more than 40% (**Fig. 4.3A**). Overall, the signal was increased in all conditions, but $JUN_{Z\text{-}eGFP}$ VLP uptake in IFNα- and LPS-stimulated DCs, which express higher levels of Siglec-1, was increased compared to iDCs (**Fig. 4.3B**). In addition, and to confirm that $JUN_{Z\text{-}eGFP}$ VLP capture was Siglec-1 dependent, we used commercial anti-Siglec-1 monoclonal antibodies (mAbs) to functionally block the viral recognition of this receptor. In the case of stimulated DCs, mAbs blocked $JUN_{Z\text{-}eGFP}$ VLP uptake, confirming that viral recognition is via Siglec-1 (**Fig. 4.3D and 4.3E**). Yet, this Siglec-1 dependency was not observed for iDCs (**Fig. 4.3C**). Overall, immuno-labelling of $JUN_{Z\text{-}eGFP}$ VLP with anti-eGFP Abs improved the detection range of VLP uptake and demonstrated that it was Siglec-1 dependent in IFN and LPS-stimulated DCs. However, we still observed a Siglec-1 independent binding in iDCs that resembled to the unspecific uptake previously detected in Raji WT and Raji R116A (**Fig. 4.2A**). Hence, we decided to investigate the possible source of this background signal by analysing the content of VLP stocks.

We first checked the viral production in the pellet from HEK 293T cells transfected with the plasmid coding for $JUN_{Z\text{-}eGFP}$ by Western-Blot (WB). Since there is no commercial anti-JUN_Z mAb available, we used an anti-eGFP mAb to indirectly detect the chimeric $JUN_{Z\text{-}eGFP}$ protein (37 kDa). The results showed that along the viral $JUN_{Z\text{-}eGFP}$ protein, soluble eGFP was also present (**Fig. 4.3D**). Moreover, the intensity of the bands in the WB suggested that the produced amount of both proteins was similar (**Fig. 4.3D**). We next used a size exclusion centrifugal filtering device (pore diameter 100 kDa) that allowed the soluble eGFP (27 kDa) to be separated from the VLPs after centrifugation. The flow-through sample had an eGFP concentration of approximately half the eGFP signal of the input sample measured by ELISA (**Fig. 4.3E**). Since prior VLP quantification method was based on an ELISA detecting eGFP, this result suggested that the initial $JUN_{Z\text{-}eGFP}$ VLP concentration had been overestimated due to the presence of soluble eGFP. Moreover, this finding could also explain the eGFP background signals detected in cells lacking Siglec-1 such as Raji WT and R116A cells.

To test this possibility, we next used the concentrated $JUN_{Z\text{-}eGFP}$ VLP stock to repeat the uptake experiment in Raji cells. Mean uptake in Raji Siglec-1 cells was increased, while uptake detected in Raji WT and Raji R116A cells was reduced (**Fig. 4.3F**). Since we improved specificity of $JUN_{Z\text{-}eGFP}$ VLP uptake by filtering the VLPs, we used this strategy with primary DCs as well. We confirmed previous findings showing that $JUN_{Z\text{-}eGFP}$ VLP capture was higher

in IFNα- and LPS-stimulated DCs compared to iDCs (**Fig. 4.3G**). Furthermore, filtered and concentrated $JUN_{Z\text{-}eGFP}$ VLPs exhibited even higher uptake levels than previously (**Fig. 4.2C and 4.3B**), with around a 60% uptake observed in both IFNα- and LPS-stimulated DCs (**Fig. 4.3G**). Moreover, using filtered stocks we again confirmed that Junín VLP uptake in DCs is dependent on Siglec-1, as seen by pre-treatment of the cells with an anti-Siglec-1 mAb (**Fig. 4.3H**). In this filtered and improved VLP system we detected for the first time a blocking effect of the anti-Siglec-1 mAb in iDCs (**Fig. 4.3H**). Overall, these results indicate that soluble eGFP generated via VLP production interfered with uptake experiments and generated an unspecific background signal also present in the immunostaining protocol, which amplified soluble eGFP. However, $JUN_{Z\text{-}eGFP}$ VLP filtration removed soluble eGFP, allowing us to verify Siglec-1 capacity to interact with these viral particles.

Siglec-1 recognizes several enveloped viruses and drives their polarization and engulfment within virus containing compartments (VCCs), which are continuous with the plasma membrane and connected to the extracellular space[81,82]. To elucidate whether Siglec-1 also recruits arenavirus to these compartments, we investigated viral uptake by confocal microscopy (**Fig. 4.3I and 4.3J)**. LPS-activated DCs exposed to fluorescent arenavirus VLPs showed $JUN_{Z\text{-}eGFP}$ VLPs attached to Siglec-1 receptors, which polarize (**Fig. 4.3I**) and drove VCC formation **(Fig. 4.3J**). The combination of several methods, including the detection of Siglec-1 interacting with GM1 ligands on $JUN_{Z\text{-}eGFP}$ VLP particles, the blocking effect of specific mAbs on primary DCs, and the *de novo* expression of Siglec-1 on Raji cells, along the formation of the well-known VCC provided different sources of evidence showing that Siglec-1 acts as an attachment receptor for Junín uptake.

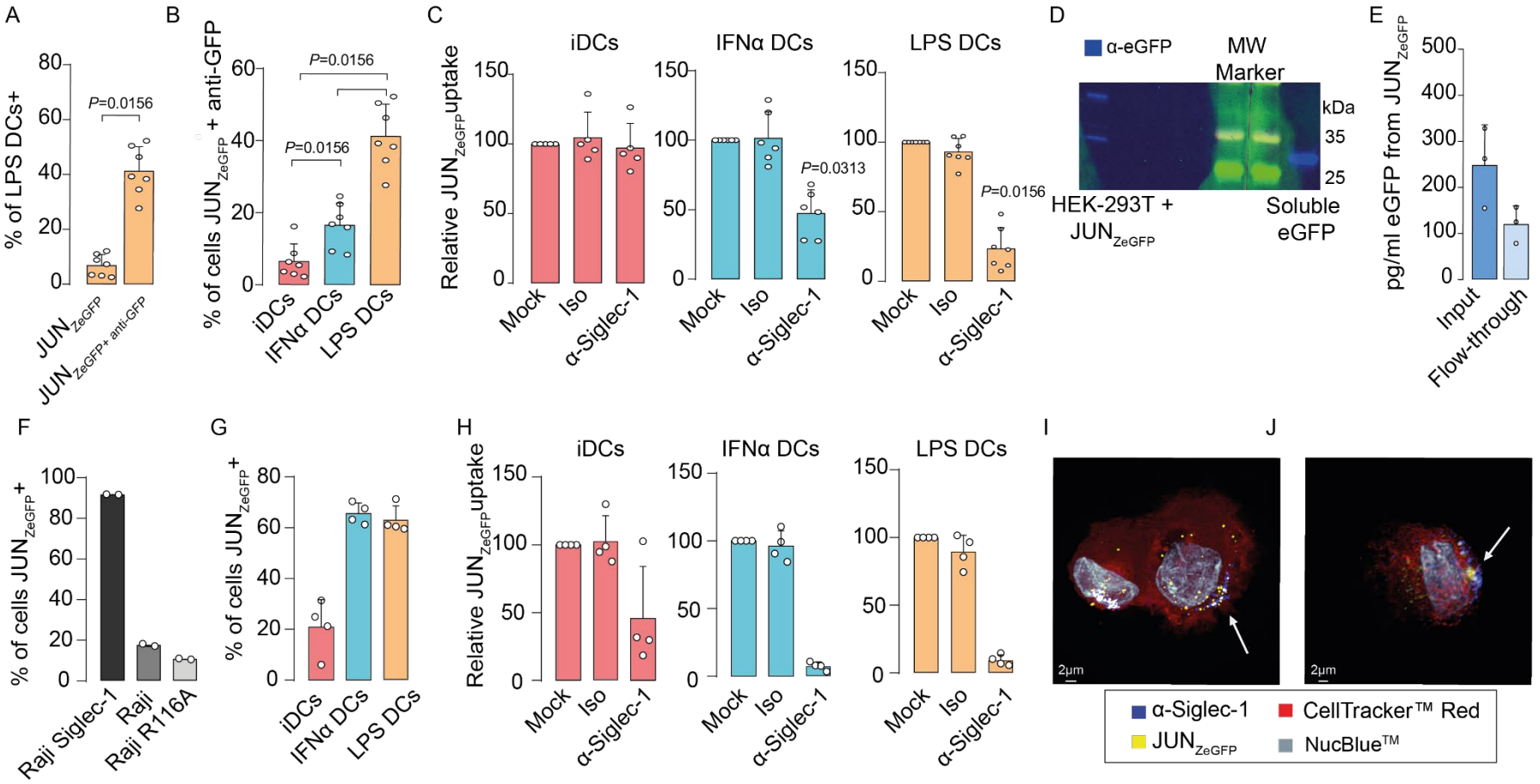

Figure 4.3 Capture overleaf

Figure 4.3. $JUN_{Z\text{-}eGFP}$ VLP filtration confirms Siglec-1 recognition. A. Comparative uptake of $JUN_{Z\text{-}eGFP}$ VLP and immunolabelled $JUN_{Z\text{-}eGFP}$ VLP by LPS activated DCs that were pulsed for 4h at 37°C and assayed by FACS. Values from seven donors and two experiments. Statistical differences were assessed with a Wilcoxon non-parametric test. **B**. Comparative uptake of immunolabelled $JUN_{Z\text{-}eGFP}$ VLP by non-activated or activated DCs that were pulsed for 4h at 37°C detected by FACS. Values from seven donors and two experiments. Statistical differences were assessed with a Wilcoxon non-parametric test. **C**. Relative uptake of different DCs pre-incubated or not with anti-Siglec-1 7-239 mAb. Values from 5 donors and two experiments. Statistical differences were assessed with a one-sample Wilcoxon test. **D**. Western-Blot analysis of HEK 293T cell pellet transfected or not with $JUN_{Z\text{-}eGFP}$ plasmid. Anti-eGFP mAb was used as an indirect way to confirm the presence of chimeric $JUN_{Z\text{-}eGFP}$ protein (~38 kDa). Bands in blue correspond to eGFP detection. On the right side, soluble eGFP (27 kDa) was added as a control. **E**. eGFP ELISA quantification results from $JUN_{Z\text{-}eGFP}$ VLPs. The concentration of eGFP of input and flow-through fractions are compared. Each point corresponds to one VLP preparation. **F**. Comparative uptake of concentrated $JUN_{Z\text{-}eGFP}$ VLPs by distinct Raji B cells that were pulsed for 1h at 37°C and assayed by FACS. Values from two replicates and one experiment. **G**. Comparative uptake of concentrated $JUN_{Z\text{-}eGFP}$ VLPs by immature or activated DCs that were pulsed for 4h at 37°C and detected by FACS. Values from four replicates and two experiments. **H**. Uptake of concentrated $JUN_{Z\text{-}eGFP}$ from DCs pre-incubated or not with an anti-Siglec-1 mAb assayed by FACS. Statistical differences were assessed with a one sample Wilcoxon test. Values from four different donors and two experiments. **I**. 3D reconstruction of LPS-activated DCs analysed by confocal microscopy pulsed with $JUN_{Z\text{-}eGFP}$ VLPs and stained with anti-Siglec-1 mAb (blue), nucleus with NucBlue (grey) and cytoplasm with Cell-tracker™ Red Far-Red Dye (red). Arrow indicates polarized VLPs **J**. 3D reconstruction of LPS-activated DCs as described in I. Arrow indicates VCC containing $JUN_{Z\text{-}eGFP}$.

4.4.4. Siglec-1 mediates the recognition and uptake of Lassa VLPs

We next tested if fluorescent Lassa VLPs generated by transfecting the Lassa protein Z fused to eGFP ($LAS_{Z\text{-}eGFP}$ VLPs) could follow the same uptake mechanism seen for Junín particles. We first analysed the pellet from $LAS_{Z\text{-}eGFP}$ transfected HEK 293T cells by WB and, as previously observed for Junín, we found soluble eGFP being produced at similar levels as the chimeric $LAS_{Z\text{-}eGFP}$ protein (**Fig. 4.4A**). In this case, a commercial anti-Lassa Z protein was available, and we were able to directly detect this viral protein. Of note, untagged eGFP viral protein was also detected (**Fig. 4.4A**). We also compared the eGFP quantity in the non-filtered and the filtrated flow-through of $LAS_{Z\text{-}eGFP}$ VLP using a GFP ELISA kit. Results showed that after filtering the VLPs through a 100 kDa pore size limit centrifugal device, the flow-through sample eGFP concentration was again around half of the input added (**Fig. 4.4B**). We then compared the unfiltered and concentrated VLP uptake in Raji cells (**Fig. 4.4C-D**). Concentrated VLPs showed certain increase in VLP uptake in Raji Siglec-1 cells, and a reduction in uptake levels in Raji WT and R116 cells (**Fig. 4.4C-D**). Overall, and as previously observed for Junín, removing the background signal derived from soluble eGFP from the VLPs improved Siglec-1-dependent capture and confirmed the key role of this receptor in arenavirus uptake.

We also replicated the experiments performed with Junín in DCs using a concentrated $LAS_{Z\text{-}eGFP}$ stock to remove soluble eGFP. We pulsed DCs with an equal amount of VLPs and observed that viral uptake was significantly increased in activated DCs expressing higher levels of Siglec-1 (**Fig. 4.4E**). When cells were pre-incubated with an anti-Siglec-1 mAb, LASZ-eGFP VLP uptake was abrogated in all DCs tested (**Fig. 4.4F**). These results indicate that both

Lassa and Junín VLPs are recognized by Siglec-1. Finally, we employed a comparable experimental approach using confocal microscopy to examine the viral uptake process of Lassa VLPs. LPS-activated DCs were exposed to $LAS_{Z\text{-}eGFP}$ VLP, and as previously found for Junín VLPs, we observed VLP attachment via Siglec-1 and polarization (**Fig. 4.4G**), leading to the formation of VCCs (**Fig. 4.4H**). These findings support the role of Siglec-1 as an attachment receptor for Lassa, facilitating viral uptake through recognition of sialic acid on $LAS_{Z\text{-}eGFP}$ VLPs.

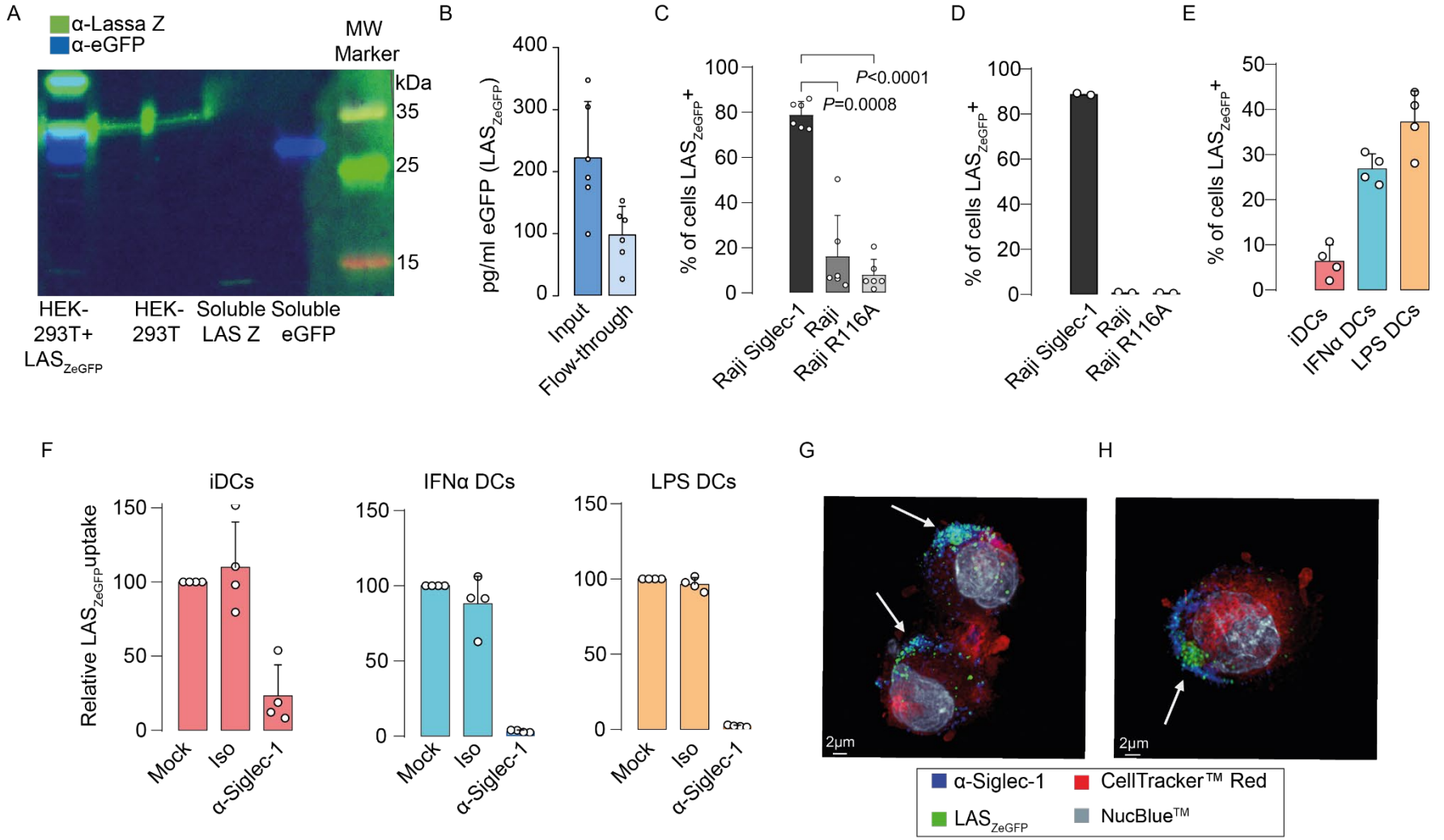

Figure 4.4 Capture overleaf

Figure 4.4. Siglec-1 mediates the recognition and uptake of Lassa VLPs. A. Western-Blot analysis of HEK 293T cell pellet transfected or not with $LAS_{Z\text{-}eGFP}$ plasmid. Antibody for the detection of Lassa Z (11 kDa) protein is shown in green. eGFP was also detected to confirm the presence of chimeric $LAS_{Z\text{-}eGFP}$ protein (~38 kDa) and is shown in blue band. Soluble eGFP (27 kDa) and soluble Lassa Z protein were added as a control. **B.** eGFP ELISA quantification from the $LAS_{Z\text{-}eGFP}$ VLP production. The concentration of eGFP of input and concentrated fractions are compared. Each point represents one VLP preparation. **C.** Uptake of non-filtered $LAS_{Z\text{-}eGFP}$ VLPs by distinct Raji B cells pulsed for 1h at 37°C and assayed by FACS. Values from six replicates and two experiments. Statistical differences were assessed with a Wilcoxon non-parametric test. **D.** Uptake of concentrated $LAS_{Z\text{-}eGFP}$ VLPs by distinct Raji B cells pulsed and assayed as previously described. Values from two replicates and one experiment. **E.** Uptake of filtered $LAS_{Z\text{-}eGFP}$ VLPs by distinct DCs that were pulsed for 4h at 37°C and analysed by FACS. Values from four donors and two experiments. **F** Uptake from DCs pre-incubated with or without commercial anti-Siglec-1 7-239 mAb. Values from four donors and two experiments. Statistical differences were assessed with one-sample Wilcoxon test. **G.** 3D reconstruction of LPS-activated DCs analysed by confocal microscopy pulsed with $LAS_{Z\text{-}eGFP}$ VLPs and stained with anti-Siglec-1 mAb (blue), nucleus with NucBlue (grey) and cytoplasm with Cell-tracker™ Red Far-Red Dye (red). Arrow indicates polarized VLPs. **H.** 3D reconstruction of LPS-activated DCs as described in G. Arrow indicates VCC containing $LAS_{Z\text{-}eGFP}$.

4.4. Conclusions

Siglec-1 is able to act as an attachment receptor for arenavirus VLPs in primary DCs. Uptake is Siglec-1 dependent and increased in cells expressing higher Siglec-1 levels on their surface, as previously shown for HIV-1, Ebola virus, and SARS-CoV-2[53,58,262,279]. This interaction can be blocked with anti-Siglec-1 antibodies, which specifically target the V-set domain and block functional viral recognition of sialylated ligands such as GM1. Given that our group has previously developed anti-Siglec-1 mAbs that block the recognition of HIV-1 and Ebola viruses[53], and that here we were able to confirm the role of this receptor on SARS-CoV-2 and Arenaviruses capture, we next wanted to address if these particular mAbs developed by our team were also effective against these new enveloped viruses.

Chapter 5 – RESULTS III: Siglec-1 as a therapeutic target for a pan-viral antibody treatment

5.1. Introduction

Siglec-1 is the key molecule for HIV-1 *trans-infection,* and it is likely to play a critical role in aiding Ebola virus propagation[53,58,68]. In the first chapter of results of this thesis we have shown that Siglec-1 can play an important role in the pathogenesis of SARS-CoV-2 virus by aiding its capture and *trans-infection* to target cells. In the second chapter, we have also showed that arenaviruses can be captured via Siglec-1 and might act as an auxiliary receptor. Preventing viral propagation in the early stages of viral infection can be critical to improve disease outcome. Nowadays antiviral treatments are limited, and a preventive strategy can provide some advantage to reduce the severity of the infection. Anti-Siglec-1 mAbs generated by our group have previously demonstrated blocking activity against enveloped viruses HIV-1 and Ebola virus in DCs. In this thesis now we have shown that SARS-CoV-2 virus uptake and *trans*-infection along with arenavirus uptake in DCs can be blocked by commercial anti-Siglec-1 mAbs. Since therapies with mAbs have demonstrated to be effective either as prophylaxis or as a therapeutic treatment[311], our anti-Siglec-1 mAbs could potentially be used as an antiviral therapy for multiple enveloped viruses.

Anti-Siglec-1 mAbs generated by our group were produced in a murine model, and therefore were not suitable for human administration. Despite their efficacy *in vitro*, murine antibodies are known to trigger an immunogenic response due to the ability of human immune system to recognize rodent antibodies and eliminate them[238]. This problem was found in the 1980s and mostly focused on replacing or removing the Fc region, which is the most immunogenic. In order to overcome it, the first step to reduce the risk of immunogenicity was to generate antigen-binding fragments (Fabs). Fabs are made of antibody variable domains, lacking the Fc region, and they can bind to target antigen without triggering the effector functions such as cell-mediated cytotoxicity or complement-dependent cytotoxicity[227,312]. Another molecular engineering approach is to engineer chimeric antibodies with human Fc regions with murine variable regions[238,313,314]. Yet even the murine antibody V-domain has a potential risk of immunogenicity[6.] That is why antibody engineering has gone a step further by humanizing murine antibodies. One of these humanization methods consist in engrafting mouse CDRs into human frameworks[255,311,314] highly reducing the risk of immunogenicity.

Here we report our approach to generate anti-Siglec-1 Fabs and humanized anti-Siglec-1 mAbs that were effectively tested in functional assays. Fabs from the murine anti-siglec-1 mAbs previously generated by our group were tested for their blocking capacity against HIV-1 viral particles. Furthermore, humanized anti-Siglec-1 mAbs adapted from the murine anti-

Siglec-1 mAbs previously generated by our group were also tested for their blocking activity against a panel of pathogenic enveloped viruses in DCs. Both products could be promising tools to combine with current antiviral treatments and generate an efficient combined therapy to fight enveloped virus propagation.

5.2. Methods

5.2.1. Ethics statement

The institutional review board on biomedical research from Hospital Germans Trias i Pujol (HUGTiP) approved this study.

5.2.2. Cell Lines

HEK293T, Raji B lymphocyte, Raji R116A, Raji Siglec-1 Vero-E6 were maintained as previously described (**Chapter 3, Material & Methods 2.3**).

5.2.3. Primary cell culture

MDDCs were obtained and activated as previously described (**Chapter 4, Materials & Methods 2.2**).

5.2.4. Viral particle generation

HIV-$1_{Gag\text{-}eGFP}$ VLP stocks were generated by transfection of HEK-293T cells with the molecular clone pGag-eGFP obtained from the US National Institutes of Health (NIH) AIDS Research and Reference Reagent Program. HEK-293T cells were transfected in T75 flasks with 30 µg of plasmid DNA using calcium phosphate (CalPhos; Clontech) and incubated during 48 h at 37ºC. Supernatants containing HIV-$1_{Gag\text{-}eGFP}$ VLPs were harvested, filtered (Millex HIV, 0.45 µm; Millipore) and frozen at -80ºC until use. The p24Gag content of viral and VLP stocks was determined by enzyme-linked immunosorbent assay (ELISA) (Perkin-Elmer).

The replication-competent HIV-1 stock was generated by transfecting HEK-293T cells with the proviral construct HIV-$1_{NFN\text{-}SX}$, an HIV-$1_{NL4\text{-}3}$ provirus that expresses the HIV-1_{JRFL} envelope glycoprotein (kindly provided by W. O'Brien). 30 µg of plasmid DNA were added to cells in T75 flasks, and transfection was performed using a calcium phosphate kit (Calphos; Clontech). Supernatants were harvested 48 h post transfection, filtered (Millex-HV, 0.45µm; Millipore) and frozen at -80ºC until use. The $p24^{Gag}$ content of VLP and HIV-1 stocks was determined by ELISA (Perkin-Elmer). $Ebo_{VP40\text{-}eGFP}$ VLPs were generated transfecting HEK-293T cells with the molecular clone CAGGS-eGFP-VP40 (kindly provided by Dr. Bieniasz).

For Ebo-$GP_{VP40\text{-}BlaM}$ VLPs, cells were transfected with molecular clones pcDNA3.1-BlaM-VP40, pcDNA3-Zaire NP and pcDNA3.1-Zaire GP (all from BEI Resources). HEK-293T cells were transfected with calcium phosphate (CalPhos; Clontech) or X-tremeGENE 9 DNA Transfection Reagent (Merck) in T75 flasks using a total of 20-30 µg of plasmid DNA at equimolar ratios. Supernatants were harvested 72h post-transfection, cleared of cellular debris by centrifugation and frozen at -80ºC until use. The VP40 content of VLP stocks was determined by a home-

made sandwich ELISA using mouse IgG1 anti-VP40 mAbs to coat Nunc MaxiSorp plates (Invitrogen) and a mouse IgG2a anti-VP40 mAb to detect bound protein (both from Fitzgerald). Goat anti-mouse IgG2a HRP (Jackson ImmunoResearch) was employed to reveal the assay. Purified VP40 protein (IT Bioservices) was used as a standard for quantification.

SARS CoV-2 was generated as previously described (**Chapter 3, Methods 2.5**)

5.2.5. Fab generation

Fabs were generated by using Pierce™ Fab Micro Preparation Kit (Thermo) and following the manufacturer instructions. After Fab generation, for the Fab purification step, we used NAb™ Protein G Spin Column Kit (Thermo) instead of NAb™ Protein A Plus Spin Column provided with the kit to try maximizing the yield.

5.2.6. Fab Wester-Blot analysis

Fabs Fc region removal was checked by Western-Blot Analysis. Anti Siglec-1 mAbs and generated Fabs were diluted in 4x Laemmli Sample Buffer for SDS-PAGE so that 1 µg of protein was loaded in each well. The analysis was run as previously described (**Chapter 4, Material & Methods 4.2.7**).

5.2.7. Fab cytometry analysis

Fabs Fc region removal was also checked by immunolabelling and cytometry analysis. 0.4 $x10^6$ Raji Siglec-1 cells were incubated for 15 minutes at RT with either anti-Siglec-1 Fabs, murine mAbs or an IgG1 Isotype control (BD Biosciences) at a constant concentration of 20 µg/ml. After this, cells were washed and AF 647 Goat anti-Mouse IgG Fcg mAb (Jackson Immuno Research) was added at a 1/500 final dilution. After being incubated for 15 minutes at RT cells were washed again and Fc region presence was checked.

5.2.8. Fab titration

Anti-Siglec-1 murine mAbs and Fabs were diluted to an 80 µg/ml final concentration in a final volume of 100 µl. Commercial anti-Siglec-1 and IgG1 Isotype control were used as controls. After this, each condition was 2:3 serially diluted 12x times to cover a concentration range from 20-0.2 µg/ml. Then, in a 96 well plate, 0.2 $x10^6$ Raji Siglec-1 cells were added to each condition and dilution. Anti-Siglec-1 murine mAb or Fab mix was added and immediately after 50 µl of $HIV_{Gag\text{-}eGFP}$ VLPs. Cells were incubated for 1 hour at 37 ºC and then washed thoroughly. Finally, VLP uptake was assessed in a Canto (BD) cytometer.

5.2.9. Fab VLP blocking experiments.

Fab blocking effect was tested in Raji Siglec-1 cells by pre-incubating $0.4x10^6$ cells with a saturating Fab final concentration of 20 µg/ml for 15 minutes and followed by 30-minute

incubation with 50 µl of $HIV_{Gag\text{-}eGFP}$ VLPs at 37 ºC. Original murine anti-Siglec-1 and IgG1 Isotype were used as controls. Cell fluorescence was checked by cytometry in Canto (BD) cytometer. After this, Fabs blocking effect was also tested in DCs with both $HIV_{Gag\text{-}eGFP}$ VLPs and HIV $_{NL43\text{-}iGFP}$ virus. In both cases $0.25x10^6$ LPS stimulated DCs were pre-incubated with a saturating Fab final concentration of 20 µg/ml for 15 minutes, followed by 1 hour incubation with 100 µl of $HIV_{Gag\text{-}eGFP}$ VLPs or HIV $_{NL43\text{-}iGFP}$ virus. Finally, VLP or virus uptake was assessed in a Canto (BD) cytometer.

5.2.10. Antibody cloning

Total RNA isolated from hybridomas was reverse transcribed into cDNA using isotype-specific anti-sense primers or universal primers following the technical manual of PrimeScriptTM 1st Strand cDNA Synthesis Kit. The antibody fragments of VH, VL, CH and CL were amplified according to the standard operating procedure of rapid amplification of cDNA ends (RACE) of GenScript and followed by sequencing analysis.

Mouse VH and VL of murine antibodies were aligned by Ig Blast-NCBI (https://www.ncbi.nlm.nih.gov/igblast) to get the closest human related V gene sequences and to identify the framework residues (FRs) and complementarity-determining regions (CDRs). For the humanization process, mouse residues forming the CDRs were retained while the FRs residues not matching between mouse and human germline were changed to the residue present in the human V gene.

Constructs with the murine VH and VL sequences of #1F5, #3F1 and #5B10 antibodies were ordered at Invitrogen to produce each antibody as both mouse/human chimeric hIgG1 and humanized CDR-engrafted hIgG1. For the light chain, constructs encoding for the whole light chain (VL + CL) were obtained directly from Invitrogen cloned into the pcDNA3.1 mammalian expression vector. For the heavy chain, constructs encoding for the VH flanked by the HindIII and NheI restriction sites were ordered at Invitrogen cloned into the pMA-RQ vector. Each VH was excised from the pMA-RQ vector by HindIII and NheI digestion and cloned into a pcDNA3.1 vector that already contained the human IgG1 constant domains. DNA encoding for anti-Siglec-1 variants to remove potential sequence liabilities was ordered at Invitrogen or generated by site directed mutagenesis. All constructs were amplified by maxiprep and sequenced for validation.

5.2.11. Antibody production

Suspension growing HEK FreeStyle™ 293-F Cells (Ref. R790-07, ThermoFisher Scientific) were cultured in FreeStyle™ 293 Expression Medium (Ref. 12338026, ThermoFisher Scientific) at 37°C with 8% CO2. The day of the transfection cells were centrifuged and seeded at density of 1E6cell/mL in fresh Freestyle medium. Plasmids encoding for the heavy and kappa chain of each antibody were transiently PEI mediated transfected (Polyethylenimine; Ref. 24765-1, Polysciences Inc.) together with 3 helper plasmids (pORF21, pORF27 and p33-SV40LT). Transfection mixtures per 100 mL of cell culture contained: 31.35 µg of heavy chain construct, 37.65 µg of light chain construct, 31 µg of helper vectors mix, 300 µg PEI and 6 mL of optiMEM (Ref. 51985026, ThermoFisher Scientific). Transiently transfected HEK293FS cells were cultured at 100 mL scale for 6 days at 37°C, 8% CO2. The culture medium was harvested by centrifugation and the antibodies were purified from the culture medium using Protein A beads and eluted using citrate buffer (20 mM citrate, 150 mM NaCl, pH=3.5) followed by neutralization with phosphate buffer (KH_2PO_4/K_2HPO_4 pH=8). Buffer was changed into 5% Glucose, 5 mM Sodium Acetate, pH4.5 by Pierce Protein Concentrator PES, 10 kDa (Ref. 88517, Pierce). Antibody concentration was determined by measuring absorbance at 280 nm. Volume was adjusted to have each antibody at 1 mg/ml.

5.2.12. Sequence liabilities prediction

Structure-based antibody prediction server SAbPred (http://opig.stats.ox.ac.uk/webapps/sabpred) was used to identify potential sequence liabilities. Afterwards, literature search was performed to identify liabilities that have already proven to have a negative impact during the manufacturing process of biological drugs [315–321].

5.2.13. Functional competition assay with Raji Siglec-1 cells

$Raji_{Siglec\text{-}1}$ cell line was generated in our lab to express constitutively Siglec-1 receptor as described previously [53]. This cell line was maintained in RPMI media (Invitrogen) supplemented with 1 mg/ml of geneticin (Invitrogen), 10% FBS (Gibco), 100 IU/ml / 100 ug/ml of penicillin/streptomycin (Capricorn).

HEK-293T (ATCC repository) were cultured in DMEM (Invitrogen) supplemented with 10% FBS, 100 U/ml of penicillin and 100 µg/ml of streptomycin at 37°C with 8% CO_2. $HIV_{Gag\text{-}eGFP}$VLPs stocks were generated by transfecting $1x10^7$ HEK-293T cells with 15 µg of pGag-eGFP plasmid using 15 µl of LipoD293 (Ver. II) reagent (Ref. SL100668, SignaGen). Supernatants containing VLPs were filtered (Millex HV, 0.45µm; Millipore) and frozen at −80°C until use. By using $HIV_{Gag\text{-}eGFP}$VLPs, we can mimic the native virus in the absence of genetic material, making them non-infectious and safe to manipulate.

Serial dilutions from 20µg/ml to 0.2 µg/ml of anti-Siglec-1 antibodies or IgG1 isotype control (AbD Serotec) were prepared in supplemented RPMI media. Then, 50µl of $HIV_{Gag\text{-}eGFP}$ VLPs were added, followed by $Raji_{Siglec\text{-}1}$ cells. Assay was performed for 60 min at 37°C. After washing with PBS, cells were suspended in PBS supplemented with 0.5% FBS and analyzed by FACS to determine VLP uptake. As non-inhibiting controls we used the corresponding mAb isotype controls, while as negative control, we used cells not exposed to the virus particles. All experiments have been performed in duplicates.

5.2.14. Blocking uptake experiments with anti-Siglec-1 hu-mAbs

HIV-1, $Ebo_{VP40\text{-}eGFP}$ and arenavirus uptake experiments were performed pulsing $0.25x10^6$ DCs with a constant amount (100 µl $HIV_{Gag\text{-}eGFP}$, 80 ng $Ebo_{VP40\text{-}eGFP}$, and 120 ng of eGFP JUN_{ZeGFP} or LAS_{ZeGFP}) of viral particles per condition at 37ºC for 4 hours. For blockade, cells were pre-incubated for 15 min at RT with 10ug/ml of anti-Siglec-1 humAbs, commercial anti-Siglec-1 mAb 7-239 (Abcam), an IgG1 isotype control (BD Biosciences) or left untreated before viral exposure. After extensive washing, cells were acquired with a Canto (BD) and the frequency of positive cells was determined using FlowJo software (TreeStar). Forward-angle and side-scatter light gating were employed to exclude dead cells and debris from all analysis. For SARS CoV-2 uptake experiments, the followed procedure was as previously described [302], but uptake levels were determined by SARS-CoV-2 Nucleocapsid protein (NP) High-sensitivity Quantitative ELISA (ImmunoDiagnostics).

5.2.15. Blocking fusion experiments with anti-Siglec-1 hu-mAbs

These experiments were performed as described previously [53]. When non-infectious Ebo-$GP_{VP40\text{-}BlaM}$ VLPs fuse with cellular membranes, they release β-lactamase that can then cleave a CCF2-AM dye loaded into the DC cytoplasm and change its fluorescence emission from fluorescein to courmarin. As opposed to the system previously used to detect viral uptake, this assay selectively detects Ebola virions entering the cytoplasm of the cell by fusion. DCs were preincubated or not with anti-Siglec-1 mAbs as previously described. A constant fusogenic amount of Ebo-$GP_{VP40\text{-}BlaM}$ VLPs was added to 0.25×10^6 cells and incubated overnight at 37 °C. The CCF2-AM substrate (Invitrogen) was added to cells following the manufacturer's instructions, to identify cells in which Ebo-$GP_{VP40\text{-}BlaM}$ cytoplasmic entry had occurred. Cells were acquired with a Canto (BD), and the percentage of positive cells was determined with FlowJo software. To use equivalent numbers of fusogenic viral particles in all entry assays, Ebo-$GP_{VP40\text{-}BlaM}$ VLP stocks were titrated in duplicate by serial 50% dilutions in Vero E6 cells (3×10^4 per well) seeded in 96-well plates, loaded with CCF2-AM substrate, and assessed by FACS.

5.2.16. Blocking trans-infection experiments with anti-Siglec-1 hu-mAbs

For HIV-1 *trans-infection* assays $0.25x10^6$ LPS matured DCs were incubated with a constant amount of $HIV\text{-}1_{NL4\text{-}3}$ for 4 h at 37ºC. For blockade, cells were pre-incubated for 15 min at RT with 10 µg/ml of anti-Siglec-1 humAbs, commercial anti-Siglec-1 7-239 mAb (Abcam), an IgG1 isotype control (BD Biosciences) or left untreated before viral exposure. After extensive washing, cells were co-cultured with the reporter cell line TZM-bl at a 1:1 ratio to measure *trans*-infection. Co-cultures were assayed for luciferase activity 48 h later (BrightGlo luciferase system; Promega) using a EnSight Multimode Plate Reader (Perkin Elmer). Background values from non-HIV-1 pulsed co-cultures were subtracted for each experiment.

For SARS-CoV-2 *trans-infection* experiments we followed the previously described method [302]. HEK-293T over-expressing the human ACE2 or lacking this molecule were used to test if SARS-CoV-2 replication competent virus was *trans*-infected. Uptake experiments with SARS-CoV-2 were performed pulsing $0.25x10^6$ LPS activated MDDCs with an MOI of 0.75 for 3 h at 37ºC. After extensive washing, cells were co-cultured at a ratio 3:1 with HEK-293T cells expressing or not ACE2. Six days later, supernatant was assayed with a SARS-CoV-2 nucleocapsid protein (NP) High-sensitivity Quantitative ELISA (ImmunoDiagnostics).

5.3. Results

5.3.1. Generation and characterization of anti-Siglec-1 Fabs

We have previously demonstrated that murine anti-Siglec-1 mAbs generated by our group can block HIV-1 and Ebola uptake and *trans*-infection or fusion respectively[53]. Over the previous chapters, we also determined that arenavirus uptake and SARS-CoV-2 uptake and *trans-infectio*n were impaired when pre-incubating cells with commercial anti-Siglec-1 mAbs. Given these findings and the potential of Siglec-1 receptor as a therapeutic antiviral target, we generated anti-Siglec-1 Fabs from anti-Siglec-1 murine mAbs.

Our group had previously identified five anti-Siglec-1 mAb clones (3F1, 1F5, 5B10, 4E8 and 6G5) which showed specific binding to Siglec-1 and demonstrated viral blocking capacity[53]. Theses antibodies displayed two different isotypes, IgG1 (3F1, 4E8 and 6G5) and IgG2b (1F5 and 5B10)[53]. After enzymatically digesting the murine mAbs, only the two IgG2b isotype mAbs -1F5 and 5B10- were correctly digested (**Figure 5.1 A**). Although 3F1 mAb with an IgG1 isotype showed fainted bands corresponding to the Fab and light chain in the WB, signal was very weak (**Figure 5.1 A**). As an alternative method to verify the correct enzymatic digestion we checked if the Fc region was still detected after protein A column purification by labelling this region using flow cytometry. Results showed that despite not being detected by WB analysis, the Fc region of 3F1 was still present (**Figure 5.1 B**). These results indicate that 1F5 y 5B10 Fabs were correctly generated.

After verifying that Fabs were correctly produced, we wanted to further investigate if they have retained their blocking activity. Therefore, we checked if the produced Fabs could block HIV-1 uptake in Siglec-1 expressing cells and compared them to the original murine mAbs.

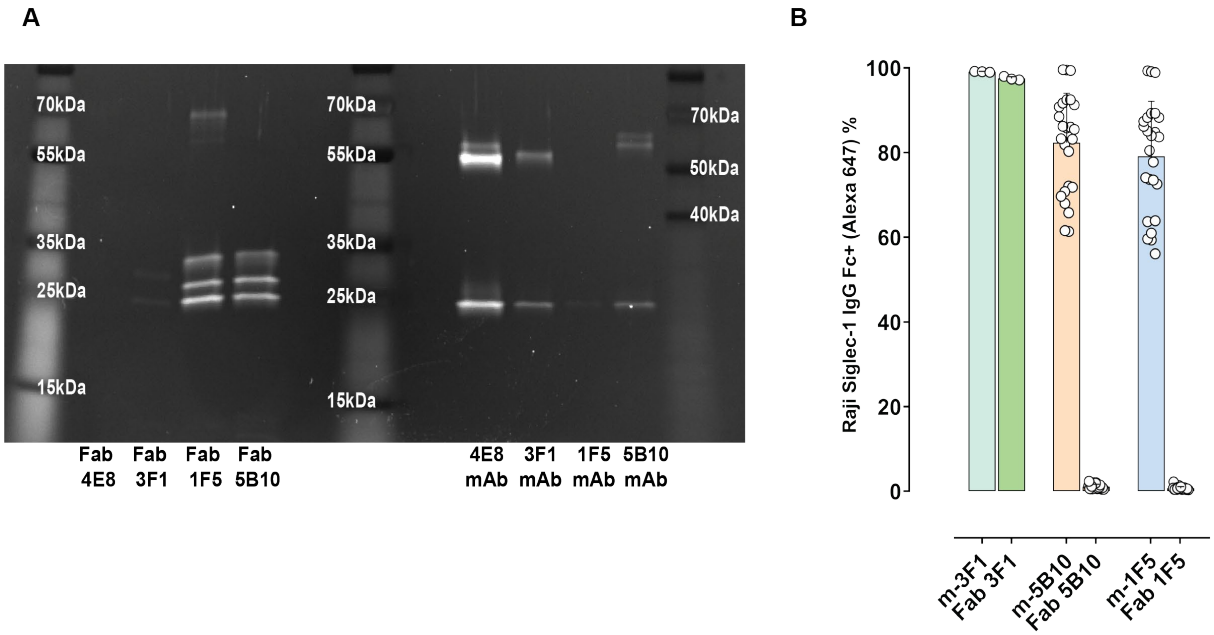

Figure 5.1 Generation and characterization of anti-Siglec-1 Fabs. A. Western-Blot analysis of Fabs and anti-Siglec-1 murine mAbs after enzymatic digestion. Non-digested mAbs show bands for both light and heavy chain (~28kDa and ~50 kDa respectively), while digested mAbs show the reduced Fc corresponding band (~32 kDa) and Reduced Fab + Light Chain (between 26-30 kDa). **B.** Comparative Fc secondary immune-labelling in Raji Siglec-1 cells labelled with generated Fabs. Murine anti-Siglec-1 mAbs were used as controls. Data show mean values and SD from 3 experiments and 25 replicas for 1F5 and 5B10, and 1 experiment and 3 replicas for 3F1.

5.3.2. Anti-Siglec-1 Fabs block HIV-1 uptake via Siglec-1.

Once Fab generation was verified, we tested if the generated Fabs retained their antiviral blocking activity. For this purpose, we used fluorescent HIV-$1_{Gag\text{-}eGFP}$ VLPs lacking the envelope glycoprotein[322–325]. A constant amount of these VLPs was added to Raji Siglec-1 cells pre-incubated with anti-Siglec-1 murine mAbs, Fabs or commercial mAbs at a constant concentration. We used an isotype control or left Raji cells untreated to compare the effect of the treatment. The anti-Siglec-1 Fabs were able to completely block HIV-$1_{Gag\text{-}eGFP}$ VLP uptake as effectively as murine mAbs or commercial mAbs used as control (**Figure 5.2 A**). We next compared the IC_{50} values required to inhibit 50% of capture comparing murine anti-Siglec-1 mAbs and generated Fabs. The IC_{50} concentration of new Fabs was slightly higher than that of the original murine mAbs (**Figure 5.2 B**). Yet, both mAbs and Fabs inhibited in a similar range, and most importantly, both mAbs and Fabs were able to completely block viral uptake at 10 µg/ml (**Figure 5.2 B**).

We next wanted to address if Fabs could also block HIV-1 uptake in primary DCs. LPS stimulated DCs were pre-incubated for 15 minutes with the Fabs, murine mAbs or commercial anti-Siglec-1 mAbs as control at 20 µg/mL saturating concentration and then, we added fluorescent HIV-$1_{Gag\text{-}eGFP}$ VLPs at a constant concentration. DCs were incubated with VLPS at

37º C for 1 hour and acquired by FACS. In both cases the tested Fabs 1F5 and 5B10 blocked HIV VLP capture at the same level as their original mAbs or the commercial control mAbs (**Figure 5.2 C**). We repeated this experiment using fluorescent replicative $HIV_{NL4.3GagiGFP}$ and confirmed that Fabs were able to completely block viral uptake mediated by LPS DCs (**Figure 5.2 D**).

Overall, the generated Fabs have demonstrated antiviral blocking activity against HIV-1Gag-eGFP VLPs in both Raji Siglec-1 cells and LPS-stimulated primary DCs, comparable to the original murine mAbs and commercial control mAbs. These findings suggest the potential of Fabs as effective agents in blocking viral uptake and highlight their utility in antibody-based therapies against enveloped viruses. In addition to the promising results of Fabs in blocking viral uptake mediated by Siglec-1, our research has also focused on the development of humanized antibodies targeting this receptor. These antibodies, engineered to retain the same anti-Siglec-1 blocking activity exhibited by the Fabs, hold potential for advancing antibody-based therapies in the fight against enveloped viral pathogens.

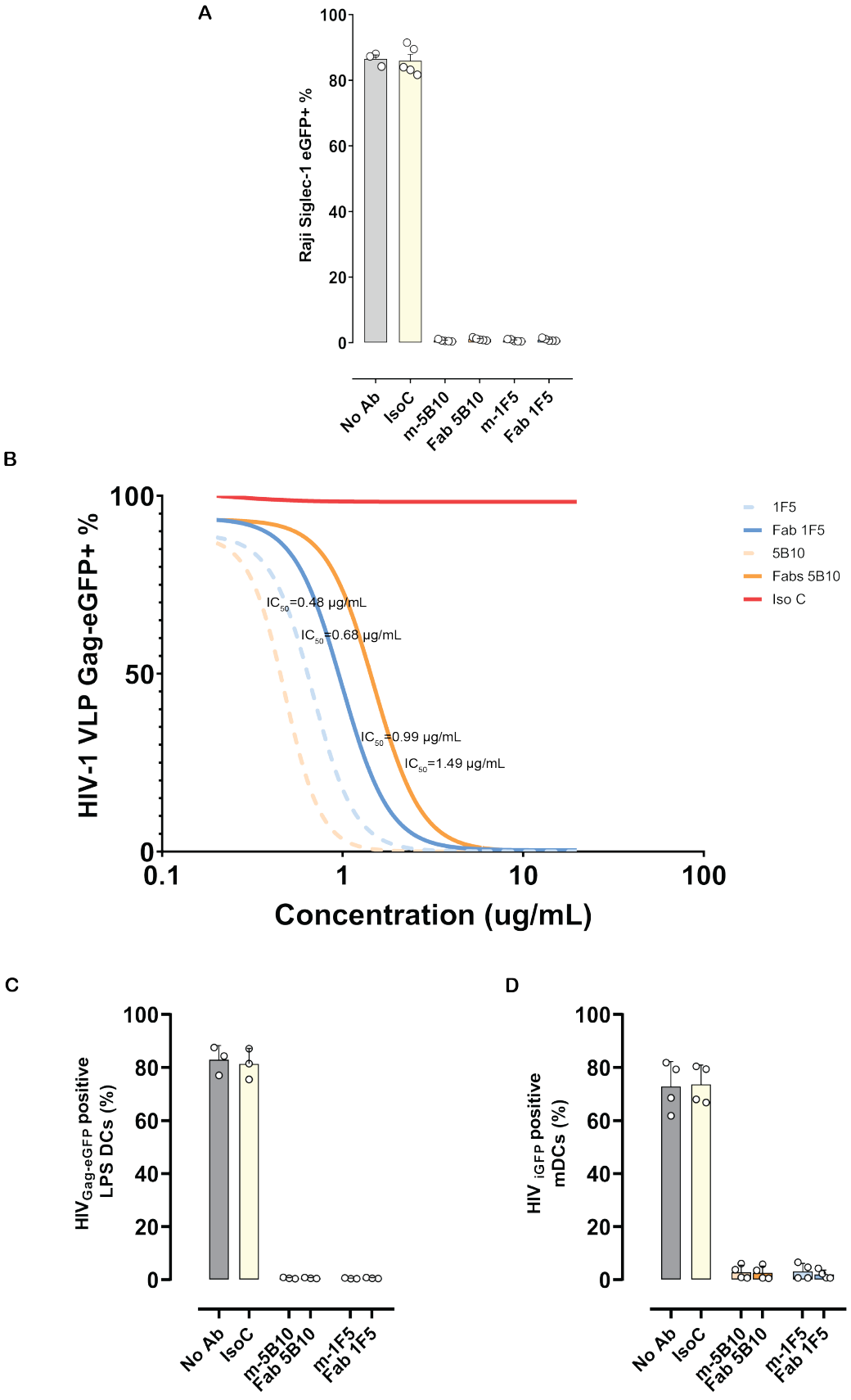

Figure 5.2: Capture overleaf

Figure 5.2 Anti-Siglec-1 Fabs block HIV-1 capture. A. HIV-$1_{Gag\text{-}eGFP}$ VLP uptake is completely blocked in Raji Siglec-1 cells pre-incubated with anti-Siglec-1 Fabs or murine mAbs. We used an IgG Isotype as control. **B.** Comparative IC_{50} values from anti-Siglec-1 Fabs and murine mAbs tested to block $HIV_{Gag\text{-}eGFP}$ VLP in Raji Siglec-1 cells. **C.** Comparative $HIV_{Gag\text{-}eGFP}$ VLP uptake in LPS DCs pre incubated with anti-Siglec-1 Fabs or mAbs Data show mean values and SD from 1 experiment and include cells from 3 donors. **D.** Comparative $HIV_{NL43\text{-}iGFP}$ virus uptake in LPS DCs pre incubated with anti-Siglec-1 Fabs or mAbs. Data show mean values and SD from 2 experiments and include cells from 4 donors.

5.3.3. Generation and characterization of anti-Siglec-1 humAbs

We selected three anti-Siglec-1 monoclonal antibodies (mAbs) to humanize based on their ability to recognize Siglec-1 cellular receptor, and block HIV-1 VLP uptake with highest efficiency [53].

The genomic sequence of these murine antibodies (clones named 1F5, 3F1 and 5B10) was extracted and sequenced from the corresponding hybridomes following the standard operating procedure of GenScript. Then, we generated a chimeric and CDR-engrafted humanized variant for the selected three candidates. For the chimeric variant, murine anti-Siglec-1 variable region of the three candidates were exchanged in a human IgG (**Figure 5.3 A**). In order to generate CDR-engrafted humanized antibodies (named h_0), mouse CDR sequences of 1F5, 3F1 and 5B10 antibodies were aligned by Ig Blast-NCBI to get the closest human related sequences and to identify the framework residues (FRs) and CDRs. Then, mouse residues forming the CDRs were retained while the FRs that were not matching between mouse and human germline were changed to the residue present in the human sequence (**Figure 5.3 A**). Chimeric and humanized CDR-engrafted antibodies were produced by transient transfection in HEK293FS cells and purified using Protein A beads.

To check if the humanization process affected the blocking capacity, we tested if the modified antibodies could block viral uptake of enveloped viruses. Thus, we performed a functional competition assay with $Raji_{Siglec\text{-}1}$ cells and HIV-1 viral like particles (VLPs) expressing eGFP as reporter gene, so that capture of viral particles is then measured by Flow Cytometry (FACS). This way, we could determine if the modified antibodies targeting Siglec-1 retained their blocking capacity and compare them to the original murine mAbs, which were used as a positive blocking control (**Figure 5.3 B-D**). We then compared the IC_{50} for each antibody (**Figure 5.3 E**). Results showed small differences in IC_{50} values between the murine, chimeric, and humanized mAbs. The chimeric variants showed slightly lower IC_{50} values in all cases, while humanized variants showed overall higher IC_{50} values. For 5B10 the humanization process completely removed its blocking capacity, and therefore, we did not continue working with this candidate.

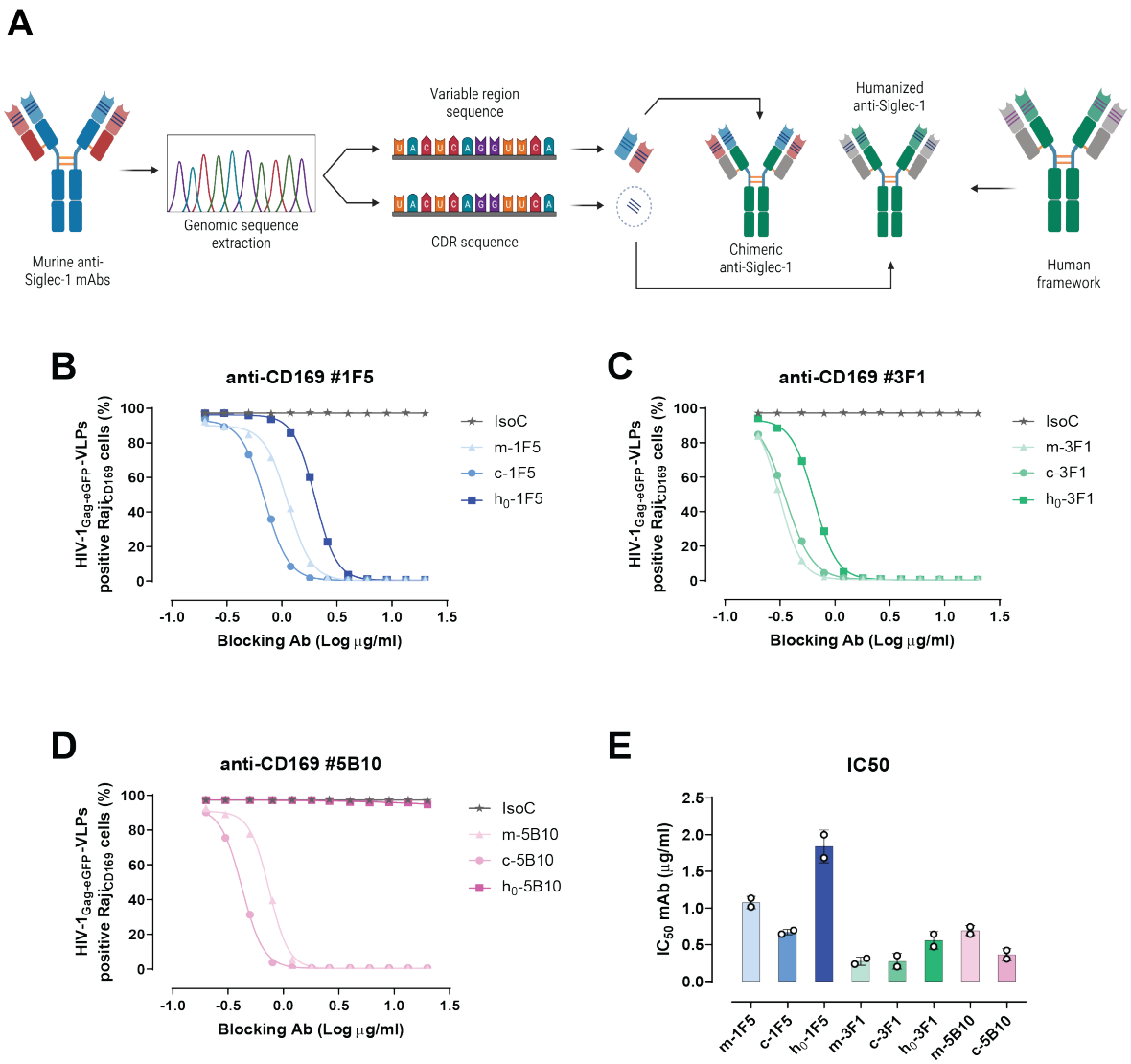

Figure 5.3. **Humanization of anti-Siglec-1-mAbs and functional validation. A.** Diagram illustrating the design of humanized and chimeric anti-Siglec-1 mAbs. **B. C. and D.** Competition for $Raji_{Siglec\text{-}1}$ cells binding between HIV-$1_{Gag\text{-}eGFP}$-VLPs for 1 h at 37 °C. As reference, antibody isotype control is used (IsoC, with grey star symbols). A comparison between original murine antibody (m-, triangle and lighter color), chimeric (c-, circle) and humanized CDR-engrafted (h_0, square and darker color) is shown for each antibody clone (1F5, **B**; 3F1, **C**; 5B10, **D**) corresponding to a non-linear fit to a variable response curve from one representative experiment out of two. **E.** IC_{50} values of individual mAbs that achieved total HIV-$1_{Gag\text{-}eGFP}$-VLP blocking effect. Data from two independent experiments. Created with BioRender.com

Despite chimeric variations showed the best IC_{50} values, the risk of immunogenicity is higher than for humanized mAbs[238]. In addition, there are antibody engineering tools available that can help improving humanized mAbs' performance[255]. Thus, we opted to continue working with the humanized variants for the 1F5 and 3F1 candidates. Before performing more experimental assays, we decided to implement some modifications in the humanized variants trying to improve their affinity/potency and stability. The sequence of the selected antibodies was analysed using SAbPred prediction server in order to find possible sequence liabilities. By this

method, we were able to maintain the conserved regions to keep the stability and correct folding of the antibodies, and we found that the humanized variants of 1F5 and 3F1 contained residues that were prone to oxidation and deamidation in their CDRs. These residues were exchanged by alternative residues that we believed could have minimal impact on the antibody features and activity while mitigating the liabilities found.

[141217]In order to analyse if these modifications alter the functionality of humanized antibodies, we generated 5 variants of h_0-1F5 antibody and 8 variants of h_0-3F1 antibody. We then performed a competition assay between HIV-$1_{Gag\text{-}eGFP}$-VLPs and those anti-Siglec-1 mAbs variants at a single concentration (**Figure 5.4 A**). All mutations introduced in h_0-1F5 antibody loose viral entry blocking capacity except for variant 4. On the other hand, mutations introduced in h_0-3F1 antibody loose viral entry blocking capacity except for variant 6. These two variants that maintained blocking activity similar to the parental antibody (named h_1-1F5 and h_1-3F1) were selected as lead candidates and were further investigated. First, we performed the same functional competition assay with $Raji_{Siglec\text{-}1}$ cells and HIV-$1_{Gag\text{-}eGFP}$ VLP with decreasing concentrations of antibody (**Figure 5.4 B**) and then compared the IC_{50} values between all candidates (**Figure 5.4 C**). h_1-3F1 mAb maintain similar blocking capacity than parental antibodies, while h_1-1F5 showed a higher IC_{50}, similarly to h_0-1F5.

After verifying that the humanization and posterior modifications did not remove the blocking capacity of candidates 1F5 and 3F1, we wanted to further investigate their blocking activity. Therefore, we tested if these candidates could block Siglec-1 interaction with a panel of enveloped viruses in primary DCs while comparing them to the original murine mAbs.

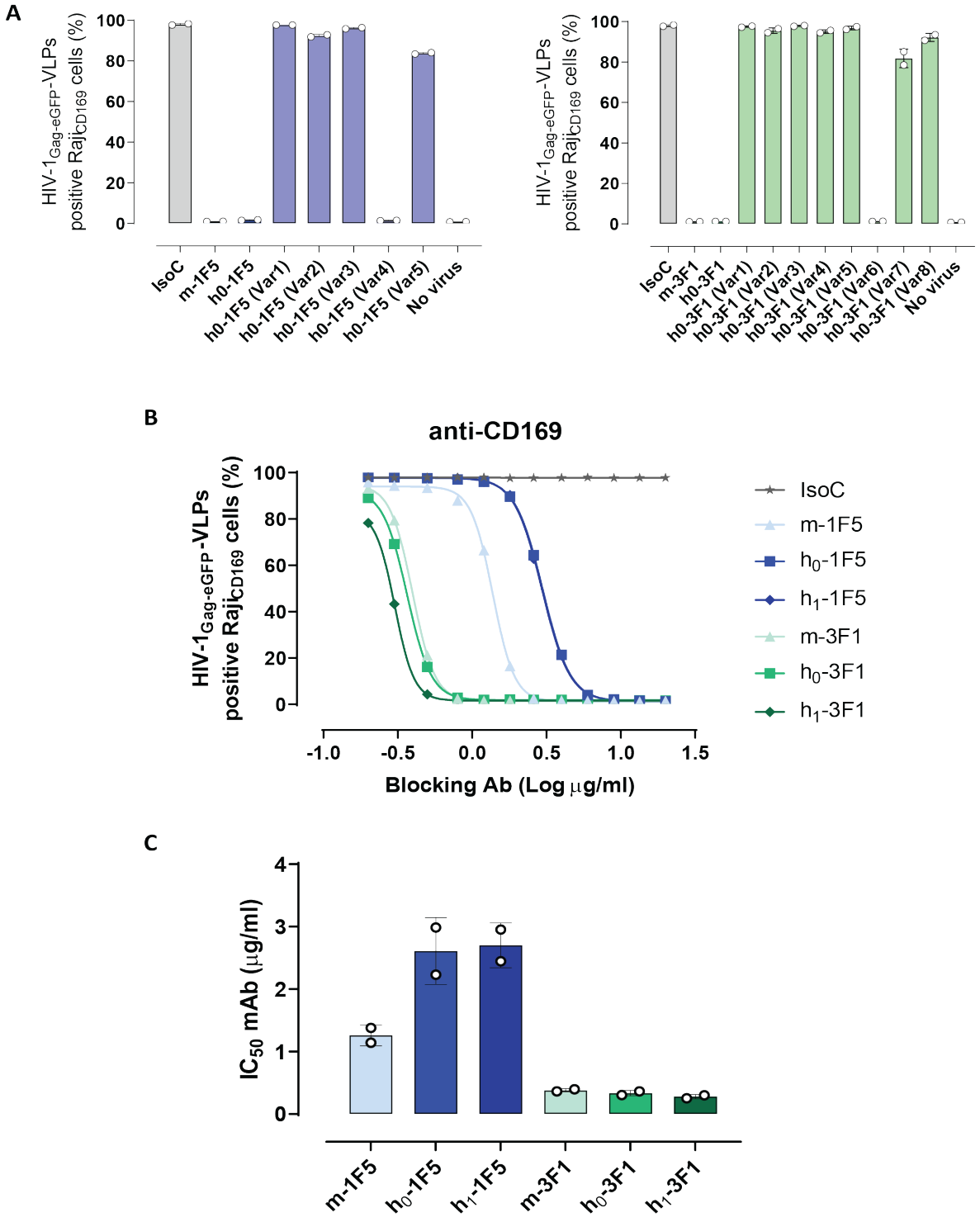

Figure 5.4 Modified humAbs retain Siglec-1 blocking activity A. Competition assay with RajiSiglec-1 cells binding and HIV-1Gag-eGFP-VLPs to test anti-Siglec-1 mAb variants to eliminate selected potential liabilities. **B**. Competition for RajiSiglec-1 cells binding between HIV-1Gag-eGFP-VLPs and anti-Siglec-1 mAbs. We tested 3 different forms of 1F5 and 3F1 antibodies: murine (m-, triangle and lighter colour), humanized (h0-, square) and modified (h1-, diamond). The comparison among these antibodies is shown with a non-linear fit to a variable response curve from one representative experiment out of two. **C**. IC_{50} values of individual mAbs were calculated with non-linear fit to a variable response curve. Data from two independent experiments.

5.3.4. Humanized anti-Siglec-1 mAbs block HIV-1 uptake and trans-infection mediated by LPS DCs

We next assessed if after optimizing the humanized anti-Siglec-1 mAbs they could block HIV-1 viral uptake and *trans*-infection. For this, we used primary MDDCs activated with LPS because it has been previously reported [53,58,134] that viral capture is higher compared to iDCs due to the increased expression of Siglec-1 on these cells. We used fluorescent HIV-$1_{NL4.3\ Gag\text{-}iGFP}$, which is as infectious as native HIV in single-round infectivity assays[326]. LPS DCs were pre-incubated with anti-Siglec-1 mAbs or an isotype control before adding a constant amount of HIV-$1_{NL4.3Gag\text{-}iGFP}$. Pre-treatment with humanized anti-Siglec-1 mAbs inhibited DC capture as effectively as murine anti-Siglec-1 mAbs (**Figure 5.5 A**). We also tested the capacity of humanized anti-Siglec-1 mAbs to block HIV-1 *trans*-infection. For this purpose, we used HIV-$1_{NL4.3}$ infectious virus. LPS treated DCs were pre-incubated with anti-Siglec-1 mAbs or isotype control and pulsed with equivalent amounts of HIV-$1_{NL4.3}$. After extensive washing, DCs were co-cultured with $CD4^+$ reporter TZM-bl cell line, and luciferase induction on these cells by HIV-$1_{NL4.3}$ was measured to assess *trans*-infection. As previously seen for viral uptake, humanized anti-Siglec-1 mAbs efficiently blocked HIV-1 *trans*-infection (**Figure 5.5 B**).

Anti-Siglec-1 humanized mAbs are able to block HIV-1 at the same level as the original murine mabs. Our group has previously demonstrated that the murine anti-Siglec-1 mAbs can also block Ebola virus viral particle uptake and cytoplasmatic entry in primary Dcs[53]. Thus, we wanted to test if humanized anti-Siglec-1 mAbs could block Ebola virus particle uptake and cytoplasmatic entry in primary DCs as well.

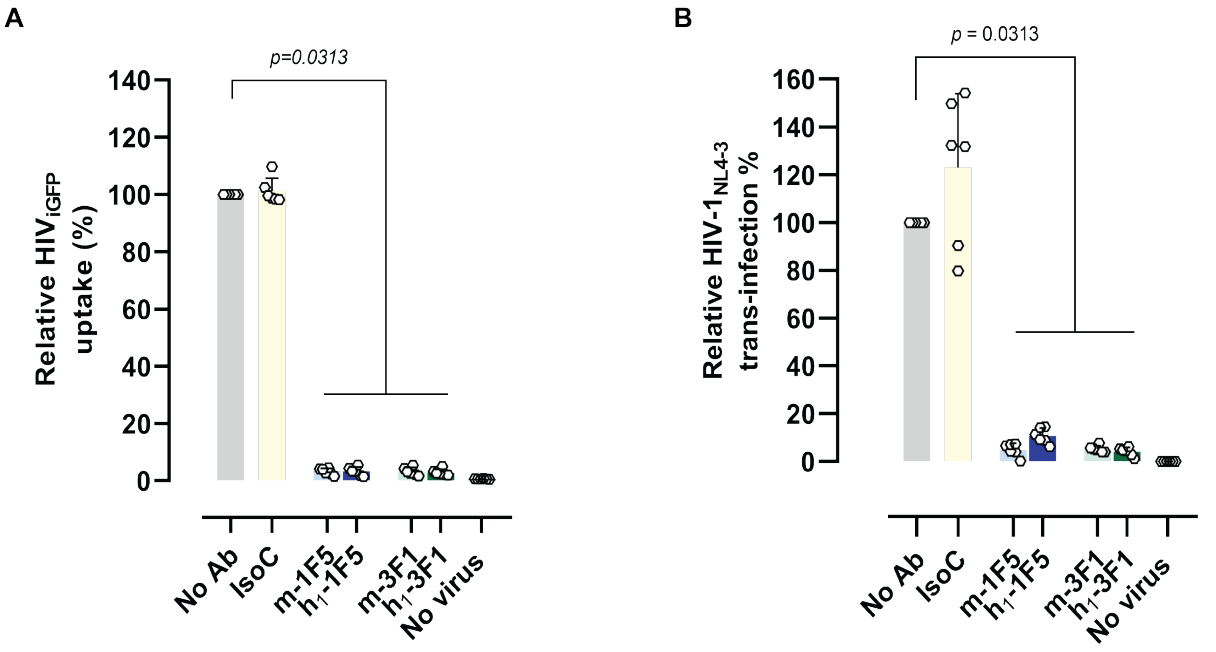

Figure 5.52. Humanized anti-Siglec-1 mAbs block DC-mediated HIV-1 uptake and trans-infection. A. Relative viral uptake of HIV-1 pulsed for 4h at 37ºC with LPS-treated DCs pre-incubated with humanized anti-Siglec-1 mAbs. Values are normalized to cells with Isotype control mAb incubation, with a mean entry of 78.8 ± 9.7% (SD) and set as 100%. Data show mean values and SD from two experiments and include cells from six donors. **B.** Relative HIV-1 trans-infection mediated by LPS-treated DCs pre-incubated with anti-Siglec-1 mAbs. Values are normalized to cells with Isotype control mAb incubation, with a mean entry of 2.83 $x10^6$ ± 2.3 $x10^6$ RLU (SD) and set at 100%. Data show mean values and SD from two independent experiments and include cells from six donors. Statistical differences were assessed using a one-sample Wilcoxon test.

5.3.5. Humanized anti-Siglec-1 mAbs block Ebola uptake and decrease cytoplasmic viral entry into LPS-stimulated DCs.

To assess if humanized anti-Siglec-1 mAbs can block Ebola uptake in primary DCs we have employed fluorescent Ebola VLPs bearing EBOV GP (Ebo-$GP_{VP40\text{-}eGFP}$ VLPs). LPS DCs were pre-incubated with anti-Siglec-1 mAbs or an isotype control before adding a constant amount of Ebo-$GP_{VP40\text{-}eGFP}$ VLPs. Pre-treatment with humanized anti-Siglec-1 mAbs inhibited DC capture at the same level as murine anti-Siglec-1 mAbs (**Figure 5.6 A**). We also tested the capacity of humanized anti-Siglec-1 mAbs to reduce cytoplasmatic entry in activated DCs. To assess if new anti-Siglec-1 mAbs could impact on cytoplasmic viral entry into activated DCs, we employed Ebola VLPs bearing the BlaM-VP40 chimeric protein and EBOV GP (Ebo-$GP_{VP40\text{-}BlaM}$ VLPs). LPS treated DCs were pre-incubated with anti-Siglec-1 mAbs, isotype control or with the CTSB inhibitor CA-074 me, a potent cytoplasmatic viral entry inhibitor[327] as control and pulsed with equivalent amounts of Ebo-$GP_{VP40\text{-}BlaM}$ VLPs. After extensive washing, cytoplasmatic entry was measured by cytometry. As previously seen for viral uptake, humanized anti-Siglec-1 mAbs efficiently blocked Ebola cytoplasmatic entry (**Figure 5.6 B**).

So far, humanized anti-Siglec-1 mAbs have demonstrated the same blocking ability as the original murine mAbs blocking HIV-1 and Ebola virus particle binding to Siglec-1. Over this thesis we have demonstrated that commercial anti-Siglec-1 mAbs, used as positive control in the development of murine anti-Siglec-1 mAbs, could block SARS-CoV-2 interaction with Siglec-1. Therefore, we wanted to further study if humanized anti-Siglec-1 mAbs were also capable of blocking this interaction.

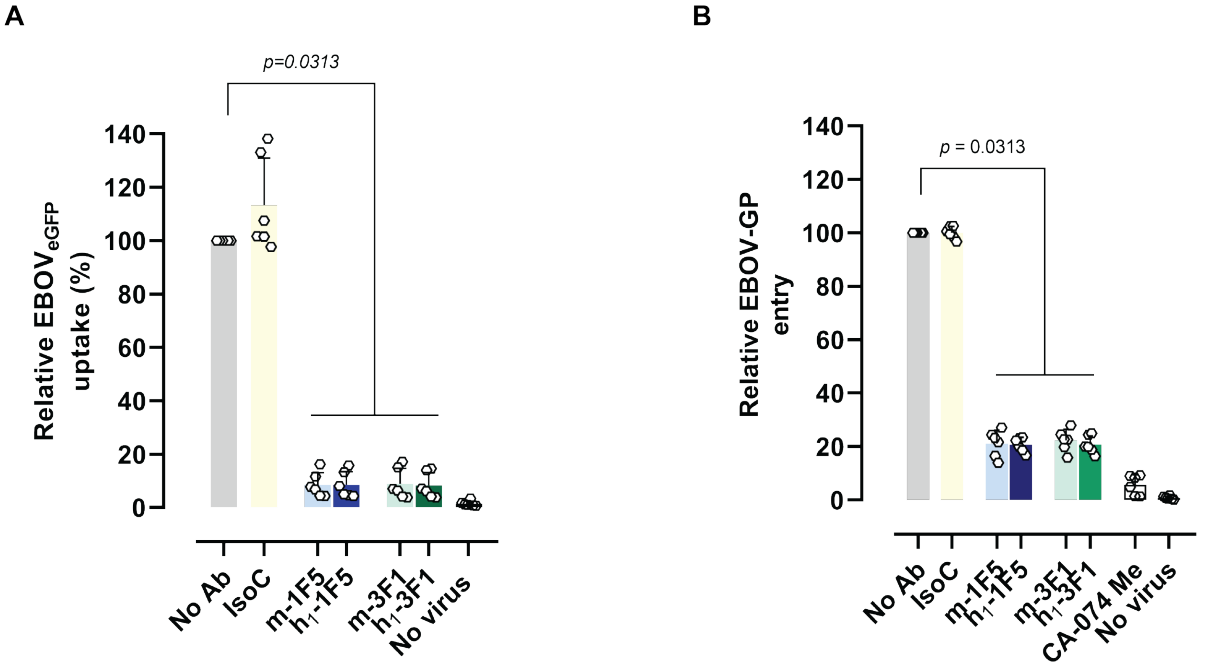

Figure 5.6. Humanized anti-Siglec-1 mAbs block DC-mediated Ebola VLP uptake and internalization. A. Relative viral uptake of Ebo-GP$_{VP40\text{-}eGFP}$ VLPs pulsed for 4 h at 37ºC with LPS-treated DCs pre-incubated with humanized anti-Siglec-1 mAbs. Values are normalized to cells with Isotype control mAb incubation, with a mean entry of 51.2 ± 18.7% (SD) and set as 100%. Data show mean values and SD from two experiments and include cells from six donors. **B.** Relative Ebo-GP$_{VP40\text{-}BlaM}$ internalization mediated by LPS-treated DCs pre-incubated with anti-Siglec-1 mAbs. Values are normalized to cells with Isotype control mAb incubation, with a mean entry of 46.8 ± 14.2% (SD) and set at 100%. Data show mean values and SD from two independent experiments and include cells from six donors. Statistical differences were assessed using a one-sample Wilcoxon test.

5.3.6. Humanized anti-Siglec-1 mAbs block SARS-CoV2 uptake and trans-infection into LPS DCs

We next assessed if humanized anti-Siglec-1 mAbs could block SARS-CoV-2 viral uptake and *trans-i*nfection. For this, we have used primary MDDCs activated with LPS. To test the blocking of viral uptake, LPS DCs were pre-incubated with anti-Siglec-1 mAbs or an isotype control before adding a constant amount of SARS-CoV-2 virus. Pre-treatment with humanized anti-Siglec-1 mAbs inhibited DC capture at the same level as murine anti-Siglec-1 mAbs (**Figure 5.7 A**). We also tested the capacity of humanized anti-Siglec-1 mAbs to block SARS-CoV-2 *trans*-infection. For this purpose, LPS treated DCs were pre-incubated with anti-Siglec-1 mAbs or isotype control and pulsed with equivalent amounts of SARS-CoV-2. After extensive

washing, DCs were co-cultured with HEK293T over-expressing ACE2 and TMPRSS2, and a viral nucleocapsid detection kit was used to assess *trans*-infection by luminometry. As previously seen for viral uptake, humanized anti-Siglec-1 mAbs efficiently blocked SARS-CoV-2 *trans*-infection (**Figure 5.7 B**).

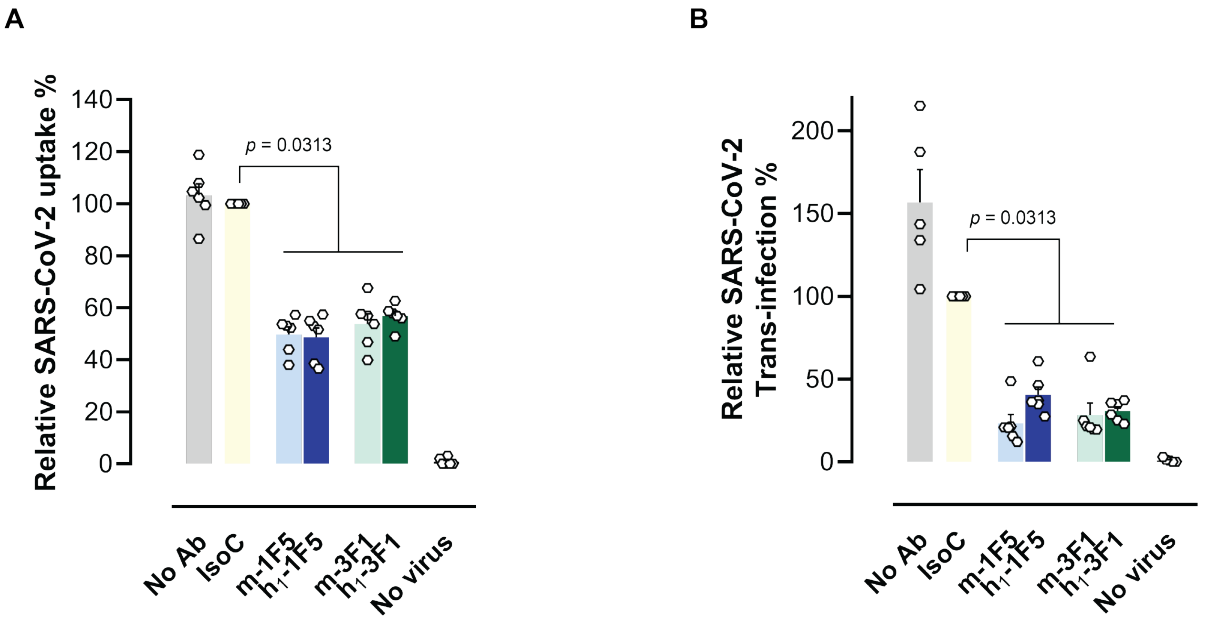

Figure 5.73. **Humanized anti-Siglec-1 mAbs block DC-mediated SARS-CoV-2 uptake and trans-infection. A.** Relative viral uptake of SARS-CoV-2 pulsed for 3h at 37ºC with LPS-treated DCs pre-incubated with humanized anti-Siglec-1 mAbs. Values are normalized to cells with Isotype control mAb incubation, with a mean entry of 13.6 ± 8.2 ng/mL (SD) and set as 100%. Data show mean values and SD from two experiments and include cells from six donors. **B.** Relative SARS-CoV-2 trans-infection mediated by LPS-treated DCs pre-incubated with anti-Siglec-1 mAbs. Values are normalized to cells with Isotype control mAb incubation, with a mean entry of 12.3 ± 2.9 ng/mL (SD) and set at 100%. Data show mean values and SD from two independent experiments and include cells from six donors. Statistical differences were assessed using a one-sample Wilcoxon test.

Anti-Siglec-1 humAbs are able to block the receptor interaction with SARS-CoV-2 as the commercial anti-Siglec-1 in previous sections. In this thesis we have shown that the commercial anti-Siglec-1 could block JUNV and LASV viral particle uptake in primary DCs. Therefore, we wanted to assess if anti-Siglec-1 humAbs could also block this interaction.

5.3.7. Humanized anti-Siglec-1 mAbs block Arenavirus uptake into LPS DCs

Finally, we wanted to assess the capacity of humanized anti-Siglec-1 mAbs to block arenavirus uptake in primary DCs. For this, we have employed fluorescent $JUN_{Z\text{-}eGFP}$ or LAS_{ZeGFP} VLPs as in previous experiments. LPS DCs were pre-incubated with anti-Siglec-1 mAbs or an isotype control before adding a constant amount of arenavirus VLPs. Pre-treatment with humanized

anti-Siglec-1 mAbs inhibited DC capture at the same level as murine anti-Siglec-1 mAbs for both arenaviruses (**Figure 5.8 A-B**).

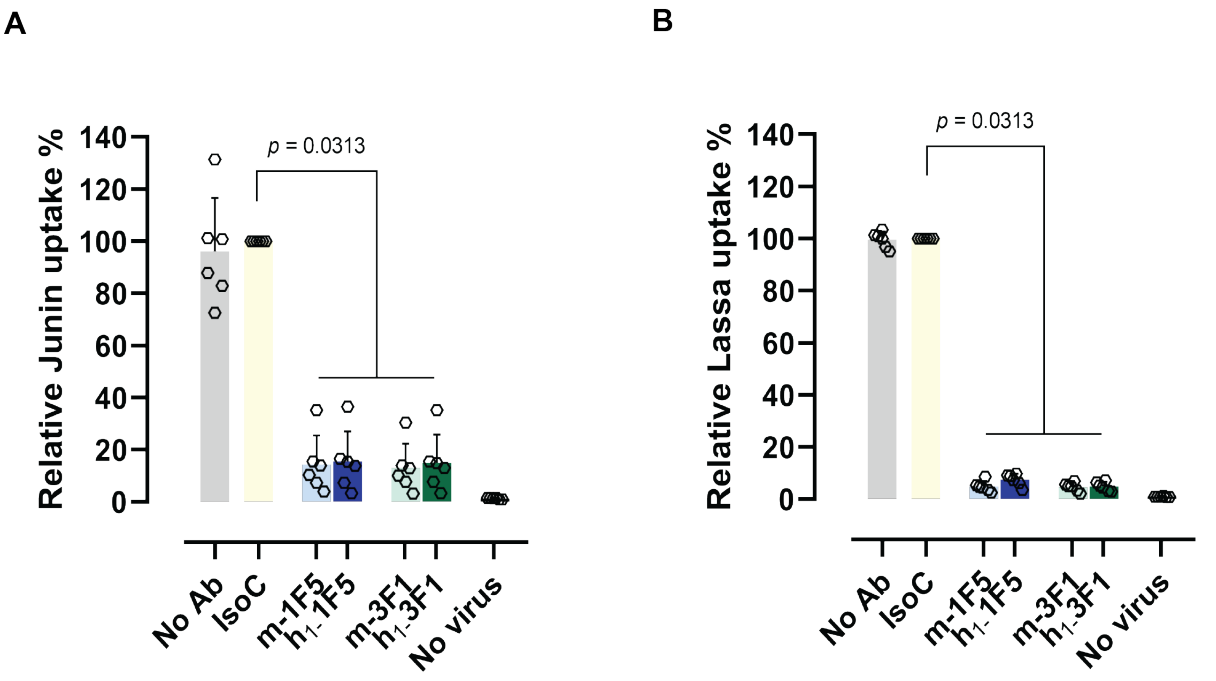

Figure 5.8. Humanized anti-Siglec-1 mAbs reduce Junín and Lassa viral uptake into activated DCs. A. Relative viral uptake of Junín Z_{eGFP} VLP pulsed for 4h at 37ºC with LPS-treated DCs pre-incubated with humanized anti-Siglec-1 mAbs. Values are normalized to cells without anti-Siglec-1 mAb incubation, with a mean entry of 35.93 ± 4.85% (SD) and set as 100%. Data show mean values and SD from two experiments and include cells from six donors. **B.** Relative viral uptake of Lassa Z_{eGFP} VLPs pulsed for 4h at 37ºC with LPS-treated DCs pre-incubated with humanized anti-Siglec-1 mAbs. Values are normalized to cells without anti-Siglec-1 mAb incubation, with a mean entry of 59.72 ± 8.95% (SD) and set as 100%. Data show mean values and SD from two experiments including cells from six donors. Statistical differences in **A** and **B** were assessed with a one-sample Wilcoxon test.

5.4. Conclusions

Over this work, we have shown the anti-Siglec-1 Fab and humAb generation, demonstrating that they retain their blocking capacity. Fabs have shown promising blocking results, although the Fab producing efficiency is low. Compared to the humanization, the Fab production procedure is simple and straight forward, although, the amount of whole IgG necessary to produce Fabs is quite high. Despite the initial steps for mAb humanization take longer and optimization can get complicated, the final yield of humanized mAbs is higher compared to Fabs. Therefore, we believe that for the intended use of anti-Siglec-1 mAbs as antiviral therapy for pathogenic enveloped viruses, the humanization approach is the most suitable.

Chapter 6 – Discussion

Immediately upon exposure to a viral infection, APCs interact with the pathogen to trigger an immune response[328–330]. Previous work has demonstrated how Siglec-1, an adhesion molecule found on the surface of activated APCs, specifically recognizes sialylated gangliosides that are present in enveloped viruses such as Ebola and HIV-1[53,68,331]. These viruses can exploit such interaction which may facilitate their systemic dissemination [67,70,332–339]. The original aim of this thesis was to study if other enveloped viruses could also interact with Siglec-1, for which we selected to focus on the arenavirus family. Similar to Ebola viruses, these are RNA enveloped viruses can cause haemorrhagic fever in humans[340,341]. However, relatively shortly after this thesis began, the COVID-19 pandemic started; and since SARS-CoV-2 is an enveloped virus as well, we decided to temporarily set aside our primary objective to first study the possible interaction between Siglec-1 and SARS-CoV-2 and gain insights into the biology of the new coronavirus. In this chapter we discuss the potential role of Siglec-1 in SARS-CoV-2 and arenavirus infection. We also address the capacity of this receptor to mediate initial events related to viral pathogenesis, aiding systemic dissemination from entry sites after infection. Moreover, we discuss the possible advantages of using humanized anti-Siglec-1 mAbs as an antiviral therapy to combat the early viral dissemination mediated by APCs via Siglec-1 receptor.

6.1. Siglec-1 in MΦs and DCs acts as an attachment receptor for SARS-CoV-2, triggering a proinflammatory response and facilitating *trans*-infection to target cells.

Previous research has emphasized the crucial function of myeloid APCs, such as MΦs and DCs, in orchestrating an antiviral inflammatory reaction, a response that becomes more pronounced in severe cases of COVID-19[137,138]. Siglec-1 is an IFN-inducible receptor on human myeloid cells, whose expression is increased upon activation of myeloid cells[54,58]. This is consistent with studies on SARS-CoV-2 infected samples obtained at early stages of infection, before symptoms onset, showing higher percentage of Siglec-1-expressing monocytes, which correlated with an increase of type I IFN levels in patients' plasma[54]. Therefore, Siglec-1 could potentially act as an uptake receptor for SARS-CoV-2 in myeloid cells.

The potential role of Siglec-1 to mediate viral uptake relies on its capacity to interact with sialylated gangliosides. Viruses budding from infected cells incorporate gangliosides, derived from the cell membrane, on their viral envelope. Among them, those containing sialyllactose

molecular motifs are specifically recognized as Siglec-1 ligands, as shown for HIV-1 and Ebola virus[53,58,68,262]. GM1 is one of these sialylated ganglioside present in the lipid envelopes of HIV-1 and Ebola virus that interacts with Siglec-1 [58,68]. Here, we identified GM1 on the SARS-CoV-2 lipidic membrane as well (**Figure 3.2H**) and showed that Siglec-1 mediates SARS-CoV-2 recognition of different viral variants of concern (**Figure 3.2D**). Hence, the incorporation of GM1 into the envelope of SARS-CoV-2 explains how Siglec-1 can interact with this virus and acts as an attachment factor for SARS-CoV-2.

Supporting the role of Siglec-1 as an attachment factor, our group has contributed to identifying that transmembrane lectins, such as DC-SIGN and L-SIGN but specially Siglec-1, act as auxiliary receptors that facilitate SARS-CoV-2 capture[342]. Furthermore, our results show that Raji cells engineered to express Siglec-1 could capture SARS-CoV-2 to a higher extent than Raji cells lacking this receptor, or Raji R116A cells, which express a mutant Siglec-1 unable to recognize sialic acids, and even other Raji cells engineered to express other lectins (**Figure 3.2B**). In addition, when Raji Siglec-1 cells were pre-incubated with anti-Siglec-1 mAbs, viral capture was blocked (**Figure 3.2C**). Overall, working with Siglec-1 transfected cellular models devoid of these types of lectins we detected a specific interaction between SARS-CoV-2 and this receptor.

It has been described that Siglec-1 is able to mediate SARS-CoV-2 entry into macrophages and promote a proinflammatory response without actively replicating in these cells[343]. This is consistent with our results that showed an increased capture of SARS-CoV-2 in activated APCs, and a direct correlation with Siglec-1 expression in these cells (**Figures 3.1F & 3.2E**). We also found that SARS-CoV-2 did not replicate in Mos. Instead, after being captured, SARS-CoV-2 is eventually processed (**Figure 3.1**). In addition, our results showed that SARS-CoV-2 capture by MΦs could also be blocked by anti-Siglec-1 mAbs (**Figure 3.2F**). These findings suggest the possible role of Siglec-1 in SARS-CoV-2 capture by MΦs, which could trigger an antiviral immune response, starting by the internalization and followed by the degradation of SARS-CoV-2. As previous studies have suggested, the capture, internalization, and processing of the virus by MΦs, might trigger a proinflammatory response by releasing cytokines related with an antiviral state such as IL-6, IL-10 or TNF [343–345]. Another study demonstrated that MΦs and DCs were able to capture SARS-CoV-2, inducing the production of multiple antiviral and proinflammatory cytokines such as IFNα, IFNβ, TNF, IL-6, IL-10 and chemokine CXCL10 without efficient replication[119]. While SARS-CoV-2 captured by MΦs leads to the virus degradation, our results showed that this is not the case for DCs.

Previous studies have shown that after exposure to SARS-CoV-2, DCs are stimulated and develop into two different types[133]. On one hand, DCs play an antiviral immune function inducing adaptive immune responses mediated by T and B cells. On the other hand, in line with our results, studies have shown that SARS-CoV-2 might impair DCs antiviral function and aid viral immune evasion[135]. A study showed that SARS-CoV-2 might be captured by DCs via heparan sulphate proteoglycans without infecting the cells and transmitting the virus to ACE2 expressing target cells[346]. Another study suggested that since DC-SIGN recognizes SARS-CoV-2[278,347,348], it might act as a trans-receptor and an immune escape decoy mechanism similar to the mechanism employed by HIV-1[135].

Our results showed that DCs can capture SARS-CoV-2 without being productively infected (**Figure 3.1**). Furthermore, activated DCs did not only capture SARS-CoV-2 in a Siglec-1-dependent manner, but also recruited the virus into a VCC that was gathered within this compartment (**Figure 3.2G & E**), as described for HIV-1 and EBOV[50,53]. Moreover, we co-cultured DCs, which have captured SARS-CoV-2, with HEK-293T cells expressing the ACE2 receptor, and we found that DCs were able to transfer the virus leading to replication in newly infected target cells (**Figure 3.3C**), following a *trans*-infection mechanism similar to what has been described for HIV-1[68,262,279]. Therefore, we believe that Siglec-1 might act as an auxiliary attachment receptor in MΦs and DCs, leading to the activation of MΦs and viral transfer to ACE2-expressing target cells via DCs.

Based on our results, we hypothesize that upon infection in the respiratory tract, SARS-CoV-2 is able to trigger an inflammatory response increasing the levels of type I IFN, and further increase Siglec-1 expression in APCs resident in the respiratory tract. Increased levels of Siglec-1 facilitate viral capture by APCs in a GP-independent manner. It is worth noting that despite SARS-CoV-2 is captured via Siglec-1 by MΦs and DCs without active replication, the response triggered is completely different. Thus, SARS-CoV-2 capture via Siglec-1 in MΦs leads to the internalization of the virus and later degradation, triggering an antiviral and inflammatory immune response. While capture by DCs, leads to SARS-CoV-2 internalization into a VCC evading the initial immune response, to later be transferred to ACE2-expressing target cells, supporting a *trans*-infection model that could aid viral spread (**Figure 6.1**).

Throughout this study we have demonstrated how SARS-CoV-2 interacts with Siglec-1, which acts as an auxiliary receptor facilitating viral capture and mediating both viral sensing promoting proinflammatory responses and *trans*-infection mechanisms. This later mechanism is aligned with what we have previously reported for HIV- 1, which could facilitate its early spread[58,68,279]. Our group has also investigated Ebola virus and showed that Siglec-1 can act

as an auxiliary receptor aiding the uptake and cytoplasmic entry of this filovirus into DCs[53]. All these results pointed out to the possibility that other enveloped viruses could interact with Siglec-1, and we therefore extended our observations to arenaviruses that share similarities with Ebola virus as they are capable of infecting DCs [340].

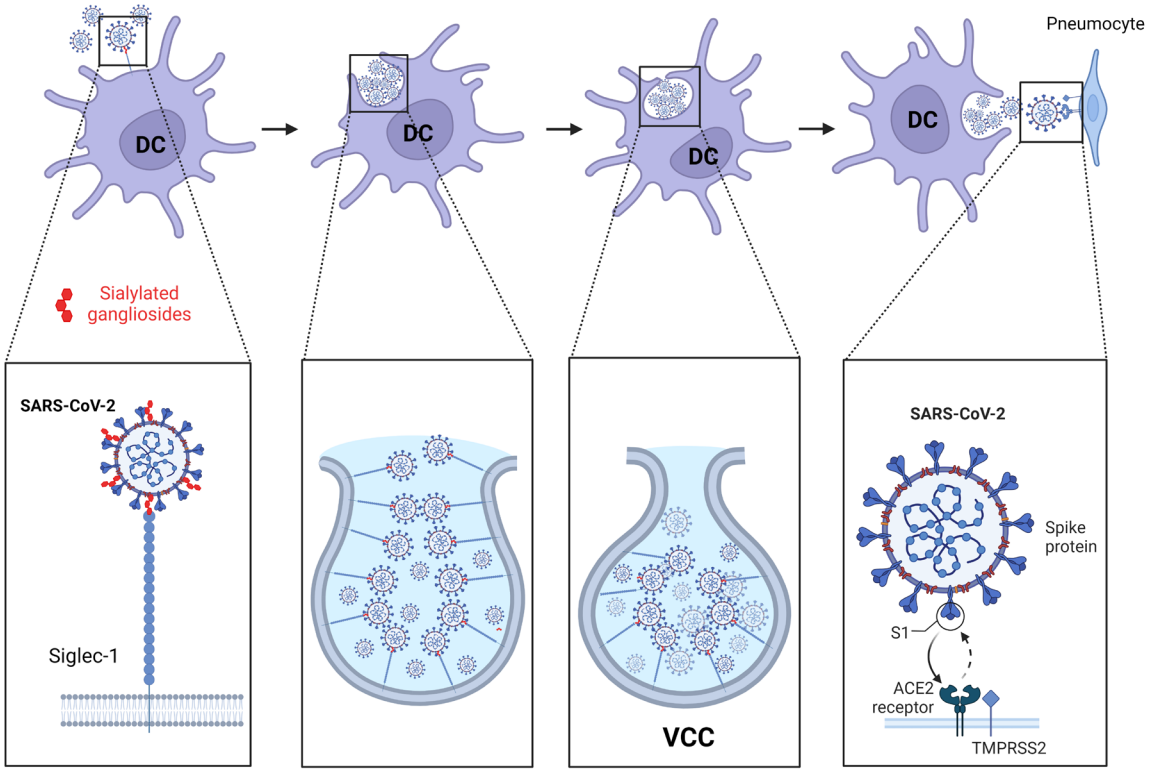

Figure 6.1 Siglec-1 is an attachment receptor that mediates the capture of SARS-CoV-2 in myeloid cells and helps its spread through *trans-infection*. Viral uptake begins when viruses are recognized by Siglec-1. Then, captured viruses concentrate forming the VCC and stay protected from the immune system without infecting the host cell. These virus-loaded cells will eventually travel to the lymph nodes where stored viruses could be released increasing the pro-inflammatory state. VCC: virus-containing-compartment. Created with BioRender.com. VCC: Virus-Containing Compartment; ACE 2: Angiotensin-Converting Enzyme 2; TMPRSS2: transmembrane serine protease 2.

6.2. Siglec-1 is an attachment receptor that contributes to arenavirus uptake

Prior studies proposed that Siglec-1 could play a role in aiding the pathogenesis of enveloped viruses [53,262,342], either acting as an auxiliary receptor facilitating viral uptake or mediating viral transmission via *trans*-infection to bystander target cells. Here we show arenaviruses are yet another family of enveloped viruses that interacts with Siglec-1 receptor, underscoring a novel mechanism for the dissemination of pathogenic arenaviruses causing haemorrhagic fevers.

Junín and Lassa viruses are transmitted to humans through contaminated food or by inhaling contaminated faeces from certain rodent species that are their natural reservoir[194,217,349,350].

Given that several subsets of APCs expressing Siglec-1 are located in the lungs[344] and the respiratory track[351], and APCs are the primary target of arenaviruses in the early stages of the infection[194,196,352], Siglec-1 could mediate viral binding and facilitate viral uptake. Furthermore, hTfR1 and αDG, canonical receptors for Junín and Lassa virus attachment respectively, or Lassa fusion receptor LAMP1, are highly expressed in airways-resident APCs[353]. Overall, these observations, combined with our findings showing that Siglec-1 facilitates the uptake of arenavirus VLP in DCs (**Figures 4.3 and 4.4**), support the hypothesis that this receptor could play a key role in early uptake of arenaviruses in the respiratory track.

Sialylated gangliosides, that bind to Siglec-1, are not viral-specific and accumulate in cell membranes where distinct enveloped viruses bud[45]. GM1 is a ganglioside shown to be present in the lipid envelopes of HIV-1, Ebola virus and, as mentioned above, also SARS-CoV-2, that interacts with Siglec-1 [53,68,302]. We have now detected GM1 in the Junín and Lassa VLPs (**Figure 4.1**) and have shown that arenaviruses uptake is dependent on Siglec-1 in cell lines and primary DCs (**Figures 4.3 and 4.4**). Blockage of Siglec-1 with specific anti-Siglec-1 mAbs halted the uptake of arenavirus VLP into DCs. In addition, Siglec-1 gathers the arenavirus VLPs and concentrates them into VCCs (**Figures 4.3 and 4.4**) as previously reported for HIV-1, Ebola virus and SARS-CoV-2[53,262,302].

JUNV primarily induces a proinflammatory response in the infected host. This response is a result of the virus' ability to trigger the release of proinflammatory cytokines and chemokines, such as IL-6, TNF and IFN-γ[352]. These molecules play a crucial role in the host's immune response to the virus by recruiting immune cells to the site of infection and promoting an antiviral defence. However, an excessive or dysregulated proinflammatory response can lead to tissue damage and contribute to the severity of the disease. It appears that the virus has developed some compensatory mechanisms to limit the extend of its inflammatory consequences such as the inhibition of RIG-1 and MDA-5 by NP and Z protein [188,354–357]. Siglec-1 is an IFN-inducible receptor that would overexpress in a proinflammatory environment such as the one triggered by JUNV infection. In the case of JUNV, Siglec-1 recognition could increase the number of infected cells at the infection site, to then travel to the lymph nodes and spread the infection to the rest of the organism. In fact, the highest levels of virus titers have been found in lymph nodes, spleen, and lungs[358] supporting the idea of lymphoid tissues acting as viral replication site. High viral titres were also recovered from visceral organs and central nervous system of rhesus macaques that were infected with JUNV via aerosol, supporting the aiding role of APCs on viral dissemination throughout the body[221,359,360]. The overexpression of Siglec-1 on the surface of APCs in addition to the immune cell recruitment

mediated by the proinflammatory state, could lead to increased viral uptake in APCs at infection site.

Opposite to JUNV, LASV infection does not trigger this sort of IFN-mediated immune response, allowing the virus to propagate quietly[144,196,224,225,361]. Infection of APCs with LASV via Siglec-1 binding could favour immune suppression and silent replication, and once these cells travel to the lymph node, the virus can continue infecting and immunosuppressing tissue resident APCs, and even disseminate to other tissues where the virus could infect other target cells. While the highest virus titres have been detected in the spleen, lymph nodes and lungs, studies have found LASV in tissues, such as the liver, far from the infection site along with infected immune cells [145,362]. Altogether, the data suggest that arenaviruses might use Siglec-1 expressed on the surface of APCs as an auxiliary attachment receptor to aid viral uptake in the early stages of the infection, in a similar way as it has been proposed for EBOV[53] (**Figure 6.2**).

We have shown how anti-Siglec-1 mAbs can block arenavirus VLPs uptake in primary DCs (**Figures 4.3 and 4.4**). We believe that Siglec-1 might be a promising therapeutic target for an antibody-based antiviral therapy of pathogenic enveloped viruses. The existence of individuals lacking Siglec-1 expression reveals that this receptor is not essential for life[363], indicating that therapeutic blockade of Siglec-1 is unlikely to result in critical adverse effects. This contrasts to other host targets, such as the canonical LASV receptor αDG-1, which leads to a muscular dystrophy disorder when blocked by antibodies[364,365]. By targeting a non-essential cellular host factor such as Siglec-1 that interacts with viral gangliosides, potential viral evasion through adaptation mechanisms could also be limited. Our results indicate the potential of anti-Siglec-1 mAbs for providing cross-protection against different arenaviruses, increasing their broad-spectrum potential against other life-threatening enveloped viruses such as Ebola virus or SARS-CoV-2.

Future experiments should further help clarify the potential use of Siglec-1 mAbs in more physiological arenavirus. One option is to use VLPs of Lassa and Junín containing their respective GP proteins to analyse the effect of anti-Siglec-1 mAbs in the viral fusion mechanism. Another approach could be using non-pathogenic reference model arenaviruses, such as Lymphocytic choriomeningitis virus or JUNV attenuated vaccine Candid1. Finally, although we lack a BSL4 facility, it would be encouraging to be able to do experiments with fully infectious EBOV or Lassa virus.

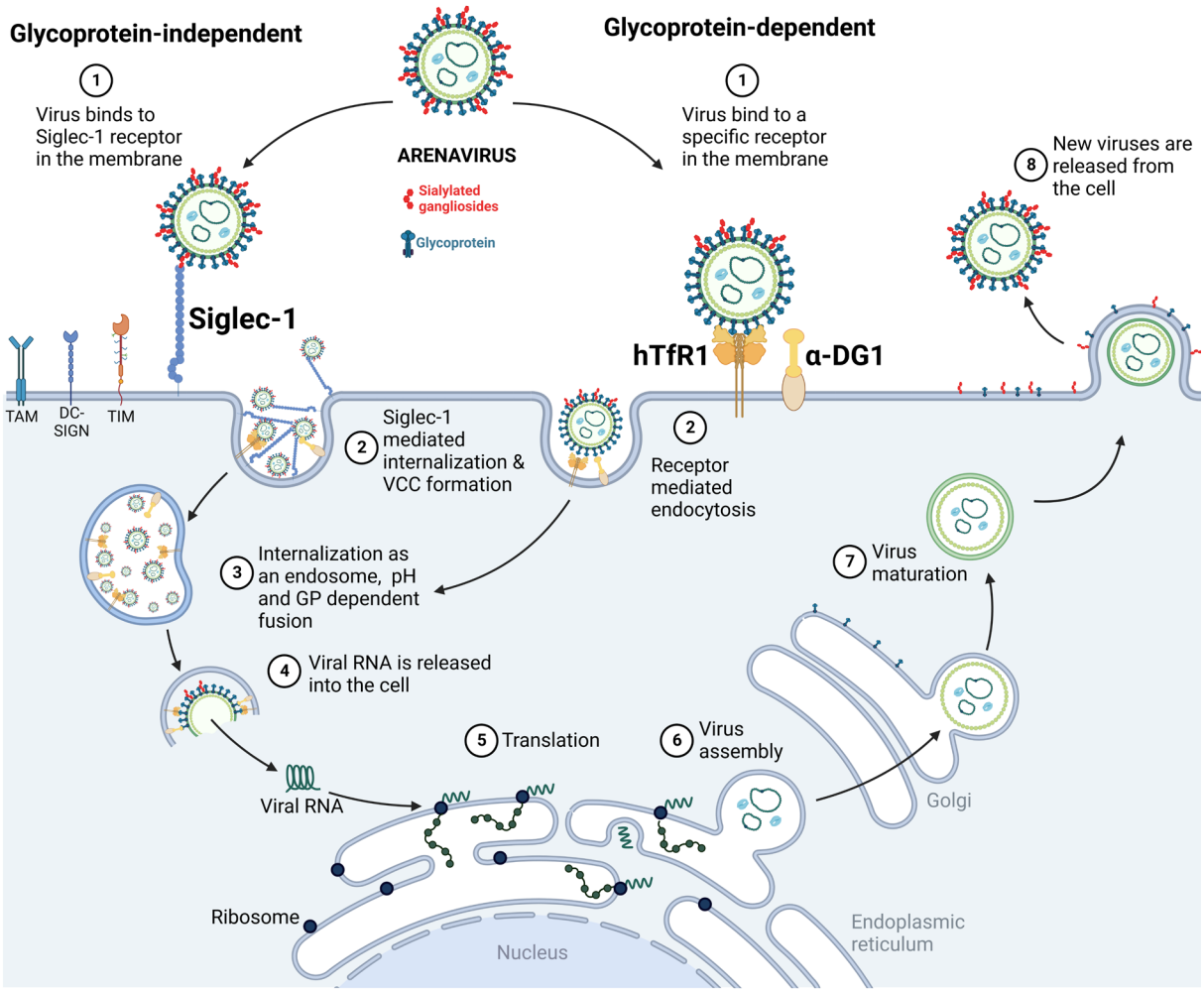

Figure 6.2 Siglec-1 is an attachment receptor aiding arenavirus entry into myeloid cells. Arenavirus attachment via glycoprotein dependent receptors or glycoprotein-independent pathway. Created with BioRender.com. hTRF1: Human Trans-Ferrin Receptor 1; α-DG1: Alpha Dystroglycan 1; RNA: Ribonucleic Acid.

6.3. Humanized anti-Siglec-1 antibodies as a potential antiviral treatment

Over this thesis, we have shown that SARS-CoV-2, Junín, and Lassa viruses share a common mechanism for viral uptake via Siglec-1, which is expressed on activated APCs, facilitating viral dissemination in the early stages of the infection as previously reported for HIV-1 and Ebola virus. We have also shown how anti-Siglec-1 mAbs are able to block this pathway **(Figures 3.2, 3.3, 4.2 & 4.3)**. Blocking Siglec-1 could be an interesting approach to reduce early dissemination of HIV-1, Ebola virus, SARS-CoV-2 and arenaviruses. Based on our results; we consider that an antiviral therapy-based on anti-Siglec-1 mAbs might be a promising tactic to reduce initial viral dissemination.

Nowadays there are 13 approved mAbs to treat viral diseases[366], most of them targeting viral-related domains. One exception that targets a host factor is Ibalizumab, a non-immunosuppressive humanised mAb that binds CD4, the primary receptor for HIV-1, and

inhibits HIV-1 from entering cells[261]. Since 2018, it has been approved, in combination with other antiretroviral drugs, for patients with limited treatment options[80]. Similarly, Leronlimab is another mAb which is currently undergoing clinical trials in phase 2b/3 for HIV-1 treatment. It is a mAb targeting CCR5 receptor, which has shown effectivity blocking HIV-1 entry in $CD4^+$ T cells[367]. Therefore, there are encouraging results showing efficacy after targeting a host factor instead of a viral target. They represent a promising landscape to develop new antiviral therapies that might be less prone to viral evasion due to mutations in the virus. Yet, to become fully effective, these approaches need to overcome limitations, such as the possible immunogenicity triggered by Ab treatments, especially when they have been generated in animals.

For the majority of approved antibody-based therapies, the predominant approach involves the utilization of human antibodies. This is accomplished either by employing convalescent patient sera obtained from individuals previously infected, the subsequently purifying the antibodies derived from these patients, or through the expression of IgG constructs that replicate the sequences of human antibodies. Yet, those derived from animals can be modified to avoid risks such as immunogenicity, making them safer therapies and capable to obtain the approval from pharmaceutical regulatory agencies. To reach the clinic, mAbs need to be adapted to avoid the generation of anti-drug antibodies, while improving their efficiency and stability [238,240,248]. There are different methods by which murine mAbs can be modified to become safer in humans, such as: enzymatic digestion to obtain Fabs, chimerization, or humanization. After developing a set of murine mAbs against human Siglec-1, we modified them to produce mAbs that could be safely used in humans. Thus, we generated Fabs and humanized the original murine mAbs to further test their capacity to interfere with the uptake of a viral panel composed by HIV-1, Ebola virus, SARS-CoV-2 and Junín and Lassa arenaviruses.

We first tested the possible use of murine anti-Siglec-1 Fabs. Currently there are only 4 Fabs approved for medical use, but none of them are intended to treat infectious diseases[366]. We decided to follow this strategy since it required a simple enzymatic digestion and if proven effective, could provide a useful tool to treat viral infections. The anti-Siglec-1 Fabs that we have generated showed a slightly higher IC_{50} value than their respective original murine mAbs (**Figure 5.2B**). Despite a higher IC_{50} value, they completely blocked HIV-1 interaction with Siglec-1 in primary DCs (**Figure 5.2C**) probing their efficacy. Fabs offer a series of advantages over mAbs, such as a reduced reactivity due to the lack of an Fc region (**Figure 6.3**), and a better capacity to reach tissues due to their smaller size. Yet, they also present some disadvantages, such as a shorter half-life or poor stability, which can be solved with different

strategies. In the case of reduced half-life, either adding some sequence modifications or the conjugation with other molecules such as fatty acids can improve it[245,246]. Yet sometimes their low yield and their limited production efficiency hamper their clinical use. Nanobodies were developed as an alternative to the limitations of Fabs, and their use has increased over the last years. Nanobodies are heavy chain antibodies based on distinct Ig structures found naturally in sharks and camelids. The structure of nanobodies is unique, composed of a single heavy chain with one variable domain (**Figure 6.3**). Although nanobodies have a higher stability, better solubility, and lower production cost [368,369], their animal origin also poses immunogenicity challenges. Therefore, and although developing nanobodies against Siglec-1 could be an interesting option, having already Fabs with blocking activity against Siglec-1 from the original murine mAbs **(Figure 5.2)** is still relevant as it could reduce the chances to generate autoantibodies.

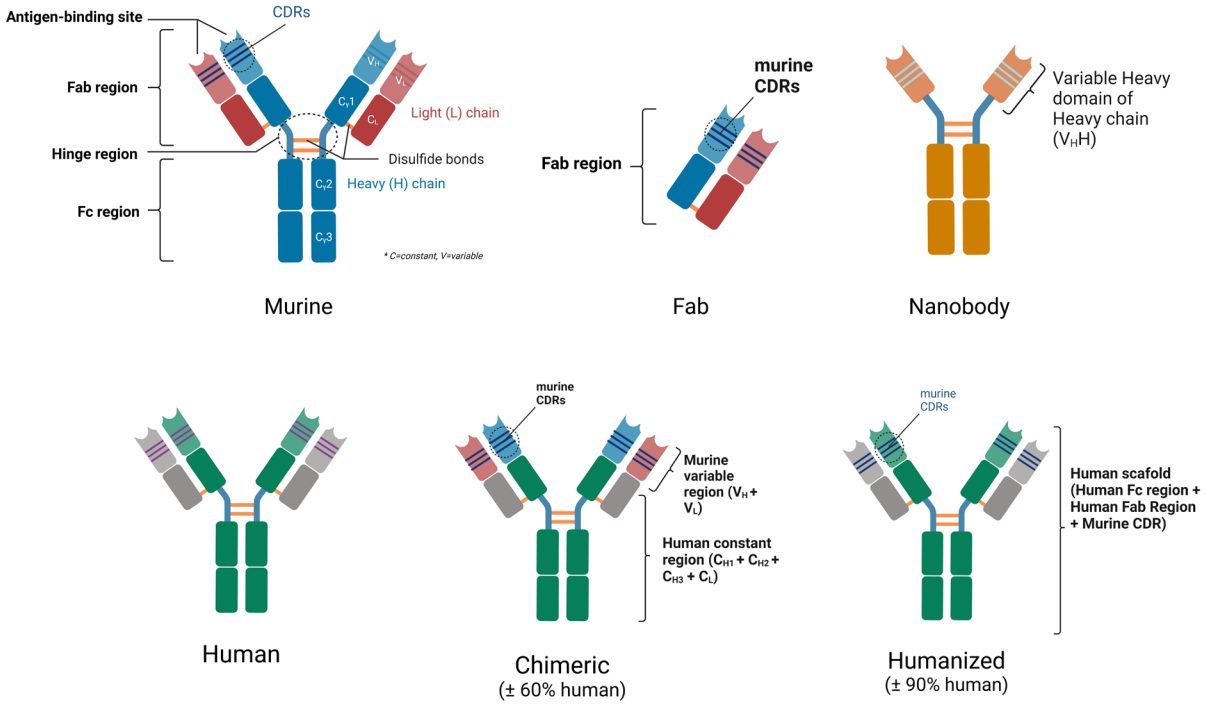

Figure 6.3. Different antibodies and their differences. Complete IgG structure is common for all antibodies, and it is not related to their origin. Modifications to reach the clinic aim to minimize the risks associated to differences in animal derived mAbs. Fabs lacking the Fc region can be generated by enzymatic digestion to avoid Fc generated immunogenicity. Chimeric or Humanized mAbs, depending on the percentage of humanization achieved, can be engineered to be as similar as possible to human IgG mAbs retaining the original antigen recognition capacity. Nanobodies differ considerably from IgGs in size and structure, being much smaller and containing a single V_HH per heavy chain, and no light chains.

In collaboration with Sanquin, an institute that provides blood services in the Netherlands on a not-for-profit basis, our group has also humanized the murine anti-Siglec-1 mAbs previously generated. We showed how the humanization process did not affect their ability to block Siglec-

1 **(Figure 5.2)**. Once we had confirmed that the blocking effect had been retained, we proceeded to optimize them. Performing some modifications to the antibody sequence allowed us to improve stability and production while retaining their blocking activity **(Figure 5.2)**. The modifications and analysis performed to the first generation of humanized mAbs (h_0) allowed us to obtain optimized anti-Siglec-1 humAbs (h_1) that retained blocking activity against different enveloped viruses **(Figure 5.3)**. After successful humanization of the murine mAbs, they retained their blocking activity, with IC_{50} values similar to the original mAbs (**Figure 5.3 E**).

Prior work has demonstrated that Siglec-1 is able to interact with some pathogenic enveloped viruses and it has been proposed that might be involved in viral dissemination. We believe that the mechanism of Siglec-1 as attachment receptor for virus uptake is similar in all cases. This initial step will subsequently facilitate that the final infection through specific viral receptors could be in *cis* (Ebola virus/Arenavirus) or *trans* (HIV-1/SARS-CoV-2)[58,65,68,262,279,370] (**Figure 6.4A**).

Previous studies showing promising results from mAbs targeting host factors[231], support the potential use of humanized anti-Siglec-1 mAbs to block early viral uptake. These antibodies offer an antiviral treatment targeting a cellular receptor which is likely to play a role in the recognition of multiple pathogenic enveloped viruses and is less likely to be subject to immune evasion due to mutations in viral factors.

As shown by our results, humanized anti-Siglec-1 can block viral uptake for the tested viral panel (**Figure 5.3**). Furthermore, our data suggests that blocking early viral uptake could disrupt further viral dissemination and cell-to-cell transfer during early infection (**Figure 5.3**). However, it is worth noting that, according to data shown in other studies, Siglec-1 receptor block does not have a measurable impact on HIV-1 acquisition or AIDS outcomes *in vivo*[363] and therefore, it is likely that anti-Siglec-1 mAbs might be useful as a complementary therapy in combination with other antivirals treatments.

Currently there are highly effective treatments that can target these early stages for HIV-1 infection[371,372], vaccines that protect against Junín virus infection[177,210,373], or SARS-CoV-2's most virulent effects[263]. Hence, an antiviral treatment focused on Siglec-1 should not be intended to replace these treatments but could provide additional advantage fighting the early stages of infection in combination with these approaches. Our group contributed to show that Siglec-1 influences the neutralizing activity of SARS-CoV-2 targeted mAbs, modulating their protective ability[342], a piece of evidence that further supports the potential use of Siglec-1 targeted mAbs. For other potential infections with emerging enveloped viruses that do not yet

have an effective treatment, it could serve as a protective treatment to help contain future epidemics.

Over this thesis, we have shown the protective effect of anti-Siglec-1 hu-mAbs in the uptake of different enveloped viruses. Our results suggest that Siglec-1 might act as an auxiliary receptor involved in early viral dissemination. Because viruses use other attachment receptors to enter host cells, additional factors are involved in their pathogenesis and therefore this potential antiviral therapy should be combined with other therapies. Most likely anti-Siglec-1 hu-mAbs will not completely disrupt the viral pathogenic process; most viruses, if not all, bind with variable affinity to a variety of attachment receptors in the surface of human cells. These receptors will help bring the virus closer to its final canonical receptor in the same cell or to potentially shuttle the virus (as in the case of DCs) to the final target cells, facilitating in both cases an effective dissemination of the virus. But its possible use to block the early dissemination of different enveloped viruses makes Siglec-1 a promising therapeutic target. In addition, previous studies have shown that individuals null for Siglec-1 do not present clinical manifestations related to the absence of this molecule[363], and therefore, if future clinical trials are performed, toxicity is expected to be low. Taken together, we have generated two anti-Siglec-1 humanized mAbs that reduce HIV-1 and SARS-CoV-2 *trans*-infection, and EBOV and arenavirus viral particle uptake (**Figure 6.4**).

To advance the development of an antibody-based antiviral therapy with anti-Siglec-1 mAbs, now that we have shown that they work *in vitro* with a panel of distant viruses such as HIV-1, EBOV, SARS-CoV-2 and arenaviruses, the next steps involve testing these mAbs in animal models. Since SARS-CoV-2 and arenavirus pathogenesis has already been studied in non-human primates[260,272,374], we believe this would be a suitable animal model to test the efficacy of anti-Siglec-1 mAbs.

Overall, through this thesis we have demonstrated that Siglec-1 is a receptor participating in the viral capture of three distant viruses such as SARS-CoV-2 and arenaviruses. The results showed in this work support the idea that targeting Siglec-1 could offer cross-protection against SARS-CoV-2, arenaviruses, and other enveloped viruses that exploit APCs for viral dissemination, leading to the development of new broad-spectrum antivirals for future outbreaks.

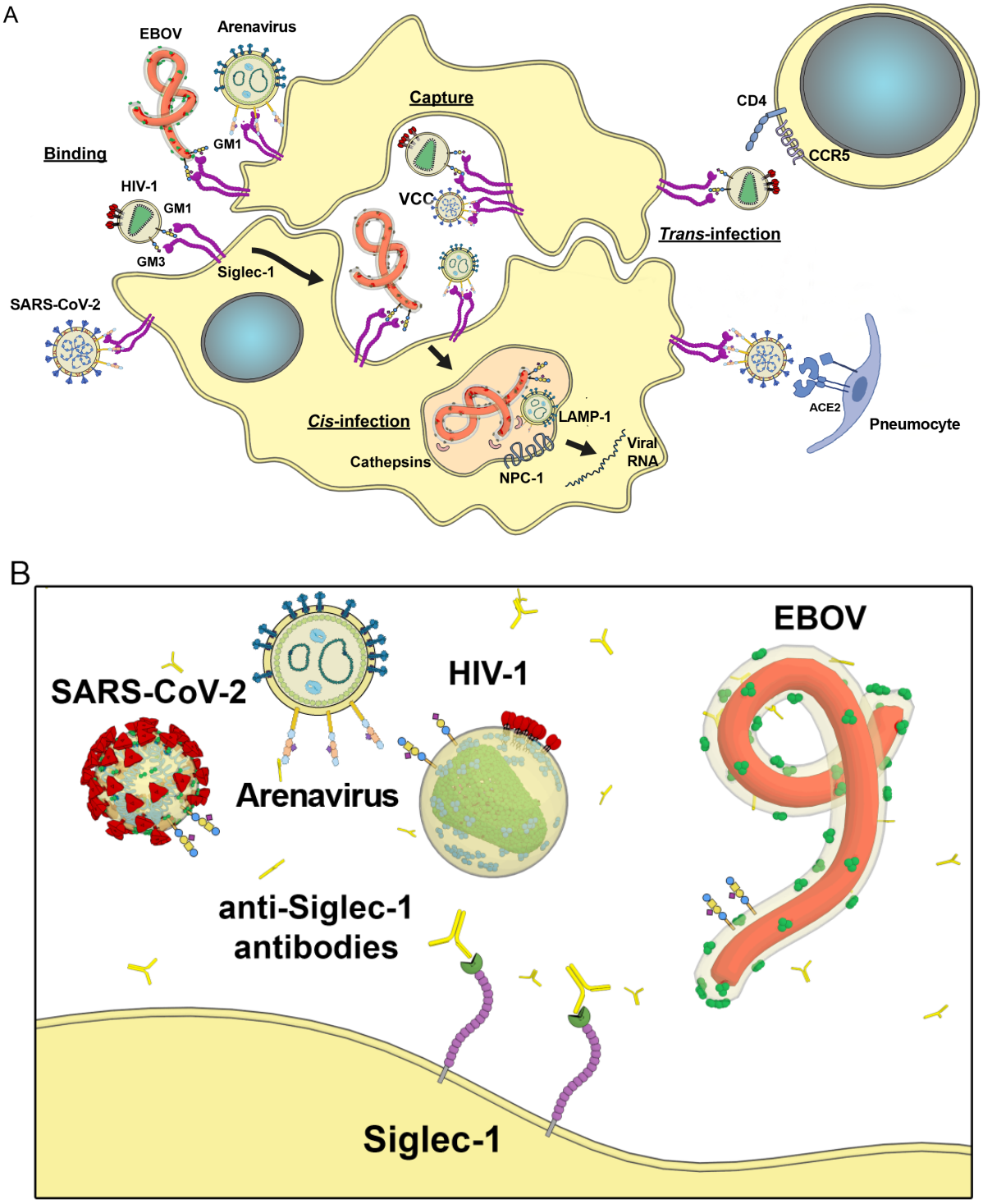

Figure 6.4 Humanized anti-Siglec-1 as potential antiviral treatment. A. We have demonstrated that Siglec-1 might play a critical role in early stages of different enveloped virus capture by DCs, therefore we believe it has potential as therapeutic target. **B.** Humanized anti-Siglec-1 mAbs could be used to disrupt early viral dissemination by blocking DCs viral capture through Siglec-1. Adapted from Ref[45].

Chapter 7 – Conclusions

AIM 1: To test if Siglec-1 receptor can recognize other envelope viruses such as SARS-CoV-2 and facilitate its spreading.

- Siglec-1 recognizes SARS-CoV-2 and mediates viral capture by monocyte-derived DCs directing it to the same virus-containing compartment as HIV-1 or Ebola.
- Siglec-1 *trans*-infects SARS-CoV-2 particles accumulated in the same virus-containing compartment as HIV-1 or Ebola from activated monocyte-derived DCs to target cells.

AIM 2: To determine if Siglec-1 can also recognize other pathological enveloped virus such as arenavirus and act as an attachment receptor.

- Siglec-1 recognizes Junín and Lassa arenavirus VLPs and mediates capture by monocyte-derived DCs, directing the particles to the same virus-containing compartment as HIV-1 or Ebola.

AIM 3: To produce Fabs and humanize anti-Siglec-1 antibodies and test their capacity to block the interaction with different enveloped viruses to determine their potential as a future treatment to fight or prevent viral infections.

- Anti-Siglec-1 Fabs can be produced by enzymatically removing the Fc region while still blocking HIV-1 uptake in activated monocyte-derived DCs.
- Humanized anti-Siglec-1 mAbs block viral uptake of HIV-1, Ebola VLPs, SARS-CoV-2 and arenavirus VLPs in activated monocyte-derived DCs.
- Humanized anti-Siglec-1 mAbs disrupt HIV-1 and SARS-CoV-2 *trans-infection* to target cells and the cytoplasmic entry of Ebola viral particles into activated monocyte-derived DCs.
- Promising *in vitro* results targeting Siglec-1 support further *in vivo* research to test the use of anti-Siglec-1 mAbs as an antiviral therapy for distinct enveloped viruses.

Chapter 8. References

1. Altfeld, M. & Gale, M. Innate immunity against HIV-1 infection. *Nat Immunol* **16**, 554–562 (2015).

2. Primorac, D. *et al.* Adaptive Immune Responses and Immunity to SARS-CoV-2. *Front Immunol* **13**, 1–13 (2022).

3. Rydyznski Moderbacher, C. *et al.* Antigen-Specific Adaptive Immunity to SARS-CoV-2 in Acute COVID-19 and Associations with Age and Disease Severity. *Cell* **183**, 996-1012.e19 (2020).

4. Rustagi, A. & Gale, M. Innate Antiviral Immune Signaling, Viral Evasion and Modulation by HIV-1. *J Mol Biol* **426**, 1161–1177 (2014).

5. Mogensen, T. H. Pathogen Recognition and Inflammatory Signaling in Innate Immune Defenses. *Clin Microbiol Rev* **22**, 240–273 (2009).

6. Iwasaki, A. & Medzhitov, R. Toll-like receptor control of the adaptive immune responses. *Nat Immunol* **5**, 987–995 (2004).

7. Kawai, T. & Akira, S. Innate immune recognition of viral infection. *Nat Immunol* **7**, 131–137 (2006).

8. Kawai, T. & Akira, S. The role of pattern-recognition receptors in innate immunity: Update on toll-like receptors. *Nat Immunol* **11**, 373–384 (2010).

9. Boehme, K. W., Guerrero, M. & Compton, T. Human Cytomegalovirus Envelope Glycoproteins B and H Are Necessary for TLR2 Activation in Permissive Cells. *The Journal of Immunology* **177**, 7094–7102 (2006).

10. Cuevas, C. D. & Ross, S. R. Toll-Like Receptor 2-Mediated Innate Immune Responses against Junín Virus in Mice Lead to Antiviral Adaptive Immune Responses during Systemic Infection and Do Not Affect Viral Replication in the Brain. *J Virol* **88**, 7703–7714 (2014).

11. Okumura, A., Pitha, P. M., Yoshimura, A. & Harty, R. N. Interaction between Ebola Virus Glycoprotein and Host Toll-Like Receptor 4 Leads to Induction of Proinflammatory Cytokines and SOCS1. *J Virol* **84**, 27–33 (2010).

12. Del Cornò, M. *et al.* HIV-1 gp120 signaling through TLR4 modulates innate immune activation in human macrophages and the biology of hepatic stellate cells. *J Leukoc Biol* **100**, 599–606 (2016).

13. Singh, H., Koury, J. & Kaul, M. Innate Immune Sensing of Viruses and Its Consequences for the Central Nervous System. *Viruses* **13**, 170 (2021).

14. Rudd, B. D., Burstein, E., Duckett, C. S., Li, X. & Lukacs, N. W. Differential Role for TLR3 in Respiratory Syncytial Virus-Induced Chemokine Expression. *J Virol* **79**, 3350–3357 (2005).

15. Wang, Q. *et al.* MDA5 and TLR3 initiate pro-inflammatory signaling pathways leading to rhinovirus-induced airways inflammation and hyperresponsiveness. *PLoS Pathog* **7**, (2011).

16. Rudd, B. D. *et al.* Deletion of TLR3 Alters the Pulmonary Immune Environment and Mucus Production during Respiratory Syncytial Virus Infection. *The Journal of Immunology* **176**, 1937–1942 (2006).

17. Iwakiri, D. *et al.* Epstein-Barr virus (EBV)-encoded small RNA is released from EBV-infected cells and activates signaling from toll-like receptor 3. *Journal of Experimental Medicine* **206**, 2091–2099 (2009).

18. Reinert, L. S. *et al.* TLR3 deficiency renders astrocytes permissive to herpes simplex virus infection and facilitates establishment of CNS infection in mice. *Journal of Clinical Investigation* **122**, 1368–1376 (2012).

19. Melchjorsen, J. *et al.* Activation of Innate Defense against a Paramyxovirus Is Mediated by RIG-I and TLR7 and TLR8 in a Cell-Type-Specific Manner. *J Virol* **79**, 12944–12951 (2005).

20. Lund, J. M. *et al.* Recognition of single-stranded RNA viruses by Toll-like receptor 7. *Proc Natl Acad Sci U S A* **101**, 5598–5603 (2004).

21. Triantafilou, K. *et al.* Human cardiac inflammatory responses triggered by Coxsackie B viruses are mainly Toll-like receptor (TLR) 8-dependent. *Cell Microbiol* **7**, 1117–1126 (2005).

22. Zhang, Y. *et al.* HCV RNA Activates APCs via TLR7/TLR8 while Virus Selectively Stimulates Macrophages Without Inducing Antiviral Responses. *Sci Rep* **6**, 1–13 (2016).

23. Alter, G. *et al.* Single-Stranded RNA Derived from HIV-1 Serves as a Potent Activator of NK Cells. *The Journal of Immunology* **178**, 7658–7666 (2007).

24. Varani, S. *et al.* Human Cytomegalovirus Differentially Controls B Cell and T Cell Responses through Effects on Plasmacytoid Dendritic Cells. *The Journal of Immunology* **179**, 7767–7776 (2007).

25. Lim, W. H., Kireta, S., Russ, G. R. & Coates, P. T. H. Human plasmacytoid dendritic cells regulate immune responses to Epstein-Barr virus (EBV) infection and delay EBV-related mortality in humanized NOD-SCID mice. *Blood* **109**, 1043–1050 (2007).

26. Hochrein, H. *et al.* Herpes simplex virus type-1 induces IFN-α production via Toll-like receptor 9-dependent and -independent pathways. *Proceedings of the National Academy of Sciences* **101**, 11416–11421 (2004).

27. Fiola, S., Gosselin, D., Takada, K. & Gosselin, J. TLR9 Contributes to the Recognition of EBV by Primary Monocytes and Plasmacytoid Dendritic Cells. *The Journal of Immunology* **185**, 3620–3631 (2010).

28. Yu, H.-R. *et al.* IFN-α production by human mononuclear cells infected with varicella-zoster virus through TLR9-dependent and -independent pathways. *Cell Mol Immunol* **8**, 181–188 (2011).

29. Lund, J., Sato, A., Akira, S., Medzhitov, R. & Iwasaki, A. Toll-like Receptor 9–mediated Recognition of Herpes Simplex Virus-2 by Plasmacytoid Dendritic Cells. *J Exp Med* **198**, 513–520 (2003).

30. Takeuchi, O. & Akira, S. Pattern Recognition Receptors and Inflammation. *Cell* **140**, 805–820 (2010).

31. Loo, Y. M. & Gale, M. Immune Signaling by RIG-I-like Receptors. *Immunity* **34**, 680–692 (2011).

32. Kato, H. *et al.* Cell type-specific involvement of RIG-I in antiviral response. *Immunity* **23**, 19–28 (2005).

33. Zheng, Y. *et al.* Severe acute respiratory syndrome coronavirus 2 (SARS-CoV-2) membrane (M) protein inhibits type I and III interferon production by targeting RIG-I/MDA-5 signaling. *Signal Transduct Target Ther* **5**, 299 (2020).

34. Chatterjee, B. *et al.* Internalization and endosomal degradation of receptor-bound antigens regulate the efficiency of cross presentation by human dendritic cells. *Blood* **120**, 2011–2020 (2012).

35. Ribeiro, C. M. S. *et al.* Receptor usage dictates HIV-1 restriction by human TRIM5α in dendritic cell subsets. *Nature* **540**, 448–452 (2016).

36. Bermejo-Jambrina, M. *et al.* C-type lectin receptors in antiviral immunity and viral escape. *Front Immunol* **9**, 1–12 (2018).

37. Chiffoleau, E. C-type lectin-like receptors as emerging orchestrators of sterile inflammation represent potential therapeutic targets. *Front Immunol* **9**, 1–9 (2018).

38. Miller, J. L. *et al.* The Mannose Receptor Mediates Dengue Virus Infection of Macrophages. *PLoS Pathog* **4**, e17 (2008).

39. Moris, A. *et al.* DC-SIGN promotes exogenous MHC-I–restricted HIV-1 antigen presentation. *Blood* **103**, 2648–2654 (2004).

40. Hoving, J. C., Wilson, G. J. & Brown, G. D. Signalling C-Type lectin receptors, microbial recognition and immunity. *Cell Microbiol* **16**, 185–194 (2014).

41. Chen, S. T. *et al.* CLEC5A regulates Japanese encephalitis virus-induced neuroinflammation and lethality. *PLoS Pathog* **8**, (2012).

42. Chen, S. T. *et al.* CLEC5A is critical for dengue-virus-induced lethal disease. *Nature* **453**, 672–676 (2008).

43. Teng, O. *et al.* CLEC5A-Mediated Enhancement of the Inflammatory Response in Myeloid Cells Contributes to Influenza Virus Pathogenicity In Vivo. *J Virol* **91**, (2017).

44. Rempel, H., Calosing, C., Sun, B. & Pulliam, L. Sialoadhesin Expressed on IFN-Induced Monocytes Binds HIV-1 and Enhances Infectivity. *PLoS One* **3**, e1967 (2008).

45. Raïch-Regué, D. *et al.* Role of Siglecs in viral infections: A double-edged sword interaction. *Mol Aspects Med* **90**, 101113 (2023).

46. Pulliam, L., Sun, B. & Rempel, H. Invasive chronic inflammatory monocyte phenotype in subjects with high HIV-1 viral load. *J Neuroimmunol* **157**, 93–98 (2004).

47. Crocker, P. R. *et al.* Sialoadhesin, a macrophage sialic acid binding receptor for haemopoietic cells with 17 immunoglobulin-like domains. *EMBO Journal* **13**, 4490–4503 (1994).

48. Munday, J., Floyd, H. & Crocker, P. R. Sialic acid binding receptors (siglecs) expressed by macrophages. *J Leukoc Biol* **66**, 705–711 (1999).

49. Crocker, P. R., Paulson, J. C. & Varki, A. Siglecs and their roles in the immune system. *Nat Rev Immunol* **7**, 255–266 (2007).

50. Gutiérrez-Martínez, E. *et al.* Actin-regulated Siglec-1 nanoclustering influences HIV-1 capture and virus-containing compartment formation in dendritic cells. *Elife* **12**, 1–31 (2023).

51. Hartnell, A. *et al.* Characterization of human sialoadhesin, a sialic acid binding receptor expressed by resident and inflammatory macrophage populations. *Blood* **97**, 288–296 (2001).

52. Eakin, A. J. *et al.* Siglec-1 and -2 as potential biomarkers in autoimmune disease. *Proteomics Clin Appl* **10**, 635–644 (2016).

53. Perez-Zsolt, D. *et al.* Anti-Siglec-1 antibodies block Ebola viral uptake and decrease cytoplasmic viral entry. *Nat Microbiol* (2019) doi:10.1038/s41564-019-0453-2.

54. Bedin, A.-S. S. *et al.* Monocyte CD169 Expression as a Biomarker in the Early Diagnosis of Coronavirus Disease 2019. *Journal of Infectious Diseases* **223**, 562–567 (2021).

55. Doehn, J.-M. *et al.* CD169/SIGLEC1 is expressed on circulating monocytes in COVID-19 and expression levels are associated with disease severity. *Infection* **49**, 757–762 (2021).

56. Oh, D. S., Oh, J. E., Jung, H. E. & Lee, H. K. Transient Depletion of CD169+ Cells Contributes to Impaired Early Protection and Effector CD8+ T Cell Recruitment against Mucosal Respiratory Syncytial Virus Infection. *Front Immunol* **8**, (2017).

57. Camara, A. *et al.* CD169 + macrophages in lymph node and spleen critically depend on dual RANK and LTbetaR signaling. *Proceedings of the National Academy of Sciences* **119**, (2022).

58. Puryear, W. B. *et al.* Interferon-Inducible Mechanism of Dendritic Cell-Mediated HIV-1 Dissemination Is Dependent on Siglec-1/CD169. *PLoS Pathog* **9**, (2013).

59. McDonald, D. *et al.* Recruitment of HIV and Its Receptors to Dendritic Cell-T Cell Junctions. *Science (1979)* **300**, 1295–1297 (2003).

60. Perot, B. P., García-Paredes, V., Luka, M. & Ménager, M. M. Dendritic Cell Maturation Regulates TSPAN7 Function in HIV-1 Transfer to CD4+ T Lymphocytes. *Front Cell Infect Microbiol* **10**, 1–17 (2020).

61. Ruffin, N. *et al.* Constitutive Siglec-1 expression confers susceptibility to HIV-1 infection of human dendritic cell precursors. *Proceedings of the National Academy of Sciences* **116**, 21685–21693 (2019).

62. Hrecka, K. *et al.* Vpx relieves inhibition of HIV-1 infection of macrophages mediated by the SAMHD1 protein. *Nature* **474**, 658–661 (2011).

63. Laguette, N. *et al.* SAMHD1 is the dendritic- and myeloid-cell-specific HIV-1 restriction factor counteracted by Vpx. *Nature* **474**, 654–657 (2011).

64. Puryear, W. B., Yu, X., Ramirez, N. P., Reinhard, B. M. & Gummuluru, S. HIV-1 incorporation of host-cell-derived glycosphingolipid GM3 allows for capture by mature dendritic cells. *Proc Natl Acad Sci U S A* **109**, 7475–7480 (2012).

65. Izquierdo-Useros, N. *et al.* Sialyllactose in viral membrane gangliosides is a novel molecular recognition pattern for mature dendritic cell capture of HIV-1. *PLoS Biol* **10**, (2012).

66. Perez-Zsolt, D. *et al.* Dendritic Cells From the Cervical Mucosa Capture and Transfer HIV-1 via Siglec-1. *Front Immunol* **10**, 1–14 (2019).

67. Cameron, P. U. *et al.* Dendritic Cells Exposed to Human Immunodeficiency Virus Type-1 Transmit a Vigorous Cytopathic Infection to CD4 $^{+}$ T Cells. *Science (1979)* **257**, 383–387 (1992).

68. Izquierdo-Useros, N. *et al.* Siglec-1 Is a Novel Dendritic Cell Receptor That Mediates HIV-1 Trans-Infection Through Recognition of Viral Membrane Gangliosides. *PLoS Biol* **10**, (2012).

69. Sewald, X. *et al.* Retroviruses use CD169-mediated trans-infection of permissive lymphocytes to establish infection. *Science (1979)* **350**, 563–567 (2015).

70. Geisbert, T. W. *et al. Pathogenesis of Ebola Hemorrhagic Fever in Cynomolgus Macaques Evidence that Dendritic Cells Are Early and Sustained Targets of Infection*. *American Journal of Pathology* vol. 163 (2003).

71. Baseler, L., Chertow, D. S., Johnson, K. M., Feldmann, H. & Morens, D. M. The Pathogenesis of Ebola Virus Disease. *Annual Review of Pathology: Mechanisms of Disease* **12**, 387–418 (2017).

72. Bosio, C. M. *et al.* Ebola and Marburg Viruses Replicate in Monocyte-Derived Dendritic Cells without Inducing the Production of Cytokines and Full Maturation. *J Infect Dis* **188**, 1630–1638 (2003).

73. Lubaki, N. M. *et al.* The Ebola Interferon Inhibiting Domains Attenuate and Dysregulate Cell-Mediated Immune Responses. *PLoS Pathog* **12**, 1–34 (2016).

74. Davey, R. A. *et al.* Mechanisms of Filovirus Entry. in *Annals of the rheumatic diseases* vol. 35 323–352 (2017).

75. Dominguez-Soto, A. *et al.* The DC-SIGN–related lectin LSECtin mediates antigen capture and pathogen binding by human myeloid cells. *Blood* **109**, 5337–5345 (2007).

76. Simmons, G. *et al.* DC-SIGN and DC-SIGNR bind Ebola glycoproteins and enhance infection of macrophages and endothelial cells. *Virology* **305**, 115–123 (2003).

77. Jemielity, S. *et al.* TIM-family Proteins Promote Infection of Multiple Enveloped Viruses through Virion-associated Phosphatidylserine. *PLoS Pathog* **9**, e1003232 (2013).

78. Bavari, S. *et al.* Lipid raft microdomains: A gateway for compartmentalized trafficking of Ebola and Marburg viruses. *Journal of Experimental Medicine* **195**, 593–602 (2002).

79. Villinger, F. *et al.* Markedly Elevated Levels of Interferon (IFN)-σ, IFN-α, Interleukin (IL)-2, IL-10, and Tumor Necrosis Factor-α Associated with Fatal Ebola Virus Infection. *J Infect Dis* **179**, S188–S191 (1999).

80. Kreuels, B. *et al.* A Case of Severe Ebola Virus Infection Complicated by Gram-Negative Septicemia. *New England Journal of Medicine* **371**, 2394–2401 (2014).

81. Hyun, J. Y., Reuter, M. A. & McDonald, D. HIV traffics through a specialized, surface-accessible intracellular compartment during trans-infection of T cells by mature dendritic cells. *PLoS Pathog* **4**, (2008).

82. Izquierdo-Useros, N. *et al.* Dynamic Imaging of Cell-Free and Cell-Associated Viral Capture in Mature Dendritic Cells. *Traffic* **12**, 1702–1713 (2011).

83. Jackson, C. B., Farzan, M., Chen, B. & Choe, H. Mechanisms of SARS-CoV-2 entry into cells. *Nature Reviews Molecular Cell Biology* vol. 23 3–20 Preprint at https://doi.org/10.1038/s41580-021-00418-x (2022).

84. Mistry, P. *et al.* SARS-CoV-2 Variants, Vaccines, and Host Immunity. *Front Immunol* **12**, 1–21 (2022).

85. Gorbalenya, A. E. *et al.* The species Severe acute respiratory syndrome-related coronavirus: classifying 2019-nCoV and naming it SARS-CoV-2. *Nat Microbiol* **5**, 536–544 (2020).

86. Lu, R. *et al.* Genomic characterisation and epidemiology of 2019 novel coronavirus: implications for virus origins and receptor binding. *The Lancet* **395**, 565–574 (2020).

87. Zhou, P. *et al.* A pneumonia outbreak associated with a new coronavirus of probable bat origin. *Nature* **579**, 270–273 (2020).

88. Perlman, S. & Netland, J. Coronaviruses post-SARS: update on replication and pathogenesis. *Nat Rev Microbiol* **7**, 439–450 (2009).

89. Zhang, Y.-Z. & Holmes, E. C. A Genomic Perspective on the Origin and Emergence of SARS-CoV-2. *Cell* **181**, 223–227 (2020).

90. Lamers, M. M. & Haagmans, B. L. SARS-CoV-2 pathogenesis. *Nat Rev Microbiol* **20**, 270–284 (2022).

91. Salzberger, B. *et al.* Epidemiology of SARS-CoV-2. *Infection* **49**, 233–239 (2021).

92. Koelle, K., Martin, M. A., Antia, R., Lopman, B. & Dean, N. E. The changing epidemiology of SARS-CoV-2. *Science (1979)* **375**, 1116–1121 (2022).

93. He, X. *et al.* Temporal dynamics in viral shedding and transmissibility of COVID-19. *Nat Med* **26**, 672–675 (2020).

94. Kremer, C. *et al.* Authors' response: Estimating the generation interval for COVID-19 based on symptom onset data. *Eurosurveillance* **25**, 18–19 (2020).

95. Cobey, S. Modeling infectious disease dynamics. *Science (1979)* **368**, 713–714 (2020).

96. Fraser, C., Riley, S., Anderson, R. M. & Ferguson, N. M. Factors that make an infectious disease outbreak controllable. *Proceedings of the National Academy of Sciences* **101**, 6146–6151 (2004).

97. Notes, C.-. C or r e sp ondence Successful Elimination of Covid-19 Transmission in New Zealand. **56**, 2020–2022 (2020).

98. Van Tan, L. COVID-19 control in Vietnam. *Nat Immunol* **22**, 261–261 (2021).

99. Harvey, W. T. *et al.* SARS-CoV-2 variants, spike mutations and immune escape. *Nat Rev Microbiol* **19**, 409–424 (2021).

100. Plante, J. A. *et al.* Spike mutation D614G alters SARS-CoV-2 fitness. *Nature* **592**, 116–121 (2021).

101. Yu, I. T. S. *et al.* Evidence of Airborne Transmission of the Severe Acute Respiratory Syndrome Virus. *New England Journal of Medicine* **350**, 1731–1739 (2004).

102. Li, Y., Huang, X., Yu, I. T. S., Wong, T. W. & Qian, H. Role of air distribution in SARS transmission during the largest nosocomial outbreak in Hong Kong. *Indoor Air* **15**, 83–95 (2005).

103. van Doremalen, N. *et al.* Aerosol and Surface Stability of SARS-CoV-2 as Compared with SARS-CoV-1. *New England Journal of Medicine* **382**, 1564–1567 (2020).

104. Wu, Y. *et al.* Prolonged presence of SARS-CoV-2 viral RNA in faecal samples. *Lancet Gastroenterol Hepatol* **5**, 434–435 (2020).

105. Harrison, A. G., Lin, T. & Wang, P. Mechanisms of SARS-CoV-2 Transmission and Pathogenesis. *Trends Immunol* **41**, 1100–1115 (2020).

106. Arons, M. M. *et al.* Presymptomatic SARS-CoV-2 Infections and Transmission in a Skilled Nursing Facility. *New England Journal of Medicine* **382**, 2081–2090 (2020).

107. Wölfel, R. *et al.* Virological assessment of hospitalized patients with COVID-2019. *Nature* **581**, 465–469 (2020).

108. Rothe, C. *et al.* Transmission of 2019-nCoV Infection from an Asymptomatic Contact in Germany. *New England Journal of Medicine* **382**, 970–971 (2020).

109. Nandi Partha Sarathi, I. O. M. A. K. D. P. L. O. F. S. H. S. M. G. C. S. K. B. Adult Cardiac Surgery During the COVID-19 Pandemic: A Tiered Patient Triage Guidance Statement. *Ann Thorac Surg* **110**, 697–700 (2020).

110. Ahn, J. H. *et al.* Nasal ciliated cells are primary targets for SARS-CoV-2 replication in the early stage of COVID-19. *Journal of Clinical Investigation* **131**, 1–14 (2021).

111. Khan, M. *et al.* Visualizing in deceased COVID-19 patients how SARS-CoV-2 attacks the respiratory and olfactory mucosae but spares the olfactory bulb. *Cell* **184**, 5932-5949.e15 (2021).

112. Hoffmann, M. *et al.* SARS-CoV-2 Cell Entry Depends on ACE2 and TMPRSS2 and Is Blocked by a Clinically Proven Protease Inhibitor. *Cell* **181**, 271-280.e8 (2020).

113. Nguyen, L. *et al.* Sialic acid-containing glycolipids mediate binding and viral entry of SARS-CoV-2. *Nat Chem Biol* **18**, 81–90 (2022).

114. Laporte, M. & Naesens, L. Airway proteases: an emerging drug target for influenza and other respiratory virus infections. *Current Opinion in Virology* vol. 24 16–24 Preprint at https://doi.org/10.1016/j.coviro.2017.03.018 (2017).

115. Baron, J. *et al.* Matriptase, HAT, and TMPRSS2 Activate the Hemagglutinin of H9N2 Influenza A Viruses. *J Virol* **87**, 1811–1820 (2013).

116. Lu, Q. *et al.* SARS-CoV-2 exacerbates proinflammatory responses in myeloid cells through C-type lectin receptors and Tweety family member 2. *Immunity* **54**, 1304-1319.e9 (2021).

117. Melms, J. C. *et al.* A molecular single-cell lung atlas of lethal COVID-19. *Nature* **595**, 114–119 (2021).

118. Hui, K. P. Y. *et al.* Tropism, replication competence, and innate immune responses of the coronavirus SARS-CoV-2 in human respiratory tract and conjunctiva: an analysis in ex-vivo and in-vitro cultures. *Lancet Respir Med* **8**, 687–695 (2020).

119. Zheng, J. *et al.* Severe Acute Respiratory Syndrome Coronavirus 2–Induced Immune Activation and Death of Monocyte-Derived Human Macrophages and Dendritic Cells. *J Infect Dis* **223**, 785–795 (2021).

120. Blair, H. A. Remdesivir: A Review in COVID-19. *Drugs* 1215–1237 (2023) doi:10.1007/s40265-023-01926-0.

121. Nguyenla, X. *et al.* Discovery of SARS-CoV-2 antiviral synergy between remdesivir and approved drugs in human lung cells. *Sci Rep* **12**, 18506 (2022).

122. Tian, L. *et al.* Molnupiravir and Its Antiviral Activity Against COVID-19. *Front Immunol* **13**, 1–20 (2022).

123. Tian, H. *et al.* Efficacy and safety of paxlovid (nirmatrelvir/ritonavir) in the treatment of COVID-19: An updated meta-analysis and trial sequential analysis. *Rev Med Virol* 1–13 (2023) doi:10.1002/rmv.2473.

124. Carter, P. J. & Rajpal, A. Designing antibodies as therapeutics. *Cell* **185**, 2789–2805 (2022).

125. Westendorf, K. *et al.* LY-CoV1404 (bebtelovimab) potently neutralizes SARS-CoV-2 variants. *Cell Rep* **39**, 110812 (2022).

126. Gupta, A. *et al.* Early Treatment for Covid-19 with SARS-CoV-2 Neutralizing Antibody Sotrovimab. *New England Journal of Medicine* **385**, 1941–1950 (2021).

127. Martonik, D. *et al.* Effect of antiviral and immunomodulatory treatment on a cytokine profile in patients with COVID-19. *Front Immunol* **14**, 1–17 (2023).

128. Tanaka, H. *et al.* Propensity-Score Matched Analysis of the Effectiveness of Baricitinib in Patients With Coronavirus Disease 2019 (COVID-19) Using Nationwide Real-World Data: An Observational Matched Cohort Study From the Japan COVID-19 Task Force. *Open Forum Infect Dis* **10**, 1–10 (2023).

129. Chaudhuri, D. *et al.* Corticosteroids in COVID-19 and non-COVID-19 ARDS: a systematic review and meta-analysis. *Intensive Care Med* **47**, 521–537 (2021).

130. Stasi, C., Fallani, S., Voller, F. & Silvestri, C. Treatment for COVID-19: An overview. *Eur J Pharmacol* **889**, 173644 (2020).

131. Shoham, S. *et al.* Vaccines and therapeutics for immunocompromised patients with COVID-19. *EClinicalMedicine* **59**, 101965 (2023).

132. Peebles, R. S. & Graham, B. S. Viruses, dendritic cells and the lung. *Respir Res* **2**, 245–249 (2001).

133. Wang, X. *et al.* The role of dendritic cells in COVID-19 infection. *Emerg Microbes Infect* **12**, (2023).

134. Izquierdo-Useros, N. *et al.* Maturation of Blood-Derived Dendritic Cells Enhances Human Immunodeficiency Virus Type 1 Capture and Transmission. *J Virol* **81**, 7559–7570 (2007).

135. Cai, G. *et al.* SARS-CoV-2 impairs dendritic cells and regulates DC-SIGN gene expression in tissues. *Int J Mol Sci* **22**, 1–20 (2021).

136. Smed-Sörensen, A. *et al.* Differential Susceptibility to Human Immunodeficiency Virus Type 1 Infection of Myeloid and Plasmacytoid Dendritic Cells. *J Virol* **79**, 8861–8869 (2005).

137. Bain, W. G. *et al.* Lower Respiratory Tract Myeloid Cells Harbor SARS-Cov-2 and Display an Inflammatory Phenotype. *Chest* **159**, 963–966 (2021).

138. Merad, M. & Martin, J. C. Pathological inflammation in patients with COVID-19: a key role for monocytes and macrophages. *Nature Reviews Immunology* vol. 20 355–362 Preprint at https://doi.org/10.1038/s41577-020-0331-4 (2020).

139. Wen, W. *et al.* Immune cell profiling of COVID-19 patients in the recovery stage by single-cell sequencing. *Cell Discov* **6**, (2020).

140. Liao, M. *et al.* Single-cell landscape of bronchoalveolar immune cells in patients with COVID-19. *Nat Med* **26**, 842–844 (2020).

141. Collin, M. & Bigley, V. Human dendritic cell subsets: an update. *Immunology* **154**, 3–20 (2018).

142. Quemener, A. M. & Galibert, M. D. Antisense oligonucleotide: A promising therapeutic option to beat COVID-19. *Wiley Interdiscip Rev RNA* **13**, 1–12 (2022).

143. Hartenian, E. *et al.* The molecular virology of coronaviruses. *Journal of Biological Chemistry* **295**, 12910–12934 (2020).

144. Mateer, E. J., Maruyama, J., Card, G. E., Paessler, S. & Huang, C. Lassa Virus but Not Highly Pathogenic New World Arenaviruses Restrict Immunostimulatory dsRNA Accumulation During Infection. *J Virol* **94**, 1–19 (2020).

145. Marie-Laurence Moraz & Stefan Kunz. Pathogenesis of arenavirus hemorrhagic fevers. *Expert Rev Anti Infect Ther* **9**, 49–59 (2011).

146. Lukashevich, I. S., de la Torre, J. C. & Torre, J. C. de la. Special Issue “Arenaviruses 2020”. *Viruses* **13**, 703 (2021).

147. Sarute, N. & Ross, S. R. New World Arenavirus Biology. *Annu Rev Virol* **4**, 141–158 (2017).

148. Maes, P. *et al.* Taxonomy of the order Bunyavirales: second update 2018. *Arch Virol* **164**, 927–941 (2019).

149. Kuhn, J. H. *et al.* 2020 taxonomic update for phylum Negarnaviricota (Riboviria: Orthornavirae), including the large orders Bunyavirales and Mononegavirales. *Arch Virol* **165**, 3023–3072 (2020).

150. Radoshitzky, S. R. *et al.* ICTV virus taxonomy profile: Arenaviridae. *Journal of General Virology* **100**, 1200–1201 (2019).

151. Howard, C. R. & Simpson, D. I. H. The Biology of the Arenaviruses. *Journal of General Virology* **51**, 1–14 (1980).

152. Romanowski, V., Scientific, N., Scientific, N. & Bender, C. "Argentine Hemorrhagic Fever". in *Viral Hemorrhagic Fevers* (eds. Singh, S. K. & Ruzek, D.) 317–338 (CRC Press, 2013).

153. Enria, D. A., Briggiler, A. M. & Sánchez, Z. Treatment of Argentine hemorrhagic fever. *Antiviral Res* **78**, 132–139 (2008).

154. Fichet-Calvet, E. & Rogers, D. J. Risk Maps of Lassa Fever in West Africa. *PLoS Negl Trop Dis* **3**, e388 (2009).

155. Ogbu, O., Ajuluchukwu, E. & Uneke, C. J. Lassa fever in West African sub-region: an overview. *J Vector Borne Dis* **44**, 1–11 (2007).

156. Richmond, J. K. & Baglole, D. J. Lassa fever: Epidemiology, clinical features, and social consequences. *Br Med J* **327**, 1271–1275 (2003).

157. Garry, R. F. Lassa fever — the road ahead. *Nat Rev Microbiol* **21**, 87–96 (2023).

158. WHO. Disease Outbreaks News. https://www.who.int/emergencies/disease-outbreak-news.

159. WHO. Lassa Fever. https://www.afro.who.int/health-topics/lassa-fever.

160. Crowcroft, N. Management of Lassa Fever in European countries. *Eurosurveillance* **7**, 50–52 (2002).

161. Charrel, R. N. & de Lamballerie, X. Zoonotic aspects of arenavirus infections. *Vet Microbiol* **140**, 213–220 (2010).

162. Salazar-Bravo, J., Ruedas, L. A. & Yates, T. L. Mammalian Reservoirs of Arenaviruses. in 25–63 (2002). doi:10.1007/978-3-642-56029-3_2.

163. Robinson, J. E. *et al.* Most neutralizing human monoclonal antibodies target novel epitopes requiring both Lassa virus glycoprotein subunits. *Nat Commun* **7**, (2016).

164. Charrel, R. N., de Lamballerie, X. & Emonet, S. Phylogeny of the genus Arenavirus. *Curr Opin Microbiol* **11**, 362–368 (2008).

165. Childs, J. E., Mills, J. N. & Glass, G. E. Rodent-Borne Hemorrhagic Fever Viruses: A Special Risk for Mammalogists? *J Mammal* **76**, 664 (1995).

166. Gallo, G. L., López, N. & Loureiro, M. E. The Virus–Host Interplay in Junín Mammarenavirus Infection. *Viruses* **14**, 1134 (2022).

167. Fisher-Hoch, S. P. *et al.* Review of cases of nosocomial Lassa fever in Nigeria: The high price of poor medical practice. *Bmj* **311**, 857 (1995).

168. Ajayi, N. A. *et al.* Containing a Lassa fever epidemic in a resource-limited setting: outbreak description and lessons learned from Abakaliki, Nigeria (January–March 2012). *International Journal of Infectious Diseases* **17**, e1011–e1016 (2013).

169. Frame, J. D., Gocke, D. J., Baldwin, J. M. & Troup, J. M. Lassa Fever, a New Virus Disease of Man from West Africa. *Am J Trop Med Hyg* **19**, 670–676 (1970).

170. Stephenson, E. H., Larson, E. W. & Dominik, J. W. Effect of environmental factors on aerosol-induced lassa virus infection. *J Med Virol* **14**, 295–303 (1984).

171. Schlie, K. *et al.* Viral Protein Determinants of Lassa Virus Entry and Release from Polarized Epithelial Cells. *J Virol* **84**, 3178–3188 (2010).

172. McKee, Jr., K. T., Enria, D. A. & Barrera Oro, J. G. Junin (Argentine Hemorrhagic Fever). in *Vaccines for Biodefense and Emerging and Neglected Diseases* (ed. Sunit K . Singh Daniel Ruzek) 537–550 (Elsevier, 2009). doi:10.1016/B978-0-12-369408-9.00029-9.

173. Huang, C. *et al.* Highly Pathogenic New World and Old World Human Arenaviruses Induce Distinct Interferon Responses in Human Cells. *J Virol* **89**, 7079–7088 (2015).

174. Shao, J., Liang, Y. & Ly, H. Human Hemorrhagic Fever Causing Arenaviruses: Molecular Mechanisms Contributing to Virus Virulence and Disease Pathogenesis. *Pathogens* **4**, 283–306 (2015).

175. Radoshitzky, S. R. *et al.* Transferrin receptor 1 is a cellular receptor for New World haemorrhagic fever arenaviruses. *Nature* **446**, 92–96 (2007).

176. Helguera, G. *et al.* An Antibody Recognizing the Apical Domain of Human Transferrin Receptor 1 Efficiently Inhibits the Entry of All New World Hemorrhagic Fever Arenaviruses. *J Virol* **86**, 4024–4028 (2012).

177. Droniou-Bonzom, M. E. *et al.* Substitutions in the Glycoprotein (GP) of the Candid#1 Vaccine Strain of Junin Virus Increase Dependence on Human Transferrin Receptor 1 for Entry and Destabilize the Metastable Conformation of GP. *J Virol* **85**, 13457–13462 (2011).

178. Flanagan, M. L. *et al.* New World Clade B Arenaviruses Can Use Transferrin Receptor 1 (TfR1)-Dependent and -Independent Entry Pathways, and Glycoproteins from Human Pathogenic Strains Are Associated with the Use of TfR1. *J Virol* **82**, 938–948 (2008).

179. Martinez, M. G. *et al.* Utilization of human DC-SIGN and L-SIGN for entry and infection of host cells by the New World arenavirus, Junín virus. *Biochem Biophys Res Commun* **441**, 612–617 (2013).

180. Martinez, M. G., Cordo, S. M. & Candurra, N. A. Characterization of Junín arenavirus cell entry. *Journal of General Virology* **88**, 1776–1784 (2007).

181. Rojek, J. M., Sanchez, A. B., Nguyen, N. T., de la Torre, J.-C. J.-C. & Kunz, S. Different Mechanisms of Cell Entry by Human-Pathogenic Old World and New World Arenaviruses. *J Virol* **82**, 7677–7687 (2008).

182. Martinez, M. G., Forlenza, M. B. & Candurra, N. A. Involvement of cellular proteins in Junin arenavirus entry. *Biotechnol J* **4**, 866–870 (2009).

183. Castilla, V., Mersich, S. E., Candurra, N. A. & Damonte, E. B. The entry of Junin virus into Vero cells. *Arch Virol* **136**, 363–374 (1994).

184. Igonet, S. *et al.* X-ray structure of the arenavirus glycoprotein GP2 in its postfusion hairpin conformation. *Proceedings of the National Academy of Sciences* **108**, 19967–19972 (2011).

185. Klewitz, C., Klenk, H.-D. & ter Meulen, J. Amino acids from both N-terminal hydrophobic regions of the Lassa virus envelope glycoprotein GP-2 are critical for pH-dependent membrane fusion and infectivity. *Journal of General Virology* **88**, 2320–2328 (2007).

186. Di Simone, C., Zandonatti, M. A. & Buchmeier, M. J. Acidic pH Triggers LCMV Membrane Fusion Activity and Conformational Change in the Glycoprotein Spike. *Virology* **198**, 455–465 (1994).

187. Eschli, B. *et al.* Identification of an N-Terminal Trimeric Coiled-Coil Core within Arenavirus Glycoprotein 2 Permits Assignment to Class I Viral Fusion Proteins. *J Virol* **80**, 5897–5907 (2006).

188. Fan, L., Briese, T. & Lipkin, W. I. Z Proteins of New World Arenaviruses Bind RIG-I and Interfere with Type I Interferon Induction. *J Virol* **84**, 1785–1791 (2010).

189. Brouillette, R. B. *et al.* TIM-1 Mediates Dystroglycan-Independent Entry of Lassa Virus. *J Virol* **92**, 1–15 (2018).

190. Oppliger, J., Torriani, G., Herrador, A. & Kunz, S. Lassa Virus Cell Entry via Dystroglycan Involves an Unusual Pathway of Macropinocytosis. *J Virol* **90**, 6412–6429 (2016).

191. Kunz, S., Rojek, J. M., Perez, M., Spiropoulou, C. F. & Oldstone, M. B. A. Characterization of the Interaction of Lassa Fever Virus with Its Cellular Receptor α-Dystroglycan. *J Virol* **79**, 5979–5987 (2005).

192. Cao, W. *et al.* Identification of α-dystroglycan as a receptor for lymphocytic choriomeningitis virus and Lassa fever virus. *Science (1979)* **282**, 2079–2081 (1998).

193. Herrador, A. *et al.* Dynamic Dystroglycan Complexes Mediate Cell Entry of Lassa Virus. *mBio* **10**, 1–20 (2019).

194. Baize, S. *et al.* Lassa Virus Infection of Human Dendritic Cells and Macrophages Is Productive but Fails to Activate Cells. *The Journal of Immunology* **172**, 2861–2869 (2004).

195. Goncalves, A.-R. A.-R. *et al.* Role of DC-SIGN in Lassa Virus Entry into Human Dendritic Cells. *J Virol* **87**, 11504–11515 (2013).

196. Schaeffer, J. *et al.* Lassa virus activates myeloid dendritic cells but suppresses their ability to stimulate T cells. *PLoS Pathog* **14**, 1–25 (2018).

197. Walker, D. H. *et al.* Pathologic and virologic study of fatal Lassa fever in man. *Am J Pathol* **107**, 349–56 (1982).

198. Shimojima, M., Ströher, U., Ebihara, H., Feldmann, H. & Kawaoka, Y. Identification of Cell Surface Molecules Involved in Dystroglycan-Independent Lassa Virus Cell Entry. *J Virol* **86**, 2067–2078 (2012).

199. Stott, R. J., Strecker, T. & Foster, T. L. Distinct Molecular Mechanisms of Host Immune Response Modulation by Arenavirus NP and Z Proteins. *Viruses* **12**, 784 (2020).

200. Hulseberg, C. E., Fénéant, L., Szymańska, K. M. & White, J. M. Lamp1 increases the efficiency of lassa virus infection by promoting fusion in less acidic endosomal compartments. *mBio* **9**, 1–14 (2018).

201. Jae, L. T. *et al.* Lassa virus entry requires a trigger-induced receptor switch. *Science (1979)* **344**, 1506–1510 (2014).

202. Brisse, M. E. & Ly, H. Hemorrhagic fever-causing arenaviruses: Lethal pathogens and potent immune suppressors. *Frontiers in Immunology* vol. 10 Preprint at https://doi.org/10.3389/fimmu.2019.00372 (2019).

203. Caì, Y. *et al.* Recombinant Lassa Virus Expressing Green Fluorescent Protein as a Tool for High-Throughput Drug Screens and Neutralizing Antibody Assays. *Viruses* **10**, 655 (2018).

204. Müller, H. *et al.* Adjuvant formulated virus-like particles expressing native-like forms of the Lassa virus envelope surface glycoprotein are immunogenic and induce antibodies with broadly neutralizing activity. *NPJ Vaccines* **5**, 1–17 (2020).

205. Wang, M. *et al.* Construction and immunological evaluation of an adenoviral vector-based vaccine candidate for lassa fever. *Viruses* **13**, (2021).

206. Mateo, M. *et al.* Vaccines inducing immunity to Lassa virus glycoprotein and nucleoprotein protect macaques after a single shot. *Sci Transl Med* **11**, 1–18 (2019).

207. Cai, Y. *et al.* A lassa virus live-attenuated vaccine candidate based on rearrangement of the intergenic region. *mBio* **11**, 1–18 (2020).

208. Purushotham, J., Lambe, T. & Gilbert, S. Vaccine platforms for the prevention of Lassa fever. *Immunol Lett* **215**, (2019).

209. Garry, R. F. Lassa fever — the road ahead. *Nat Rev Microbiol* **21**, 87–96 (2023).

210. Gowen, B. B. *et al.* Second-Generation Live-Attenuated Candid#1 Vaccine Virus Resists Reversion and Protects against Lethal Junín Virus Infection in Guinea Pigs. *J Virol* **95**, (2021).

211. Sulis, G., Peebles, A. & Basta, N. E. Lassa fever vaccine candidates: A scoping review of vaccine clinical trials. *Tropical Medicine & International Health* **28**, 420–431 (2023).

212. Madu, I. G. *et al.* A potent Lassa virus antiviral targets an arenavirus virulence determinant. *PLoS Pathog* **14**, e1007439 (2018).

213. Gowen, B. B. *et al.* Potent inhibition of arenavirus infection by a novel fusion inhibitor. *Antiviral Res* **193**, 105125 (2021).

214. Furuta, Y. *et al.* Favipiravir (T-705), a novel viral RNA polymerase inhibitor. *Antiviral Res* **100**, 446–454 (2013).

215. McLay, L., Liang, Y. & Ly, H. Comparative analysis of disease pathogenesis and molecular mechanisms of New World and Old World arenavirus infections. *Journal of General Virology* **95**, 1–15 (2014).

216. Sevilla, N. *et al.* Immunosuppression and Resultant Viral Persistence by Specific Viral Targeting of Dendritic Cells. *Journal of Experimental Medicine* **192**, 1249–1260 (2000).

217. Baize, S. *et al.* Early and Strong Immune Responses Are Associated with Control of Viral Replication and Recovery in Lassa Virus-Infected Cynomolgus Monkeys. *J Virol* **83**, 5890–5903 (2009).

218. Johnson, K. M. *et al.* Clinical Virology of Lassa Fever in Hospitalized Patients. *Journal of Infectious Diseases* **155**, 456–464 (1987).

219. Marta, R. F. *et al.* Proinflammatory cytokines and elastase-α-1-antitrypsin in Argentine hemorrhagic fever. *American Journal of Tropical Medicine and Hygiene* **60**, 85–89 (1999).

220. Heller, M. V., Saavedra, M. C., Falcoff, R., Maiztegui, J. I. & Molinas, F. C. Increased Tumor Necrosis Factor- Levels in Argentine Hemorrhagic Fever. *Journal of Infectious Diseases* **166**, 1203–1204 (1992).

221. Levis, S. C. *et al.* Correlation between endogenous interferon and the clinical evolution of patients with Argentine hemorrhagic fever. *J Interferon Res* **5**, 383–389 (1985).

222. Groseth, A. *et al.* Tacaribe Virus but Not Junin Virus Infection Induces Cytokine Release from Primary Human Monocytes and Macrophages. *PLoS Negl Trop Dis* **5**, e1137 (2011).

223. Maiztegui, JulioI., Fernandez, NestorJ. & De Damilano, AlbaJ. Efficacy of immune plasma in treatment of argentine hæmorrhagic fever and association between treatment and a late neurological syndrome. *The Lancet* **314**, 1216–1217 (1979).

224. Qi, X. *et al.* Cap binding and immune evasion revealed by Lassa nucleoprotein structure. *Nature* **468**, 779–785 (2010).

225. Hastie, K. M., Kimberlin, C. R., Zandonatti, M. A., MacRae, I. J. & Saphire, E. O. Structure of the Lassa virus nucleoprotein reveals a dsRNA-specific 3' to 5' exonuclease activity essential for immune suppression. *Proc Natl Acad Sci U S A* **108**, 2396–2401 (2011).

226. Lyu, X. *et al.* The global landscape of approved antibody therapies. *Antib Ther* **5**, 233–257 (2022).

227. Stanfield, R. L. & Wilson, I. A. Antibody structure. *Antibodies for Infectious Diseases* 49–62 (2015) doi:10.1128/9781555817411.ch3.

228. Dreyfus, C. *et al.* Highly Conserved Protective Epitopes on Influenza B Viruses. *Science (1979)* **337**, 1343–1348 (2012).

229. Parren, P. W. H. I. & Burton, D. R. The antiviral activity of antibodies in vitro and in vivo. *Adv Immunol* **77**, 195–262 (2001).

230. Han, J. *et al.* Effects of Anti-G and Anti-F Antibodies on Airway Function after Respiratory Syncytial Virus Infection. *Am J Respir Cell Mol Biol* **51**, 143–154 (2014).

231. Dibo, M. *et al.* Antibody Therapy for the Control of Viral Diseases: An Update. *Curr Pharm Biotechnol* **20**, 1108–1121 (2019).

232. PREVAIL II Writing Group *et al.* A Randomized, Controlled Trial of ZMapp for Ebola Virus Infection. *New England Journal of Medicine* **375**, 1448–1456 (2016).

233. Ottoni, M. P. *et al.* Ebola-negative neonates born to Ebola-infected mothers after monoclonal antibody therapy: a case series. *Lancet Child Adolesc Health* **4**, 884–888 (2020).

234. Tiller, K. E. & Tessier, P. M. Advances in Antibody Design. *Annu Rev Biomed Eng* **17**, 191–216 (2015).

235. Nelson, A. L. Antibody fragments. *MAbs* **2**, 77–83 (2010).

236. Shepard, H. M., Phillips, G. L., Thanos, C. D. & Feldmann, M. Developments in therapy with monoclonal antibodies and related proteins. *Clinical Medicine, Journal of the Royal College of Physicians of London* **17**, 220–232 (2017).

237. Wu, H., Nie, Y., Huse, W. D. & Watkins, J. D. Humanization of a murine monoclonal antibody by simultaneous optimization of framework and CDR residues. *J Mol Biol* **294**, 151–162 (1999).

238. Waldmann, H. Human Monoclonal Antibodies: The Benefits of Humanization. in 1–10 (2019). doi:10.1007/978-1-4939-8958-4_1.

239. Deluca, K. F. *et al.* Generation and diversification of recombinant monoclonal antibodies. *Elife* **10**, (2021).

240. Safdari, Y., Farajnia, S., Asgharzadeh, M. & Khalili, M. Antibody humanization methods - A review and update. *Biotechnol Genet Eng Rev* **29**, 175–186 (2013).

241. Holliger, P. & Hudson, P. J. Engineered antibody fragments and the rise of single domains. *Nat Biotechnol* **23**, 1126–1136 (2005).

242. Chames, P., Van Regenmortel, M., Weiss, E. & Baty, D. Therapeutic antibodies: successes, limitations and hopes for the future. *Br J Pharmacol* **157**, 220–233 (2009).

243. Shahidian, A., Ghassemi, M., Mohammadi, J. & Hashemi, M. Immunotherapy. in *Bio-Engineering Approaches to Cancer Diagnosis and Treatment* 69–114 (Elsevier, 2020). doi:10.1016/B978-0-12-817809-6.00004-2.

244. Cumber, A. J., Ward, E. S., Winter, G., Parnell, G. D. & Wawrzynczak, E. J. Comparative stabilities in vitro and in vivo of a recombinant mouse antibody FvCys fragment and a bisFvCys conjugate. *J Immunol* **149**, 120–6 (1992).

245. Mazaheri, S. *et al.* Improvement of Certolizumab Fab' properties by PASylation technology. *Sci Rep* **10**, (2020).

246. Zhang, Q.-B. *et al.* Extending the in vivo Half-Life of Adalimumab Fab via Sortase A-Mediated Conjugation of Adalimumab Fab with Modified Fatty Acids. *Pharmaceutical Fronts* **02**, e160–e167 (2020).

247. SANZ, L., CUESTA, Á. M., COMPTE, M. & ÁLVAREZ-VALLINA, L. Antibody engineering: facing new challenges in cancer therapy. *Acta Pharmacol Sin* **26**, 641–648 (2005).

248. Almagro, J. C. & Fransson, J. Humanization of antibodies. *Frontiers in Bioscience* **13**, 1619–1633 (2008).

249. Lu, R. M. *et al.* Development of therapeutic antibodies for the treatment of diseases. *J Biomed Sci* **27**, (2020).

250. Robert, R. *et al.* Germline humanization of a murine Aβ antibody and crystal structure of the humanized recombinant Fab fragment. *Protein Science* **19**, 299–308 (2010).

251. Pelat, T. *et al.* Germline Humanization of a Non-human Primate Antibody that Neutralizes the Anthrax Toxin, by in Vitro and in Silico Engineering. *J Mol Biol* **384**, 1400–1407 (2008).

252. Cheung, N.-K. V., Guo, H., Hu, J., Tassev, D. V. & Cheung, I. Y. Humanizing murine IgG3 anti-GD2 antibody m3F8 substantially improves antibody-dependent cell-mediated cytotoxicity while retaining targeting in vivo. *Oncoimmunology* **1**, 477–486 (2012).

253. Foote, J. & Winter, G. Antibody framework residues affecting the conformation of the hypervariable loops. *J Mol Biol* **224**, 487–499 (1992).

254. Pavlinkova, G. *et al.* Effects of humanization and gene shuffling on immunogenicity and antigen binding of anti-TAG-72 single-chain Fvs. *Int J Cancer* **94**, 717–726 (2001).

255. Kuramochi, T., Igawa, T., Tsunoda, H. & Hattori, K. Humanization and Simultaneous Optimization of Monoclonal Antibody. in 213–230 (2019). doi:10.1007/978-1-4939-8958-4_9.

256. Hwang, W. Y. K. & Foote, J. Immunogenicity of engineered antibodies. *Methods* **36**, 3–10 (2005).

257. Schroff, R. W., Foon, K. A., Beatty, S. M., Oldham, R. K. & Morgan, A. C. Human anti-murine immunoglobulin responses in patients receiving monoclonal antibody therapy. *Cancer Res* **45**, 879–85 (1985).

258. Miller, R., Oseroff, A., Stratte, P. & Levy, R. Monoclonal antibody therapeutic trials in seven patients with T-cell lymphoma. *Blood* **62**, 988–995 (1983).

259. Golub, E. S. *Monoclonal Antibodies*. *Brenner's Encyclopedia of Genetics: Second Edition* (2013). doi:10.1016/B978-0-12-374984-0.00969-4.

260. Zeitlin, L. *et al.* Therapy for Argentine hemorrhagic fever in nonhuman primates with a humanized monoclonal antibody. *Proc Natl Acad Sci U S A* **118**, 1–8 (2021).

261. Jacobson, J. M. *et al.* Safety, Pharmacokinetics, and Antiretroviral Activity of Multiple Doses of Ibalizumab (formerly TNX-355), an Anti-CD4 Monoclonal Antibody, in Human Immunodeficiency Virus Type 1-Infected Adults. *Antimicrob Agents Chemother* **53**, 450–457 (2009).

262. Izquierdo-Useros, N. *et al.* HIV-1 Capture and Transmission by Dendritic Cells: The Role of Viral Glycolipids and the Cellular Receptor Siglec-1. *PLoS Pathog* **10**, (2014).

263. Fiolet, T., Kherabi, Y., MacDonald, C.-J., Ghosn, J. & Peiffer-Smadja, N. Comparing COVID-19 vaccines for their characteristics, efficacy and effectiveness against SARS-CoV-2 and variants of concern: a narrative review. *Clinical Microbiology and Infection* **28**, 202–221 (2022).

264. Berlin, D. A., Gulick, R. M. & Martinez, F. J. Severe Covid-19. *New England Journal of Medicine* **383**, 2451–2460 (2020).

265. Hadjadj, J. *et al.* Impaired type I interferon activity and inflammatory responses in severe COVID-19 patients. *Science (1979)* **369**, 718–724 (2020).

266. Huang, C. *et al.* Clinical features of patients infected with 2019 novel coronavirus in Wuhan, China. *The Lancet* **395**, 497–506 (2020).

267. Mehta, P. *et al.* COVID-19: consider cytokine storm syndromes and immunosuppression. *The Lancet* vol. 395 1033–1034 Preprint at https://doi.org/10.1016/S0140-6736(20)30628-0 (2020).

268. del Valle, D. M. *et al.* An inflammatory cytokine signature predicts COVID-19 severity and survival. *Nat Med* **26**, 1636–1643 (2020).

269. Garcia-Carretero, R., Vazquez-Gomez, O., Gil-Prieto, R. & Gil-de-Miguel, A. Hospitalization burden and epidemiology of the COVID-19 pandemic in Spain (2020–2021). *BMC Infect Dis* **23**, 1–11 (2023).

270. CDC. COVID-19 Data Tracker. https://covid.cdc.gov/covid-data-tracker/#datatracker-home.

271. Tzotzos, S. J., Fischer, B., Fischer, H. & Zeitlinger, M. Incidence of ARDS and outcomes in hospitalized patients with COVID-19: A global literature survey. *Crit Care* **24**, 1–4 (2020).

272. Hoang, T. N. *et al.* Baricitinib treatment resolves lower-airway macrophage inflammation and neutrophil recruitment in SARS-CoV-2-infected rhesus macaques. *Cell* **184**, 460-475.e21 (2021).

273. Geijtenbeek, T. B. H. *et al.* Identification of DC-SIGN, a Novel Dendritic Cell–Specific ICAM-3 Receptor that Supports Primary Immune Responses. *Cell* **100**, 575–585 (2000).

274. Moller-Tank, S. & Maury, W. Ebola Virus Entry: A Curious and Complex Series of Events. *PLoS Pathog* **11**, e1004731 (2015).

275. Martines, R. B., Ng, D. L., Greer, P. W., Rollin, P. E. & Zaki, S. R. Tissue and cellular tropism, pathology and pathogenesis of Ebola and Marburg viruses. *Journal of Pathology* **235**, 153–174 (2015).

276. Alvarez, C. P. *et al.* C-Type Lectins DC-SIGN and L-SIGN Mediate Cellular Entry by Ebola Virus in cis and in trans . *J Virol* **76**, 6841–6844 (2002).

277. Lin, G. *et al.* Differential N-Linked Glycosylation of Human Immunodeficiency Virus and Ebola Virus Envelope Glycoproteins Modulates Interactions with DC-SIGN and DC-SIGNR. *J Virol* **77**, 1337–1346 (2003).

278. Thépaut, M. *et al.* DC/L-SIGN recognition of spike glycoprotein promotes SARS-CoV-2 trans-infection and can be inhibited by a glycomimetic antagonist. *PLoS Pathog* **17**, e1009576 (2021).

279. Pino, M. *et al.* HIV-1 immune activation induces Siglec-1 expression and enhances viral trans-infection in blood and tissue myeloid cells. *Retrovirology* **12**, (2015).

280. Chan, R. *et al.* Retroviruses Human Immunodeficiency Virus and Murine Leukemia Virus Are Enriched in Phosphoinositides. *J Virol* **82**, 11228–11238 (2008).

281. Feizpour, A. *et al.* Quantifying Lipid Contents in Enveloped Virus Particles with Plasmonic Nanoparticles. *Small* **11**, 1592–1602 (2015).

282. Kalvodova, L. *et al.* The Lipidomes of Vesicular Stomatitis Virus, Semliki Forest Virus, and the Host Plasma Membrane Analyzed by Quantitative Shotgun Mass Spectrometry. *J Virol* **83**, 7996–8003 (2009).

283. Pillay, S. *et al.* Illumina Nextera DNA Flex library construction and sequencing for SARS-CoV-2: Adapting COVID-19 ARTIC protocol V.1 Genes In 1 collection Coronavirus Method Development Community KRISP. (2020) doi:10.17504/protocol.

284. Ewels, P. A. *et al.* The nf-core framework for community-curated bioinformatics pipelines. *Nat Biotechnol* **38**, 276–278 (2020).

285. Ou, X. *et al.* Characterization of spike glycoprotein of SARS-CoV-2 on virus entry and its immune cross-reactivity with SARS-CoV. *Nat Commun* **11**, (2020).

286. Trinité, B. *et al.* SARS-CoV-2 infection elicits a rapid neutralizing antibody response that correlates with disease severity. *Sci Rep* **11**, 1–10 (2021).

287. Tenorio, R. *et al.* Reovirus σNS and μNS proteins remodel the endoplasmic reticulum to build replication neo-organelles. *mBio* **9**, (2018).

288. Dalskov, L. *et al.* SARS-CoV-2 evades immune detection in alveolar macrophages. *EMBO Rep* **21**, 1–10 (2020).

289. Yilla, M. *et al.* SARS-coronavirus replication in human peripheral monocytes/macrophages. *Virus Res* **107**, 93–101 (2005).

290. Tynell, J. *et al.* Middle east respiratory syndrome coronavirus shows poor replication but significant induction of antiviral responses in human monocyte-derived macrophages and dendritic cells. *Journal of General Virology* **97**, 344–355 (2016).

291. Giron, L. B. *et al.* Plasma Markers of Disrupted Gut Permeability in Severe COVID-19 Patients. *Front Immunol* **12**, 1–16 (2021).

292. Panchal, R. G. *et al. In vivo oligomerization and raft localization of Ebola virus protein VP40 during vesicular budding*. https://www.pnas.org (2003).

293. Lorizate, M. & Kräusslich, H. G. Role of lipids in virus replication. *Cold Spring Harb Perspect Biol* **3**, 1–20 (2011).

294. Happi, A. N., Happi, C. T. & Schoepp, R. J. Lassa fever diagnostics: past, present, and future. *Curr Opin Virol* **37**, 132–138 (2019).

295. Kolokoltsova, O. A. *et al.* RIG-I enhanced interferon independent apoptosis upon Junin virus infection. *PLoS One* **9**, 1–8 (2014).

296. Mareze, V. A. *et al.* Tests in mice of a dengue vaccine candidate made of chimeric Junin virus-like particles and conserved dengue virus envelope sequences. *Appl Microbiol Biotechnol* **100**, 125–133 (2016).

297. Macher, A. M. & Wolfe, M. S. Historical Lassa fever reports and 30-year clinical update. *Emerg Infect Dis* **12**, 835–837 (2006).

298. Salami, K., Gouglas, D., Schmaljohn, C., Saville, M. & Tornieporth, N. A review of Lassa fever vaccine candidates. *Curr Opin Virol* **37**, 105–111 (2019).

299. Mantlo, Paessler & Huang. Differential Immune Responses to Hemorrhagic Fever-Causing Arenaviruses. *Vaccines (Basel)* **7**, 138 (2019).

300. Joseph, S. & Campbell, K. P. Lassa fever virus binds matriglycan—A polymer of alternating xylose and glucuronate—On α-dystroglycan. *Viruses* **13**, (2021).

301. Moreno, H., Möller, R., Fedeli, C., Gerold, G. & Kunz, S. Comparison of the Innate Immune Responses to Pathogenic and Nonpathogenic Clade B New World Arenaviruses. *J Virol* **93**, 1–19 (2019).

302. Perez-Zsolt, D. *et al.* SARS-CoV-2 interaction with Siglec-1 mediates trans-infection by dendritic cells. *Cell Mol Immunol* **18**, 2676–2678 (2021).

303. Borio, C. S. *et al.* Antigen vehiculization particles based on the Z protein of Junin virus. *BMC Biotechnol* **12**, 80 (2012).

304. Li, D. *et al.* An Ebola Virus-Like Particle-Based Reporter System Enables Evaluation of Antiviral Drugs In Vivo under Non-Biosafety Level 4 Conditions . *J Virol* **90**, 8720–8728 (2016).

305. Ziegler, C. M. *et al.* A proteomic survey of Junín virus interactions with human proteins reveals host factors required for arenavirus replication. *J Virol* JVI.01565-17 (2017) doi:10.1128/jvi.01565-17.

306. Ziegler, C. M. *et al.* Host-driven phosphorylation appears to regulate the budding activity of the Lassa virus matrix protein. *Pathogens* **7**, 5–8 (2018).

307. Capul, A. A. & de la Torre, J. C. A cell-based luciferase assay amenable to high-throughput screening of inhibitors of arenavirus budding. *Virology* **382**, 107–114 (2008).

308. Li, S. *et al.* Acidic pH-Induced Conformations and LAMP1 Binding of the Lassa Virus Glycoprotein Spike. *PLoS Pathog* **12**, e1005418 (2016).

309. Branco, L. M. *et al.* Lassa virus-like particles displaying all major immunological determinants as a vaccine candidate for Lassa hemorrhagic fever. *Virol J* **7**, 279 (2010).

310. Beutler, B. Innate immunity: An overview. *Mol Immunol* **40**, 845–859 (2004).

311. Marasco, W. A. & Sui, J. The growth and potential of human antiviral monoclonal antibody therapeutics. *Nat Biotechnol* **25**, 1421–1434 (2007).

312. Aubrey, N. & Billiald, P. Antibody Fragments Humanization: Beginning with the End in Mind. in 231–252 (2019). doi:10.1007/978-1-4939-8958-4_10.

313. Morrison, S. L., Johnson, M. J., Herzenberg, L. A. & Oi, V. T. Chimeric human antibody molecules: Mouse antigen-binding domains with human constant region domains. *Proc Natl Acad Sci U S A* **81**, 6851–6855 (1984).

314. Yamada, T. Therapeutic Monoclonal Antibodies. *Keio J Med* **60**, 37–46 (2011).

315. Chelius, D., Render, D. S. & Bondarenko, P. v. Identification and characterization of deamidation sites in the conserved regions of human immunoglobulin gamma antibodies. *Anal Chem* **77**, 6004–6011 (2005).

316. Lu, X. *et al.* Deamidation and isomerization liability analysis of 131 clinical-stage antibodies. *MAbs* **11**, 45 (2019).

317. Wakankar, A. A. *et al.* Aspartate isomerization in the complementarity-determining regions of two closely related monoclonal antibodies. *Biochemistry* **46**, 1534–1544 (2007).

318. Hageman, T. *et al.* Impact of Tryptophan Oxidation in Complementarity-Determining Regions of Two Monoclonal Antibodies on Structure-Function Characterized by Hydrogen-Deuterium Exchange Mass Spectrometry and Surface Plasmon Resonance. *Pharm Res* **36**, (2018).

319. Qiu, H. *et al.* Engineering an anti-CD52 antibody for enhanced deamidation stability. *MAbs* **11**, 1266–1275 (2019).

320. Pavon, J. A. *et al.* Selective Tryptophan Oxidation of Monoclonal Antibodies: Oxidative Stress and Modeling Prediction. *Anal Chem* **91**, 2192–2200 (2019).

321. van de Bovenkamp, F. S. *et al.* Variable Domain N-Linked Glycans Acquired During Antigen-Specific Immune Responses Can Contribute to Immunoglobulin G Antibody Stability. *Front Immunol* **9**, (2018).

322. Schwartz, S. *et al. Mutational Inactivation of an Inhibitory Sequence in Human Immunodeficiency Virus Type 1 Results in Rev-Independent gag Expression*. *JOURNAL OF VIROLOGY* (1992).

323. Hermida-Matsumoto, L. & Resh, M. D. Localization of human immunodeficiency virus type 1 Gag and Env at the plasma membrane by confocal imaging. *J Virol* **74**, 8670–8679 (2000).

324. Perlman, M. & Resh, M. D. Identification of an intracellular trafficking and assembly pathway for HIV-1 Gag. *Traffic* **7**, 731–745 (2006).

325. Lindwasser, O. W. & Resh, M. D. Myristoylation as a target for inhibiting HIV assembly: Unsaturated fatty acids block viral budding. *Proc Natl Acad Sci U S A* **99**, 13037–13042 (2002).

326. Hübner, W. *et al.* Sequence of Human Immunodeficiency Virus Type 1 (HIV-1) Gag Localization and Oligomerization Monitored with Live Confocal Imaging of a Replication-Competent, Fluorescently Tagged HIV-1. *J Virol* **81**, 12596–12607 (2007).

327. Martinez, O. *et al.* Zaire Ebola virus entry into human dendritic cells is insensitive to cathepsin L inhibition. *Cell Microbiol* **12**, 148–157 (2010).

328. Banchereau, J. & Steinman, R. M. Dendritic cells and the control of immunity. *Nature* **392**, 245–252 (1998).

329. Steinman, R. M. The Dendritic Cell System and its Role in Immunogenicity. *Annu Rev Immunol* **9**, 271–296 (1991).

330. Wilson, N. S. & Villadangos, J. A. Regulation of antigen presentation and cross-presentation in the dendritic cell network: Facts, hypothesis, and immunological implications. *Adv Immunol* **86**, 241–305 (2005).

331. Akiyama, H. *et al.* Virus Particle Release from Glycosphingolipid-Enriched Microdomains Is Essential for Dendritic Cell-Mediated Capture and Transfer of HIV-1 and Henipavirus. *J Virol* **88**, 8813–8825 (2014).

332. Farrell, H. E. *et al.* Murine cytomegalovirus spreads by dendritic cell recirculation. *mBio* **8**, 1–13 (2017).

333. De Witte, L. *et al.* DC-SIGN and CD150 have distinct roles in transmission of measles virus from dendritic cells to T-Lymphocytes. *PLoS Pathog* **4**, (2008).

334. Spira, A. I. *et al.* Cellular targets of infection and route of viral dissemination after an intravaginal inoculation of simian immunodeficiency virus into rhesus macaques. *Journal of Experimental Medicine* **183**, 215–225 (1996).

335. Ren, X. X. *et al.* The molecule of DC-SIGN captures enterovirus 71 and confers dendritic cell-mediated viral trans-infection. *Virol J* **11**, 1–9 (2014).

336. Schönrich, G. & Raftery, M. J. Dendritic cells as Achilles' heel and Trojan horse during varicella zoster virus infection. *Front Microbiol* **6**, 1–6 (2015).

337. Pham, A. M., Langlois, R. A. & tenOever, B. R. Replication in cells of hematopoietic origin is necessary for dengue virus dissemination. *PLoS Pathog* **8**, (2012).

338. de Jong, M. A. W. P., de Witte, L., Bolmstedt, A., van Kooyk, Y. & Geijtenbeek, T. B. H. Dendritic cells mediate herpes simplex virus infection and transmission through the C-type lectin DC-SIGN. *Journal of General Virology* **89**, 2398–2409 (2008).

339. Knight, S. C. & Patterson, S. BONE MARROW–DERIVED DENDRITIC CELLS, INFECTION WITH HUMAN IMMUNODEFICIENCY VIRUS, AND IMMUNOPATHOLOGY. *Annu Rev Immunol* **15**, 593–615 (1997).

340. Mahanty, S. *et al.* Cutting Edge: Impairment of Dendritic Cells and Adaptive Immunity by Ebola and Lassa Viruses. *The Journal of Immunology* **170**, 2797–2801 (2003).

341. Israeli, H., Cohen-Dvashi, H., Shulman, A., Shimon, A. & Diskin, R. Mapping of the Lassa virus LAMP1 binding site reveals unique determinants not shared by other old world arenaviruses. *PLoS Pathog* **13**, e1006337 (2017).

342. Lempp, F. A. *et al.* Lectins enhance SARS-CoV-2 infection and influence neutralizing antibodies. *Nature* **598**, 342–347 (2021).

343. Jalloh, S. *et al.* CD169-mediated restrictive SARS-CoV-2 infection of macrophages induces pro-inflammatory responses. *PLoS Pathog* **18**, e1010479 (2022).

344. Ural, B. B. *et al.* Identification of a nerve-associated, lung-resident interstitial macrophage subset with distinct localization and immunoregulatory properties. *Sci Immunol* **5**, (2020).

345. Yeung, S. T., Ovando, L. J., Russo, A. J., Rathinam, V. A. & Khanna, K. M. CD169+ macrophage intrinsic IL-10 production regulates immune homeostasis during sepsis. *Cell Rep* **42**, 112171 (2023).

346. Bermejo-Jambrina, M. *et al.* Infection and transmission of SARS-CoV-2 depend on heparan sulfate proteoglycans. *EMBO J* **40**, 1–16 (2021).

347. Amraei, R. *et al.* CD209L/L-SIGN and CD209/DC-SIGN act as receptors for SARS-CoV-2. *bioRxiv* (2021) doi:10.1101/2020.06.22.165803.

348. Gupta, J. *et al.* SARS CoV-2 spike protein variants exploit DC-SIGN/DC-SIGNR receptor for evolution and severity: an in-silico insight. *Virusdisease* **34**, 278–296 (2023).

349. Peters, C. J. Human Infection with Arenaviruses in the Americas. in 65–74 (2002). doi:10.1007/978-3-642-56029-3_3.

350. Radoshitzky, S. R. *et al.* Receptor determinants of zoonotic transmission of New World hemorrhagic fever arenaviruses. *Proc Natl Acad Sci U S A* **105**, 2664–2669 (2008).

351. Bräutigam, K. *et al.* Comprehensive analysis of SARS-CoV-2 receptor proteins in human respiratory tissues identifies alveolar macrophages as potential virus entry site. *Histopathology* **82**, 846–859 (2023).

352. Negrotto, S. *et al.* Human Plasmacytoid Dendritic Cells Elicited Different Responses after Infection with Pathogenic and Nonpathogenic Junin Virus Strains. *J Virol* **89**, 7409–7413 (2015).

353. Karlsson, M. *et al.* A single–cell type transcriptomics map of human tissues. *Sci Adv* **7**, 1–10 (2021).

354. Martínez-Sobrido, L., Giannakas, P., Cubitt, B., García-Sastre, A. & de la Torre, J. C. Differential Inhibition of Type I Interferon Induction by Arenavirus Nucleoproteins. *J Virol* **81**, 12696–12703 (2007).

355. Shao, J., Huang, Q., Liu, X., Liang, Y. & Ly, H. Arenaviral Nucleoproteins Suppress PACT-Induced Augmentation of. *J Virol* **92**, 1–11 (2018).

356. Xing, J., Ly, H. & Liang, Y. The Z Proteins of Pathogenic but Not Nonpathogenic Arenaviruses Inhibit RIG-i-Like Receptor-Dependent Interferon Production. *J Virol* **89**, 2944–2955 (2015).

357. Xing, J., Chai, Z., Ly, H. & Liang, Y. Differential Inhibition of Macrophage Activation by Lymphocytic Choriomeningitis Virus and Pichinde Virus Is Mediated by the Z Protein N-Terminal Domain. *J Virol* **89**, 12513–12517 (2015).

358. Ambrosio, A. M., Enria, D. A. & Maiztegui, J. I. Junin Virus Isolation from Lympho-Mononuclear Cells of Patients with Argentine Hemorrhagic Fever. *Intervirology* **25**, 97–102 (1986).

359. McKee, K. T., Mahlandt, B. G., Maiztegui, J. I., Green, D. E. & Peters, C. J. Virus-specific factors in experimental Argentine hemorrhagic fever in rhesus macaques. *J Med Virol* **22**, 99–111 (1987).

360. Kenyon, R. H. *et al.* Aerosol infection of rhesus macaques with Junin virus. *Intervirology* **33**, 23–31 (1992).

361. Jiang, X. *et al.* Structures of arenaviral nucleoproteins with triphosphate dsRNA reveal a unique mechanism of immune suppression. *Journal of Biological Chemistry* **288**, 16949–16959 (2013).

362. Hensley, L. E. *et al.* Pathogenesis of lassa fever in cynomolgus macaques. *Virol J* **8**, (2011).

363. Martinez-Picado, J. *et al.* Identification of siglec-1 null individuals infected with HIV-1. *Nat Commun* **7**, 1–7 (2016).

364. Brown, S. C. *et al.* Dystrophic phenotype induced in vitro by antibody blockade of muscle alpha-dystroglycan-laminin interaction. *J Cell Sci* **112**, 209–216 (1999).

365. Dai, Y. *et al.* Whole exome sequencing identified a novel DAG1 mutation in a patient with rare, mild and late age of onset muscular dystrophy-dystroglycanopathy. *J Cell Mol Med* **23**, 811–818 (2019).

366. The Antibody Society. Therapeutic monoclonal antibodies approved or in regulatory review. https://www.antibodysociety.org/antibody-therapeutics-product-data/.

367. Chang, X. L. *et al.* Suppression of human and simian immunodeficiency virus replication with the CCR5-specific antibody Leronlimab in two species. *PLoS Pathog* **18**, e1010396 (2022).

368. Asaadi, Y., Jouneghani, F. F., Janani, S. & Rahbarizadeh, F. A comprehensive comparison between camelid nanobodies and single chain variable fragments. *Biomark Res* **9**, 87 (2021).

369. Wesolowski, J. *et al.* Single domain antibodies: Promising experimental and therapeutic tools in infection and immunity. *Med Microbiol Immunol* **198**, 157–174 (2009).

370. Perez-Zsolt, D. *et al.* HIV-1 Trans-Infection Mediated by DCs: The Tip of the Iceberg of Cell-to-Cell Viral Transmission. *Pathogens* **11**, 1–14 (2022).

371. Taylor, B. S., Tieu, H.-V., Jones, J. & Wilkin, T. J. CROI 2019: advances in antiretroviral therapy. *Top Antivir Med* **27**, 50–68 (2019).

372. Atta, M. G., De Seigneux, S. & Lucas, G. M. Clinical Pharmacology in HIV Therapy. *Clinical Journal of the American Society of Nephrology* **14**, 435–444 (2019).

373. Seregin, A. v. *et al.* The Glycoprotein Precursor Gene of Junin Virus Determines the Virulence of the Romero Strain and the Attenuation of the Candid #1 Strain in a Representative Animal Model of Argentine Hemorrhagic Fever. *J Virol* **89**, 5949–5956 (2015).

374. Fisher-Hoch, S. P. *et al.* Protection of rhesus monkeys from fatal Lassa fever by vaccination with a recombinant vaccinia virus containing the Lassa virus glycoprotein gene. *Proc Natl Acad Sci U S A* **86**, 317–321 (1989).

Chapter 9. Publications

Perez-Zsolt, D., Itziar Erkizia, Maria Pino, Mónica García-Gallo, Maria Teresa Martin, Susana Benet, Jakub Chojnacki, María Teresa Fernández-Figueras, Dolores Guerrero, Victor Urrea, **Xabier Muñiz-Trabudua**, Leonor Kremer, Javier Martinez- Picado* and Nuria Izquierdo-Useros*. **Anti-Siglec-1 antibodies block Ebola viral uptake and decrease cytoplasmic viral entry**. 2019. *Nature Microbiology*. 4(9):1558-1570. doi: 10.1038/s41564-019-0453-2.

*Corresponding authors

Author's contribution: The author of this thesis contributed to the current work by transfecting primary myeloid cells to produce EBOV VLPs in order to demonstrate GM1 incorporation.

Perez-Zsolt, D., Muñoz-Basagoiti, J., Rodon, J., Elosua-Bayes, M., Raïch-Regué, D., Risco, C., Sachse, M., Pino, M., Gumber, S., Paiardini, M., Chojnacki, J., Erkizia, I., **Muñiz-Trabudua, X**., Ballana, E., Riveira-Muñoz, E., Noguera-Julian, M., Paredes, R., Trinité, B., Tarrés-Freixas, F., Blanco, I., Guallar, V., Carrillo, J., Blanco, J., Telenti, A., Heyn, H., Segalés, J., Clotet, B., Martinez-Picado, J.*, Vergara-Alert, J.* and Izquierdo-Useros, N.*, 2021. **SARS-CoV-2 interaction with Siglec-1 mediates trans-infection by dendritic cells**. Cellular & Molecular Immunology, 18(12), pp.2676-2678.

*Corresponding authors

Author's contribution: The author of this thesis contributed to the current work by measuring lectin expression in cell lines by FACS used to assess the interaction between SARS-CoV-2 and Siglec-1. The author also contributed by generating high-resolution microscopy images and videos demonstrating VCC formation where the virus and the receptor accumulated.

Dàlia Raïch-Regué, Patricia Resa-Infante, Marçal Gallemí, Fernando Laguia, **Xabier Muñiz-Trabudua**, Jordana Muñoz-Basagoiti, Daniel Perez-Zsolt, Jakub Chojnacki, Susana Benet, Bonaventura Clotet, Javier Martinez-Picado, Nuria Izquierdo-Useros*, 2022. **Role of Siglecs in viral infections: A double-edged sword interaction**. Molecular Aspects of Medicine, https://doi.org/10.1016/j.mam.2022.101113.

*Corresponding authors

Author's contribution: The author of this thesis contributed to the current work by conducting extensive bibliographic research and actively participating in the writing process of the article.

Chapter 10. Acknowledgements

"Nunca puede faltar la parte de agradecimientos, la ciencia es un trabajo en equipo, y no habrías podido hacer lo que has hecho tú solo". Una frase que me dijeron al empezar el doctorado, y que no se me va a olvidar nunca. Desde el primer día que empecé a trabajar en Irsi, hasta el último, me han enseñado que en la ciencia no se llega a ningún sitio trabajando solo. Por eso no podía faltar un apartado como este, en el que quiero agradecer su ayuda a todos aquéllos que se han implicado, directa o indirectamente, en este trabajo.

En primer lugar, a **Javier** y **Nuria**, porque me dieron la oportunidad de trabajar con ellos y formar parte de su proyecto. Porque a pesar de haber hecho una entrevista de la que salí pensando que mi oportunidad de hacer un doctorado se había esfumado, (no se me va a olvidar esa entrevista en la vida), confiaron en mí y me han ayudado a lo largo de todo el doctorado. En estos 5 años he aprendido a escribir, a ponerle cariño, a dedicarle tiempo, y darle vueltas a lo que escribo hasta conseguir que todo hile y se pueda leer con la facilidad con la que se lee un cómic. He aprendido a priorizar, a valorar el esfuerzo y dedicarlo a lo que más importa. He aprendido que, para entender la cosas, a veces hay que cerrar los ojos e imaginárselo cómo si estuvieses viendo una película. También he aprendido que los colores de los gráficos son más importantes de lo que parecen, y que, aunque haya aprendido muchísimo sobre Adobe Illustrator y a hacer figuras, me trae por el camino de la amargura retocarlas. Pero, sobre todo, creo que he aprendido lo que es un buen científico y a hacer ciencia con rigurosidad, y eso es algo que me habéis aportado cada uno de los vosotros a vuestra manera.

Mila esker, **Itziar**. Ez dakit ze egin izango nuke zu gabe! Esperimentu amaitezinak egiten laguntzeagatik, zitometria ulertzea lortzeagatik, nola ez, zure patata opilengatik, baina batez ere, beti laguntzeko prest egoteagatik eta nire euskara berpizteagatik. Mila eta mila esker! A **Dani**, que fuiste quién me enseñó cómo funcionaban las cosas cuando llegué y que me guiaste los primeros meses para que no estuviese más perdido que un pulpo en un garaje. Me has enseñado muchísimo estos años, y me has ayudado mucho contagiándome tu alegría cuando había días que yo estaba de capa caída, sobre todo con los bailoteos en P3. También tengo que agradecerte que hubieses probado todo el menú de la cafetería antes de que yo llegase y me recomendases qué se podía comer y qué no. A **Judith**, por los desayunos con café y puesta al día antes de arrancar la jornada, por preocuparte siempre de que no me faltase de nada y disfrutase de la tesis. Y por supuesto de descubrirme el Can Montllor y sus calçotadas. A **Patri**, por haberte volcado en ayudarme cuándo te lo pedí, y por enseñarme lo

importante que es la organización y comprobar todo tres veces. He aprendido mucho sobre cómo hacer buena ciencia de ti. Thanks, Jakub, for your time explaining the art of microscopy and for the nerdy chats while we waited for the computer to process the awesome pictures you helped me acquire. Gracias a **Cristina**, que, aunque ahora ya no te dedicas al pipeteo, me ayudaste mucho en los últimos meses de tesis con tu experiencia. A **Fernando**, que me ha aguantado la formación y las bromas desde que entró, estoy seguro de que vas a tener una tesis espectacular con las fotos que estabas sacando. A **Sílvia**, por haberme acogido de compañero de entrenos desde el día que llegué. A **Ángel** por estar siempre dispuesto a ayudar y echar un cable cuando me hacía falta. A **Mª Carmen** por ayudarme a encontrar todo lo que me hacía falta para mis experimentos de molecular. A **Maria**, por el hornazo que nunca probé, las catas de crema de avellanas y su buen humor. A **Susana**, que, aunque no hayamos compartido mucho laboratorio, siempre me echaste un cable cuando me hizo falta. A **Lidia** por echarme un cable encontrando las 7 diferencias en las secuencias que me estaban volviendo loco. A **Mari**, **Sara** e **Irene** por estar siempre dispuestas a ayudar. Y como no, a **Victor** por ayudarme con la bioestadística que no sé si algún día llegaré a entender y que los análisis de mis resultados tengan algo de sentido.

Y no habría tenido resultados que analizar si no es por **Dalia** y **Jordana**, que junto con Dani me han acompañado cuando ha tocado ponerse el traje espacial y pasarnos las mañanas y las tardes en el laboratorio del CMCIB pipeteando SARS a ritmo de Alaska. Y siguiendo con la música, a **Carlos** por descubrirme canciones que al final he acabado escuchando en bucle y por tener siempre 5 minutos para comentar el último episodio que había salido del anime de turno. A **Macedonia**, la vecina de Carlos, que tiene la receta más peculiar de fajitas que conozco y que me ha amenizado desayunos y comidas. A todos los predocs y recién doctorados que han compartido laboratorio y largas tardes en P3, **Edurne**, **Raquel**, **Edwards**, **Clara**, **Eudald**, **Luis**, **Lucía**, **Irene**, **Ana**, y algunos más que me estaré dejando.

A aquellos que sin ser parte de Irsi me han ayudado a sacar adelante la tesis y que han colaborado con nosotros. A **Cristina Borio** y **Marcos Bilen** por sus consejos desde el otro lado del charco para resolver los misterios de los arenavirus. A la maravillosa **Elena Rebollo**, por todo el tiempo que has dedicado a explicarme cómo sacar las mejores fotografías a los virus y células con el equipo más puntero, las tardes en el Parc Científic y las alegrías al ver que habíamos conseguido sacar fotos a lo que parecía imposible.

Volviendo a Irsi, a Lidia, que siempre está dispuesta a solucionar todos los problemas. A Julián, que, si no llega a ser por él, no habría podido escribir la tesis a distancia ni estas palabras. A **Álex** no sólo por sus consejos, sino porque junto con **Roger** y **Ester**, han

conseguido catalanizarme un poco, y no hablo sólo del pa amb tomaquet y los calçots. Estic molt agraït d'haver pogut aprendre una miqueta de català i que m'heu ajudat a practicar-ho aquests anys. I encara que m'hagi calgut google translate per escriure això, gràcies a vosaltres puc defensar-me quan ho he de parlar. A **María**, por hacer las incubaciones menos aburridas, los encuentro en el office y los cafés de las 5 con Esther. A **Samandhy** por archivar todas las buenas recetas y tratar de alegrarnos a todos siempre. A **Nuria** (Pedreño senior) por aguantar mis lamentos durante las MacroPreps en molecular. A **Marisa** y a **Ruth** por oír los mismos lamentos e intentar alegrarme siempre. A **Eva**, por las recomendaciones culinarias de Premiá y salvarme el culo cuando me he quedado sin coche con el que volver del trabajo. A **Silvia M**, que además de salvarme también cuando no he tenido coche, se mudó a Premiá con Dama y se convirtió en compañera de paseos caninos. Y hablando de canes, agradecerle a **Francesc** las risas, los partidos de pádel, y sus reflejos para ir corriendo a la farmacia con el episodio del perro sangrante y salvar el viaje de ski.

No me puedo olvidar del dream team. **Arnau, Pénelope y Cristina**. Por los almuerzos improvisados, por no dejar pasar ni un cumpleaños sin su recordatorio, por acordarte de mí cada vez que vas al norte a coger olas, aunque sólo sea para dar envidia, porque nunca se me ha perdido un envío y porque si se había perdido, ya sabía dónde tenía que buscar. Por supuesto, tampoco me olvido de las chicas de muestras. **Lucía**, **Cris** y **Rafi**, que siempre me han ayudado cuando se lo he pedido y porque los desayunos en la cafetería no son lo mismo sin ellas. Tampoco serían lo mismo sin **Susana**, que hace que todo siga adelante en Irsi y me ha rescatado del almacén en múltiples ocasiones. Y cómo no acordarme de **Eli**, que siempre tiene una onza de chocolate para cuando me da el bajón de azúcar. A quién parecía que nunca le daba el bajón de azúcar a pesar de quedarse en P3 sin comer hasta bien entrada la tarde era a **Jordi**, que, en vez de saludarnos, al vernos en P3 nos preguntábamos a ver si ya habíamos comido.

Agradecer a todos los IPs de Irsi, **Cecilia Cabrera**, **Cristian Brander**, **Ester Ballana**, **Julia Garcia**, **Juliá Blanco**, **Jorge Carrillo**, **Marta Masanella**, **Nuria de la Iglesia**, y **Roger Paredes**, que siempre se nos han ofrecido su ayuda cuando la hemos necesitado.

También me gustaría agradecer a **Bonaventura Clotet** y a **Lourdes Grau** por darme la oportunidad de formar parte de IrsiCaixa. Para mí ha sido una oportunidad inigualable el poder realizar la tesis en un entorno de trabajo tan acogedor y a la vez profesional como es el de IrsiCaixa.

También me acuerdo de los que me acompañaron durante el doctorado y que ya no son parte de Irsi, pero que han formado parte de mi tesis y me han dado muy buenos momentos, A **Ana**

por todos los cotilleos, el episodio del perro sangrante en Andorra y descubrirme el almogrote. A **Miriam** por sus consejos sobre la vida de predoc y su picoteo en la terraza con vistas a Barcelona. To **Ifi**, for all those laughs at congresses and for cheering up the mood every single day. A **Sonia**, por el lavavajillas y por las risas esquiando a pesar de que Francesc casi se deja la rodilla en Andorra. A **Ferrán**, que siempre me ayudaste cuando tenía algún problema, aunque no tenías por qué, y porque siempre que salía alguna frikada nueva tenía alguien con quién comentarlo. A **Esther**, por los viajes a esquiar, las quedadas improvisadas después de los entrenos de volley, los cafés de las 5 con María y seguir en contacto a pesar de haberte ido.

A mis amigos de Bilbao, que me han acompañado durante todo el camino y me han alegrado las tardes y las noches a distancia, y me han apoyado cuando se me ha hecho cuesta arriba.

A **Isa**. Por acompañarme todos estos años y por aguantarme este último. Por estar siempre, a las duras y a las maduras, empujándome a trabajar cuando no tenía ganas y apoyándome cuando más me costaba.

Finalmente, quiero agradecer a **ama** y **aita** que me han apoyado siempre en todo lo que me propongo y que cuando me han flaqueado los ánimos o me han faltado las ganas, me han dado un empujón para seguir. Gracias por estar siempre a mi lado.